Investigating potential physiological roles of condensed tannins in roots of *Populus*: Localization and distribution in relation to nutrient ion uptake.

by

Rebecca Westley
MBiolSci, University of Sheffield, 2012

A Thesis Submitted in Partial Fulfillment
of the Requirements for the Degree of

MASTER OF SCIENCE

in the Department of Biology

Supervisory Committee

Investigating potential physiological roles of condensed tannins in roots of *Populus*: Localization and distribution in relation to nutrient ion uptake.

by

Rebecca Westley
MBiolSci, University of Sheffield, 2012

Supervisory Committee

Dr. C. Peter Constabel (Department of Biology)
Supervisor

Dr. Barbara J. Hawkins (Department of Biology)
Co-Supervisor

Dr. Patrick von Aderkas (Department of Biology)
Departmental Member

Dr. Doug Maynard (Pacific Forestry Centre)
Outside Member

Abstract

Supervisory Committee
Dr. C. Peter Constabel (Department of Biology)
Supervisor
Dr. Barbara J. Hawkins (Department of Biology)
Co-Supervisor
Dr. Patrick von Aderkas (Department of Biology)
Departmental Member
Dr. Doug Maynard (Pacific Forestry Centre)
Outside Member

Condensed tannins or proanthocyanidins (CTs) are polymeric flavonoids and common plant secondary metabolites. They are defined by their protein binding capacity, and anti-oxidant and metal chelating properties. Known functions of CTs include anti-herbivore and anti-microbial defenses. Chemical ecology studies, especially on CTs, have focussed almost exclusively on foliar chemistry and above-ground ecological interactions. However, CT concentrations in roots can match and far exceed those found in leaves, particularly in woody plant species. This suggests that CTs are also likely to have important ecological and physiological roles below-ground. A review of the literature suggests three potential roles of root CTs: 1) defense against soil pathogens and root herbivores; 2) facilitating adaptation to toxic soils through heavy metal chelation, and; 3) facilitating or modulating nutrient uptake through the binding of nutrient cations. In this thesis the relationship between root CTs and nutrient uptake will be analysed in *P. tremula* x *alba.*

Localization of CTs was determined through both quantitative and histochemical techniques. Quantitation of CTs with the 1-butanol:HCl assay clearly showed that CT

concentration was higher in the white root zone compared to the brown root zone or cork zone. This is inconsistent with the term ‘condensed tannin zone’ that is commonly used to describe the macroscopic brown zone of the root between the white zone and the cork zone in *Pinus.* The tissue specific localization of CTs in roots was determined using the CT-specific stain, 4-dimethylaminocinnamaldehyde (4-DMACA), on embedded longitudinal and fresh cross sections. These stained sections showed that CTs were present in cells on the root surface, specifically accumulating in the root cap and epidermal cells. CTs were also sporadically present in the cortical cells of the young, white root zones. CT concentration declined as distance from the root tip increased. The pattern of CT distribution, as indicated by intensity of the staining, corresponded directly to the quantitative assay results.

Growing poplars under low nitrogen availability stimulated higher root CT concentrations than when they were grown under high nitrogen availability, suggesting a link between nitrogen and CTs. Since CTs are known to bind cations *in vivo,* I hypothesized that root CTs may modulate or facilitate nutrient uptake by binding positively charged nutrient ions. The Microelectrode Ion Flux Measurement (MIFE^{TM}) technique was used to analyse specific fluxes of NH_4^+, NO_3^- and Ca^{2+} at specific root locations in poplar roots, and test for spatial correlation with CT localization. This technique was also used to compare the NH_4^+, NO_3^- and Ca^{2+} fluxes in transgenic high-CT and wild-type lines of *Populus tremula* x *alba* to test the impact of CTs on nutrient uptake directly. No correlation was found between fluxes of NH_4^+, NO_3^- or Ca^{2+} and CT distribution. The data indicate that root CTs do not influence nutrient uptake in *Populus*.

This study provides data regarding the pattern of CT distribution as well as fundamental information on nutrient uptake in *P. tremula* x *alba* roots. It provides new knowledge that will be used to stimulate investigations on other potential roles of root CTs.

Table of Contents

List of Figures

Acknowledgments

Firstly, I would like to acknowledge my funding from the NSERC CREATE Program in Forests and Climate Change through the Centre for Forest Biology at the University of Victoria. This research grant enabled me to pursue my scientific curiosity in the most beautiful place in the world!

I would like to thank my supervisors, Dr. Peter Constabel and Dr. Barbara Hawkins, and committee members, Dr. Patrick von Aderkas and Dr. Doug Maynard, for their direction, guidance and encouragement throughout this MSc project. Your thoughtful and constructive feedback has helped me to become a better biologist. I am grateful to all of the technical and research staff for tirelessly teaching me a whole realm of new techniques and offering endless support throughout my research: Brad Binges, Heather Down, Brent Gowan, Dr. Lisheng Kong, Dr. Lynn Yip and Tieling Zhang. A special thanks to Samantha Robbins for offering her time and calmly mentoring me through the MIFE experiments – your friendship and support kept me (almost) sane and I will forever appreciate your patience and selflessness. To Dr. Carol Peterson from the University of Waterloo, I am honoured to have had the chance to discuss my work with you, thank you for your insightful suggestions for the project. To Dr. Robert Burke thank you for allowing me to use your microscope and for organizing the imaging equipment on my behalf. To David Ma, thank you for so generously allowing me to use your plants for the nitrogen manipulation analysis. Further thanks go to undergraduate students Katie Wiese and Sophie Deluca for assisting me with my research and to all the students and staff in Forest Biology, you have helped to make my time at UVic enjoyable. Thank you for your support both academically and personally throughout these two years.

Lastly, to my husband, Tom, who accompanied me on this adventure to the other side of the world, you are always a source of unwavering support and encouragement - thank you.

1 Literature Review: Exploring the Potential Ecological and Physiological Roles of Condensed Tannins in Roots

1.1 Introduction to Condensed Tannins

Condensed tannins or proanthocyanidins (herein referred to as CTs) are plant secondary metabolites that are widely known for their roles in plant defenses, soil nutrient cycling, and their many applications in human medicine and diet. CTs are large polymers of flavan-3-ols, predominantly catechin and epicatechin, and are end products of the flavonoid pathway (Tsai *et al.*, 2006). The flavonoids are characterised by their C_6-C_3-C_6 skeleton. CT polymers consist of flavan-3-ol monomers joined through C_4-C_8 bonds (Figure 1.1) that vary in stereochemistry and hydroxylation (Waterman and Mole, 1994). The high numbers of hydroxyls (OH) on the aromatic rings of the flavan-3-ol polymer give CTs their high binding properties. CTs are functionally defined by their ability to bind and precipitate protein, contributing to their anti-herbivore defense mechanisms (Constabel *et al.,* 2014). CTs have also been widely observed to chelate positively charged metal ions (Osawa *et al.,* 2011; Scalbert, 1991) which may provide plants with detoxification abilities. This metal chelating property of CTs is determined by the extent of phenyl (B) ring hydroxylation and polymer size (Yoneda and Nakatsubo, 1998). Lastly, CTs have anti-oxidant properties through hydrogen or electron donations to free radicals (Quideau *et al.,* 2011). These antioxidant properties of CTs contribute to the human health benefits that are associated with a high CT diet, such as reduced risk of age-related diseases (Quideau *et al.,* 2011).

CTs are distinct from another group of tannins, the hydrolysable tannins (HTs). Both HTs and CTs are derived from the flavonoid pathway and are defined through their protein precipitating ability. HTs, however, are more derived and are more structurally diverse than CTs (Quideau *et al.*, 2011). HTs are formed through the esterification of gallic acid and its large number of derivatives (>1000) leading to this high diversity (Quideau *et al.*, 2011; Waterman and Mole, 1994). The most basic form of HT polymer, pentagalloylglucose is shown in Figure 1.2.

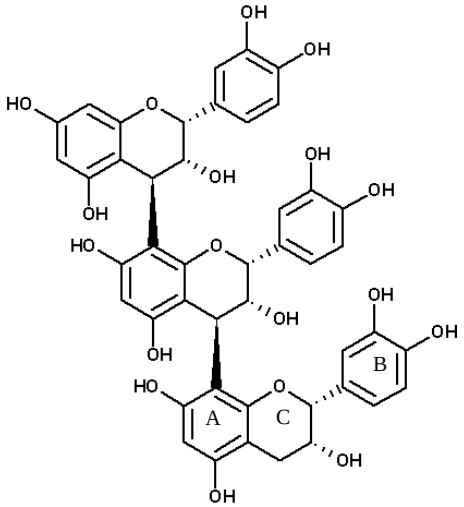

Figure 1.1 Generalised chemical structure of condensed tannins (adapted from Zifkin *et al.*, 2012).

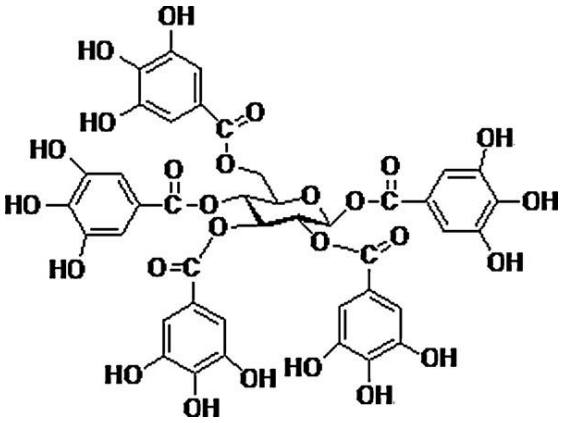

Figure 1.2 Chemical structure of the simplest hydrolysable tannin, pentagalloylglucose. (taken from Pei *et al.*, 2011)

Classed as secondary metabolites, CTs are not present in all plant species. Therefore there is high interspecies variation in CT-producing capacity. Specific genes that regulate CT synthesis have been identified in grapevine, *Populus* and many other species (Bogs *et al.*, 2007; Mellway *et al.*, 2009; Franklin, 2013). Factors that induce above-ground production of CTs have been studied. Herbivory, microbial attack and possibly UV-B are common causes of CT upregulation (Barbehenn and Constabel, 2011; Banso and Adayemo, 2007; Tegelberg and Julkunen-Titto, 2001). Ecological functions of CTs, through their inhibitory effects on nutrient cycling and ability to impact microbial communities, have also been observed (Schweitzer *et al.*, 2008).

CTs have been widely observed in the roots of plant species: from woody angiosperms to conifers to herbaceous plants (Kao *et al.*, 2002; McKenzie and Peterson, 1995a and 1995b; Stoutjesdijk *et al.*, 2001). Root cells are sloughed off into the soil through regular cell cycling. Therefore, species that produce root CTs are expected to contribute to total soil CT content and nutrient cycling. CT producing species can alter the nutrient contents of the soil and impact succession (Schimel *et al.*, 1998) potentially having wide ranging impacts on vegetative communities (Whitham *et al.*, 2006). However, little research attention has been given to the potential physiological roles of CTs within the roots of plants.

Presented here is a review of the current knowledge regarding three potential functional roles of root CTs, and identification of research priorities.

1) Defensive roles against below-ground pathogens and herbivores.

2) Adaptation for growth on heavy-metal soils (principally aluminum).

3) Facilitating nutrient uptake through cation binding.

1.2 Condensed Tannins and Defense

Feeny's (1968) landmark paper proposed that CTs can provide constitutive plant defense mechanisms against herbivores. The study uncovered the negative correlation between herbivore performance when feeding on high CT foliage: *Operophtera brumata* L. (winter moth) larval growth declined when feeding on high CT containing *Quercus* leaves (Feeny, 1968). Since this initial study, an increased accumulation of CTs following herbivore attack have also been frequently observed in *Populus*, suggesting that CT synthesis contributes to induced plant defenses (Osier and Lindroth, 2001; Peters and Constabel, 2002; Tsai *et al.*, 2006; Kosola *et al.*, 2006; Stevens *et al.*, 2014). The evidence to suggest that CTs are effective plant defense compounds has been largely correlative, i.e. an observed increase in CTs in response to herbivory, or reduced herbivore performance due to high CT diet. There have been three specific mechanisms proposed as to how CTs negatively impact herbivores: through reduced digestibility, feeding deterrence, or through toxic effects (Barbehenn and Constabel, 2011). Recent studies have endeavoured to further understand these mechanisms by which CTs act as defense compounds against herbivores.

1.2.1 Anti-digestive Properties of CTs

The initial hypothesis for anti-herbivore properties of CTs arises from their ability to bind proteins. This led to the idea that CTs bind enzymes and dietary protein in herbivores' digestive tracts inhibiting the breakdown of plant material and thus reducing growth and fitness of the herbivore (reviewed in Constabel *et al.,* 2014). Since Feeny's (1968) study, many other experiments have failed to replicate this negative correlation between high CT food sources and reduced growth and fitness of insects (Ayres *et al.,* 1997). Controlled experiments have also failed to show evidence for CTs reducing digestibility and growth in grasshoppers (Bernays, 1978) or in lepidopterans (Barbehenn *et al.,* 2009; Karowe, 1989; Boeckler *et al.,* 2014). Under high pH conditions (pH>9) hydroxyl groups on CT polymers ionise and protein binding is significantly reduced (Barbehenn and Constabel, 2011). Therefore, pH of the digestive tract may explain how CTs failed to act as anti-digestive compounds in some species. Studies concerned with the anti-herbivore effects of CTs have largely focused on lepidopteran species (Barbehenn *et al.,* 2009; Karowe, 1989; Boeckler *et al.,* 2014). Caterpillars have highly alkaline guts (pH 10) (Barbehenn *et al.,* 2009), and so it is likely that CTs are no longer able to bind to protein under these conditions. The lack of negative correlation between caterpillar growth and foliar CT concentration, suggests that CTs are not effective anti-herbivore mechanisms through reduced digestibility.

Vertebrates have acidic guts (Stevens and Hume, 2004) and there is evidence to suggest that CTs are effective anti-herbivore defense compounds that reduce digestibility. CTs within foliage bind dietary protein and can inhibit digestive enzymes at low pH. This reduces the assimilation of nitrogen by the animal and may cause nutrient limitation and

negative consequences on growth and fitness. A generalised negative correlation between high CT diets and decreased reproductive success of mammals has been observed (Wallis *et al.*, 2012), with specific case studies in ringtail possum (DeGabriel *et al.*, 2009), moose (McArt *et al.*, 2009) and beaver (Bailey *et al.*, 2004). One mechanism by which mammals have adapted to a high CT diet is by producing high levels of proline-rich salivary proteins, which bind with the CTs prior to ingestion and so reduce the amount of free CTs in the digestive tract (Mueller-Harvey, 2006).

1.2.2 Toxic Effects of CTs

Condensed tannins have been proven to have beneficial effects on mammalian health through their antioxidant properties. CTs donate a hydrogen atom or a single electron to quench harmful free radicals and prevent oxidative damage (Quideau *et al.*, 2011). At present, anti-oxidant effects have not been demonstrated in insect herbivores. The antioxidant properties of CTs are related to the pH of the herbivore's digestive tract. CTs can become harmful prooxidants at pH>9 which can lead to toxic effects (Barbehenn and Constabel, 2011). Toxic oxidative damage has been observed in non-adapted grasshoppers and lepidopterans feeding on leaves coated in tannic acid, specifically causing lesion formation in the midgut (Bernays *et al.*, 1980; Steinly and Berenbaum, 1985). Despite the antioxidant benefits of CTs, toxic effects from high CT diets have been observed in sheep and cattle causing stomach ulcerations (Mueller-Harvey, 2006).

1.2.3 Feeding Deterrent Properties of CTs.

The negative effects of CTs as anti-digestion and toxic agents have led to the proposition that CTs may function as a feeding deterrent. In addition, the protein binding and astringent properties of CTs are suggested to reduce palatability of high CT foliage (Schweitzer *et al.,* 2008). The evidence to support the idea that CTs are effective feeding deterrents is variable, and is dependent on species of both the herbivore and plant (Ayres *et al*., 1997). Feeding trials have been conducted using *Lymantria dispar* (gypsy moth caterpillar) and *Malacosoma disstria* (forest tent caterpillar) comparing food choice between wild-type (low-CT) and transgenic high-CT *Populus tremula* x *tremuloides* genotypes (Boeckler *et al.,* 2014; Mellway *et al.,* 2009). Both lepidopteran species consistently chose to feed on the transgenic high CT line, and caterpillar growth on the transgenics was enhanced compared to the wild-type control. This provides strong evidence that CTs were not an effective feeding deterrent in these studies. Engineering of the transgenic line resulted in elevated CT concentrations, but also caused shifts in the balance of other phenolics. Both lepidopterans preferentially chose to feed on the high CT transgenic line which had significantly higher CT concentrations but lower phenolic glycoside (PG) concentrations compared to the wild-type. This suggests that PGs may be a more effective feeding deterrent for lepidopterans rather than CTs. In mammals, CTs have been proven to be an effective feeding deterrent for some species but, again, this trend is not consistent, but species and plant specific (Marsh *et al.*, 2003).

1.2.4 Antimicrobial Properties of CTs

Other hypothesised defensive functions of CTs are based on their antibacterial and antifungal properties. Wounded leaves are often more susceptible to bacterial and

fungal infection, consequently the upregulation of CTs that is observed in poplar following herbivore attack may serve to protect wounded leaves (Peters and Constabel, 2002). CTs have low minimum inhibitory concentrations against bacteria including *Staphylococcus aureus* and *Escherichia coli* (Banso and Adeyemo, 2007). CTs are potent inhibitors of bacterial growth as they can bind to bacterial cell walls and consequently disrupt cellular integrity (Smith *et al.*, 2005). A significant negative relationship between CT concentration and success of fungal endophyte infection is also recorded (Bailey *et al.*, 2011; Nichols-Orion, 1991). CTs may inhibit fungal colonisation by crosslinking and inactivating enzymes and cell wall proteins (Scalbert, 1991). The metal chelating properties of CTs also cause formation of CT-metal complexes that limit available metal ions (chiefly Fe^{3+}) which are essential for fungal growth (Treutter, 2006; Scalbert, 1991). This metal precipitate may also have a secondary function in acting as a physical barrier around the root to prevent fungal colonisation (Treutter, 2006).

1.2.5 Functions of Root CTs in Defense

Root-feeding herbivores have been found to significantly reduce annual net primary productivity in a variety of plant biomes (Hunter, 2001). Damage to roots also increases the chance of fungal and bacterial infection by orders of magnitude compared to undamaged roots (Hunter, 2001). A review by Rasmann and Agrawal (2008) concluded that the diversity of below-ground herbivores is lower than that of above-ground herbivores but their impacts on plant growth and health appear to be equal. Despite this finding, few studies have looked at the roles of root CTs as below-ground defense compounds.

The distribution of root CTs throughout the plant kingdom has not been thoroughly investigated, but is believed to be similar to that of foliar CTs which are present in the majority of temperate woody species (Smolander *et al.*, 2012). Kaplan *et al.* (2008) is one of the few studies that have investigated the division of above- and below-ground chemical defenses (secondary metabolites) through herbivore manipulation experiments. In *Nicotiana tabacum* foliar herbivory induced significant increases in secondary metabolite production (not specifically CTs) in leaves, but not in roots. By contrast, root herbivory by nematodes elicited a whole plant response, with elevated secondary metabolite production in both roots and leaves (Kaplan *et al.*, 2008). This experiment provides evidence that below-ground herbivory may be especially costly to plants.

CTs have been found to be effective anti-digestive compounds in vertebrate herbivores (Wallis *et al.*, 2012; DeGabriel *et al.*, 2009; McArt *et al.*, 2009; Bailey *et al.*, 2004). Although, vertebrates are not often considered to be root eaters, many animals gain a significant proportion of their diet from roots and rhizomes. This is particularly true over-winter in deciduous biomes. For example, pocket-gophers are significant herbivores on *Populus tremuloides* roots causing a 23 % reduction in below-ground biomass of the Utah aspen forests (Stevens *et al.*, 2014). To date, no vertebrate feeding trials have been conducted comparing high and low CT roots. Transgenic *Populus* will be a key resource in addressing this question further as these allow direct comparisons to be drawn between high and low CT genotypes of the same species.

The studies of CTs as effective plant defense compounds have yielded variable outcomes, and functional correlations are typically specific to the particular herbivore-plant food source. However, in some cases, for example ringtail possums feeding on high CT *Eucalyptus*, CTs clearly provide an important anti-herbivore defense mechanism (DeGabriel *et al.*, 2009). Furthermore, in poplar, CTs are induced following damage by herbivores (Peters and Constabel, 2002). This could be a plant defensive response, perhaps due to increased vulnerability to infection by fungal and microbial pathogens following herbivore-induced wounding. CTs have been shown to have the potential to be effective defenses mechanisms against fungal and microbial pathogens (Banso and Adeyemo, 2007; Bailey *et al.*, 2011). Therefore, the inducible nature of CTs in *Populus* is consistent with the idea that CTs may play a role in anti-pathogen defense rather that anti-herbivore defense.

1.3 Condensed Tannins and Metal Toxicity

Global degradation of soils through intensive agriculture, drainage and land development have caused decreases in soil pH. Acidic soils (pH <5.0) high in charged aluminum (Al^{3+}) are common in tropical areas with high levels of weathering. Presence of toxic metals (Al, Fe) are also becoming more common in areas inhabited by plants not adapted to these conditions (Lynch and St Clair, 2004). Soil acidity, which is coupled to the presence of heavy metal cations, is a major constraint on crop productivity, as root elongation can be inhibited, thus reducing the plant's capacity for water and nutrient absorption (Barceló and Porschenreider, 2002). Understanding the mechanisms of plant adaptation to acidic soils enriched in heavy metals could provide interesting applications

to forestry and agronomy. To this end, an adaptive role of CTs has been proposed by which CTs chelate heavy metals cations and minimise the toxic effects to the plant.

1.3.1 Metal Chelating Properties of CTs

The presence of two or more hydroxyl groups on the phenyl (B) ring of CTs enables chelation (Quideau *et al.*, 2011). This binding potential is greater under acidic conditions (Waterman and Mole, 1994). In general, the binding of CTs to heavy metals reduces their toxicity in the soils. There is evidence to suggest this mechanism of CT chelation of highly toxic Al^{3+} is more effective in detoxifying Al^{3+} rich soils than the secretion of anions, for example citrate, malate and oxalate (Osawa *et al.*, 2011). These root exudates can be rapidly decomposed by soil microbes (Jones *et al.*, 1996). By contrast, CTs appear to be a longer lasting tolerance mechanism to Al^{3+} rich soils.

1.3.2 Functions of Root CTs in Heavy Metal Soils

Osawa *et al.* (2011) demonstrated the ability of root CTs to minimise the negative effects of Al^{3+} on root growth. Their study compared growth of a CT producing species *Cinnamomum camphora* (camphor tree) with non-CT producing *Glycine max* (soybean) on differing levels of Al in soils. *Cinnamomum camphora* was highly resistant to high levels of Al^{3+} (500µM), exhibiting a more than 20-fold higher tolerance than that of *G. max.* Tolerance was correlated with increased synthesis of CT containing cells on the surface of the root elongation zone. Despite *G. max* exuding up to six times higher volume of citrate than *C. camphora*, the high Al^{3+} levels prompted the onset of dormancy in the roots of *G. max*, with no observed root elongation and no active

absorptive surface. Osawa *et al.* (2011) also showed that in *C. camphora*, the rate and distance from the root tip at which the CT cells were detached from the root was greater under high Al conditions compared to the control. The Al-CT rich cells become detached, thus preventing accumulation of Al^{3+} in the newly expanding epidermal tissue. This constant turnover of CT cells were proposed to divert the toxic effects of Al^{3+} away from the epidermal cells, and epidermal expansion was not negatively impacted under the high Al^{3+} condition. An additional flavon-3-ol bioassay study (Osawa *et al.*, 2011) showed that the exogenous co-application of CT monomers (catechin and epigallocatechin) from *Camellia sinensis* (tea) with Al^{3+} reduced the accumulation of Al^{3+} by *G. max*. CTs bound to Al^{3+} within the solution, suggesting that CTs can complex Al^{3+} both within cells and in the environment.

Although CTs can provide a physiological adaptation to heavy metal soils through chelation of metal cations, there appear to be differences in CT localization between plant species that causes differences in detoxification mechanisms. Osawa *et al.* (2011) showed that CTs reduce the toxic effects of Al^{3+} in *C. camphora* through continual proliferation of CT containing cells that bind with Al^{3+} in the cytosol. The Al-CT rich cells become detached to prevent accumulation of Al^{3+} in the newly expanding epidermal tissue. In *C. sinensis*, however, free Al^{3+} ions were transported to foliage where they became bound to leaf CTs and catechin monomers. Leaf CTs have been directly attributed to the high Al tolerance exhibited by *C. sinensis* (Nagata *et al.*, 1992). In the roots of *Lotus pedunculatus* (bird's foot trefoil) a significant correlation was found between CT presence and Al accumulation within the vacuoles of the inner cortical cells, suggesting that CTs are performing a detoxifying role by removing Al from the cytoplasm

(Stoutjesdijk *et al.*, 2001). This CT accumulation was observed towards the root apex (within 1-2mm), a zone in which nutrient uptake occurs. No Al-CT complexes were detected farther than 8mm from the root tip, at which point cork was deposited and cortical cells were being lost. Cork forms a suberized protective layer in the mature parts of the roots; subsequently, this root zone is no longer capable of nutrient absorption. At high Al concentration (60 μM), deposition of cork occurred closer to the apex than at lower Al concentrations. This was thought to minimise Al uptake by reducing the area of absorptive surface, which suggests that while CTs aided growth on Al-rich soils the mechanism does not confer complete tolerance as root growth and development is still negatively impacted under high Al concentrations.

The hydrolysable tannin (HT), oenothein B, in the roots of *Eucalyptus camaladulensis* provides a similar mechanism for Al tolerance (Tahara *et al.*, 2014). *Eucalyptus camaladulensis* has the capability to grow on soil with a pH <3.5, with Al concentration in the mM range, and can accumulate up to 11 mg Al g^{-1} dry weight in root tissue (Tahara *et al.*, 2014). Oenothein B can chelate a minimum of four Al ions by the free hydroxyl groups on the HT polymer. Such binding was confirmed by the formation of a white precipitate when Al was combined in solution with oenothein B (Tahara *et al.*, 2014). Al intolerant species, which were incapable of growth and root elongation under the high Al condition, were also screened and no oenothein B was found in their root tissue, further supporting its suggested role as a defensive response against toxic metal concentrations (Tahara *et al.*, 2014). Oenothein B is not an Al specific binding agent, but does preferentially bind Al when multiple metals are present (Tahara *et al.*, 2014). This

leads to the supposition that there may be other secondary defensive compounds that bind to other metal cations.

In summary, there is clear evidence that both HTs and CTs reduce toxic effects of Al^{3+} to plants through chelation. The detoxifying role of CTs on other heavy metal ions is not as well studied. However, there is evidence to suggest that root tannins bind to Fe^{3+} in mangrove roots (Kimura and Wada, 1989). Mangroves are able to tolerate highly acidic environments which are high in Fe^{3+}. Blackening of living roots was observed in the mangroves with increased biomass, compared to those trees lacking blackened roots. This led to the discovery that tannins were binding Fe^{3+} which resulted in black ferric pigment, and provided mangroves with an effective Fe^{3+} tolerance mechanism. To my knowledge, this relationship between Fe^{3+} and root tannins in the context of Fe^{3+} toxicity has not been investigated further or been observed in other species.

1.4 Condensed Tannins and Nutrients

1.4.1 Soil Nutrient Cycling and CTs

The ecological roles of soil tannins (both CTs and HTs) on soil nutrient availability and microbial communities have been the focus of much tannin research. Tannins have the ability to alter access to soil nutrients and consequently impact plant communities (Schweitzer *et al.,* 2008; Castells *et al.,* 2005; Kraus *et al.,* 2003). Soil tannin content is typically negatively correlated to the rates of organic matter decomposition and nitrogen mineralization (Kraus *et al.,* 2003). CTs bind to amine groups (NH_2) of organic nitrogen compounds and form large inorganic complexes of low

solubility and that are resistant to decomposition (Castells *et al.*, 2005). These large nitrogen complexes can reduce nitrogen losses through leaching (Schweitzer *et al.*, 2008), and also reduce the amount of nitrogen lost to microbes. This can enhance organic nitrogen availability to mycorrhizal plants (Kraus *et al.*, 2003). CTs can further immobilize soil nitrogen by inhibiting and altering microbial communities which compete with plants for nitrogen. CTs may also be directly toxic to microbes through oxidative damage (Scalbert, 1991). CTs also readily bind with Fe^{3+} within the soil and limit availability for microbial growth (Scalbert, 1991). Direct binding of CTs to microbial enzymes can inactivate them and thus inhibit decomposition (Scalbert, 1991). Interestingly, some microbes have adapted to high tannin soils, for example via secretion of tannin-binding polymers and production of tannin resistant enzymes (Scalbert, 1991; Kraus *et al.*, 2003). Diversity in microbial tolerance to high tannin soils may partly explain the shifts in microbial communities in soils of differing tannin content.

The large insoluble nitrogen complexes resulting from high tannin content in soils, also reduce the conversion of organic nitrogen to plant-available inorganic nitrogen forms (NH_4^+ and NO_3^-).This suggests that high soil CTs could have negative consequences for plant growth. High CT leaf litter produced from *Populus balsamifera* (balsam poplar), however, provided a mechanism which enabled it to outcompete *Alnus rubra* (red alder) (Schimel *et al.*, 1998). In this situation, the high CT leaf litter reduced the ability of *A. rubra* to fix atmospheric N_2 (Schimel *et al.*, 1998) as well as limited inorganic nitrogen availability in the soil. *Alnus rubra* has higher nitrogen requirements than *P. balsamifera* for growth, therefore, increases in soil CTs induced by *P.*

balsamifera leaf litter reduced the amount of plant available nitrogen and allowed *P. balsamifera* to dominate over the competitor species (Schimel *et al.,* 1998). This study provides evidence for the importance of CTs in regulating edaphic environments and vegetation succession.

1.4.2 Nutrient Availability and CT Synthesis

The growth differentiation balance hypothesis (GDBH) (Herms and Mattson, 1992) states that under low nitrogen availability, plants will invest more in carbon-based defenses than in growth. In the case of phenolics, this relationship has been supported by a number of studies (Stout *et al.*, 1998; Glynn *et al.*, 2007; Gebauer *et al.*, 1998). Low levels of soil nitrogen have resulted in increased CT concentrations in leaves of *Populus tremuloides* (quaking aspen), *Pinus taeda* (loblolly pine) and apple cultivars (Osier and Lindroth, 2001; Gebauer *et al.*, 1998; Leser and Treutter, 2005), although it is not always clear that this increases their resistance to herbivory.

The impact of nitrogen depletion on secondary metabolite production has been particularly well studied in *Populus* in both leaves and roots. Experiments that have investigated this relationship, however, have often been studied in combination with genotype and defoliation effects (Osier and Lindroth, 2001; Kosola *et al.*, 2006; Stevens *et al.*, 2014). The increase in CT synthesis was most pronounced under low nutrients and high defoliation conditions, yet, in isolation, nutrients elicited a greater response than defoliation or genotype alone (Kosola *et al.*, 2006). The upregulation of CTs under low nitrogen has been reported for roots as well as leaves in *Populus* x *canadensis* “Eugenii”

and *P. tremuloides* (Kosola *et al.*, 2006; Stevens *et al.*, 2014). In *Populus tremuloides* the CT concentration was increased by 47 % under low nutrient conditions. This response was attributed primarily to low nitrogen availability in the low nutrient condition, rather than phosphorus or potassium limitation (Stevens *et al.*, 2014).

The GDBH was not supported in other studies, for example in *Populus deltoides* (Kosola *et al.*, 2004). A negative correlation between relative growth rate and root CT concentration was only observed in one out of the three field sites. CT synthesis did not correlate with extractable soil nitrogen. In addition, a single study using *P. tremuloides* found that CT concentration in leaves was more closely correlated with light intensity than nitrogen availability (Osier and Lindroth, 2006). This suggests that growth rate and defense are not always closely correlated and that other environmental factors may influence CT synthesis more than nitrogen availability.

In *Pseudotsuga menziesii,* potassium levels seemed to affect CT content more than nitrogen, with an increased proportion of CTs produced under low potassium regardless of nitrogen availability (Shaw *et al.*, 1998). However, the absolute quantity of total CTs was not reported, only given as a percentage of total C-derived compounds. It was difficult, therefore, to assess the impact of nutrient concentrations on total CT production and whether it was up or down regulated under nutrient deficient conditions in this species (Shaw *et al.*, 1998).

1.4.3 Functions of Root CTs in Nutrient Uptake

It is clear that CTs, from both root and foliar inputs, have a role in regulating the nitrogen cycle (Kraus *et al.,* 2003). Root CT concentrations are also observed to occur at higher concentrations when nitrogen is limiting (Stevens *et al.,* 2014; Kosola *et al.,* 2006). However it is not understood whether CTs are upregulated as an adaptive advantage to the plant itself, i.e. to enhance defense, or whether it is a consequence arising from an excess of carbon while nitrogen is limiting. Potential roles of CTs as plant defense compounds against herbivores, microbes and heavy metals have already been discussed. Non-defensive functions of root CTs, however, have been given little consideration in the literature.

As described earlier, there is strong evidence that CTs bind positively charged metal ions (Al^{3+} and Fe^{2+}) in soils (Osawa *et al.,* 2011; Treutter, 2006: Kimura and Wada, 1989). CTs have also been reported to bind and store Ca^{2+} in the vacuoles of *Mimosa pudica* and *Albizzia julibrissin* that exhibit nyctinasty (Hollins and Jaffe, 1997). In these plants Ca^{2+} is required in specific cells of the pulvini to initiate leaf movement by depolarising the cells and opening K^{+} channels (Visnovitz *et al.,* 2007). This movement of K^{+} alters turgidity of the pulvini and causes leave folding and opening. The release and reabsorption of Ca^{2+} from the vacuoles is crucial in controlling this chain of events, demonstrated by the lack of nyctinasity if Ca^{2+} channels are inhibited by Erythrosin B (Turnquist *et al.,* 1993: Hollins and Jaffe, 1997). The pulvini cells are physiologically distinct from other leaf cells due to the presence of CT-filled vacuoles. CTs were directly implicated in the absorption and release of Ca^{2+} from the vacuoles. The precise

mechanism of how CTs release the Ca^{2+} once bound is not described by the authors (Hollins and Jaffe, 1997; Visnovitz *et al.,* 2007). However these studies suggest that vacuoles of *Mimosa pudica* and *Albizzia julibrissin* pulvini have a mechanism to release CT bound Ca^{2+} upon stimulation.

The studies described above collectively suggest that CTs bind positively charged ions and metals. This has led to speculation that CTs act as a mechanism to bind and store nutrient cations in the root cells. The binding and storing of nutrient cations within CT containing vacuoles could maintain an ion gradient across the cell, thereby facilitating greater rates of cation uptake in plants with high CT concentrations within the vacuoles.

1.5 Research Objectives

This literature review has outlined three potential roles of root CTs. The ecological effects of CTs include their negative impact on soil decomposition and effects on microbial communities, and in herbivore and pathogen defenses. Physiological functions of root CTs include the detoxification of heavy metals via chelation, and a proposed effect on nutrient ion uptake.

This MSc project aims to investigate whether CTs have a physiological role in nutrient uptake. My study will focus exclusively on *Populus* using two aspen hybrids: *P. tremula* x *alba* and *P. tremula* x *tremuloides.* The research will build on previous studies that have investigated the correlation between nutrient availability and CT synthesis in *Populus* (Osier and Lindroth, 2001; Kosola *et al,* 2004 and 2006; Stevens *et al.,* 2014). In

addition, the results aim to provide new information regarding physiological roles of CTs in *Populus* roots. The availability of transgenic *Populus* lines with manipulated CT levels (Mellway *et al.,* 2009; Franklin, 2013; Yoshida *et al.,* 2015) will be extremely useful for comparative studies. These transgenics will avoid inter-species differences in physiology and allow comparison of poplar lines differing only in CT concentration.

Establishing the precise location of root CTs at a tissue and cellular level is critical for inferring possible functions of CTs. Nutrient absorption occurs in the young, unsuberized zone of the roots (Hishi, 2007) and thus CTs would be expected to accumulate in this zone if they were to play a role in modulating or facilitating nutrient fluxes. However, there are conflicting reports on root CT localization. In *Pinus* CTs were present in the older, less absorptive portion of the root (McKenzie and Peterson 1995a and 1995b). In *Populus* and rosaceous species, however, CTs have been observed to accumulate closest to the root tip (Kao *et al.,* 2002; Hoffmann *et al.,* 2012).This is consistent with the hypothesis that CTs impact nutrient uptake. Chapter 2 will focus on verifying and extending the previously observed location of root CT in *Populus* (Kao *et al.,* 2002). Both histochemical staining and quantitative assay methods will be used to achieve this.

Chapter 3 will focus on analysing correlations between root CTs and nutrients. The differences in CT concentrations under a range of nitrogen treatments will be analysed to further clarify the link between nitrogen and CT synthesis. An increase in root CT concentration with limiting nitrogen has previously been observed in *Populus* though in

different experimental contexts, i.e. in combination with defoliation and genotype (Kosola *et al.,* 2006; Stevens *et al.,* 2014). The effect of nitrogen availability on CT concentration in roots has not previously been investigated as a single experimental variable.

I will use the information gained on CT localization in wild-type (low CT) and transgenic high-CT *P. tremula* x *alba* to assess the spatial correlation between nutrient ion fluxes and CT concentration. Nutrient flux data will be generated by the Microelectrode Ion Flux Measurement (MIFE^{TM}) technique, which records nutrient fluxes at discreet locations along the root. I will analyse fluxes of NO_3^-, NH_4^+ and Ca^{2+} and compare them to CT concentrations at corresponding root positions. From this I will be able to directly address the question: do root CTs have a physiological role in modulating or facilitating nutrient uptake in *Populus*?

The specific research objectives of this study are to:

1) Establish the precise location of CTs within *Populus* roots using histochemical staining and quantitative assay methods (Chapter 1).
2) Test if soil nitrogen availability affects root CT concentrations (Chapter 2).
3) Compare the patterns of net fluxes of nitrogen (NO_3^-, NH_4^+) and calcium (Ca^{2+}) with the distribution of CTs in roots, using wild-type and high CT genotypes of *P. tremula* x *alba* (Chapter 2).

2 Localization of Condensed Tannins in Roots of Hybrid Aspen (*Populus tremula* x *alba*)

2.1 Introduction

The genus *Populus* contains over forty species and incorporates the aspens, cottonwoods and poplars (collectively referred to as poplars) (Farmer, 1996). Their wide distribution across both climatic and edaphic gradients has led to species differentiation into riparian and 'dry-land' specialists, and also into generalists that exhibit wide habitat tolerance (Farmer, 1996). In addition, their capacity for vegetative propagation has facilitated their rapid spread across landscapes. In experimental settings, poplars have become the genomic model for woody plant species following complete genome sequencing of *Populus trichocarpa* (Tuskan *et al.*, 2006).

The availability of the *P. trichocarpa* genome has led to the complete characterisation of the flavonoid pathway in *Populus* (Tsai *et al.*, 2006) and subsequent identification of the genetic mechanisms that regulate CT synthesis (discussed in Chapter 3) (Mellway *et al.*, 2009; Franklin, 2013; Yoshida *et al.*, 2015). In *Populus*, leaf CTs are induced following environmental stress and can accumulate to levels up to 25 % of leaf dry weight (Hwang and Lindroth, 1997). The inducible nature of CTs enables the plant to adjust synthesis in response to resource availability and stress (Tsai *et al.*, 2006). The high levels of inducible CTs and detailed knowledge of their regulation make *Populus* an excellent system to study functional properties of CTs.

There are many studies that have investigated the functions of foliar CTs, typically in relation to their protein binding and anti-oxidative properties. As outlined in Chapter 1, proposed functional roles of foliar CTs include: defense against herbivores (Barbehenn and Constabel, 2011) and microbial pathogens (Scalbert, 1991), and possible protection against UV-B rays due to their anti-oxidant properties (Tegelberg and Julkunen-Titto, 2001). Functions of root CTs have been given far less consideration than foliar CTs. Three potential roles of root CTs were outlined in Chapter 1. This thesis will focus on establishing CT localization in *Populus* roots and whether they have a role in modulating or facilitating nutrient uptake.

Work described in this chapter is conducted exclusively on the hybrid aspen, *Populus tremula* x *alba* (syn. *Populus canescens* (grey poplar)). *Populus tremula* (European aspen) occupies a large area across the northern portion of Europe and is adapted to short photoperiods, nutrient poor soils and cold temperatures that are characteristic of high latitudes (>50 ^{o}N) (Farmer, 1996). *Populus alba* (white poplar) is native to central and southern Europe and northern Africa, but has been widely planted as an ornamental tree in the US and Canada since the 18th century. It has now escaped into wild forests in large zones of the eastern USA (Gucker, 2010; USDA NRCS, 2015). In its native habitat, *P. alba* is a generalist poplar inhabiting diverse terrain: from dry disturbed land, to forest-steppe and floodplain woodlands. The hybrid *P. tremula* x *alba*, although non-native, is the most widespread of all poplar hybrids and is grown in all states and provinces east of Ontario due to its wide tolerance to a range of environmental conditions (Gucker, 2010; USDA NRCS, 2015).

The roots of *Populus* have been less extensively studied than the above-ground organs (Pregitzer and Friend, 1996). Poplars have fine roots and rapidly branching lateral roots (up to seven orders of branching have been recorded). Growth is rapid and roots can extend up to 10 mm day^{-1} under fertile and high moisture conditions (Pregitzer *et al.*, 1995). In young poplars, shoot growth has proven to be a good indicator of root growth (Heilman *et al.,* 1994). Nevertheless, many physiological and structural features of poplar roots are not well investigated and little is known about the branch architecture of the root systems as the tree matures (Pregitzer and Friend, 1996).

Roots are defined by generalized anatomical and developmental zones, the meristematic, elongation and maturation zones. These zones are not sharply delimited but transition gradually. Differences in local soil environments, both within and between individual trees, control the spatial development of these zones and the distances that they occur along the root. This causes root development to be very dynamic. Anatomical descriptions are, therefore, typically used to distinguish between root zones rather than predefined distances from root tip.

The meristematic zone consists of a high density of undifferentiated cells undergoing cell division. It is protected by specialized border and root cap parenchyma cells, which are covered with a pectin-like secretion which lubricates the surface of the root and aids its path through the soil. Turnover of the root cap is continuous with the outer cells being sloughed off as they become damaged and as new root cap cells are added from the meristem (Gallagher, 2013). Directly adjacent to the meristematic zone is the elongation zone, which is the very short zone (only a few mm) responsible for root

growth. Therefore the meristematic zone and root cap are the only regions that are actually being pushed through the soil, and so are most likely to incur mechanical damage. Cells differentiate in the zone of maturation into discrete dermal, ground and vascular tissue systems. The latter is enclosed by an endodermis and sealed by suberized Casparian bands that are deposited in anticlinal walls. The Casparian bands, and subsequent development of suberin lamellae inside the primary cell walls, prevent both water and solute loss, while maintaining conduction pressure through the vascular cylinder (Peterson and Enstone, 1996; Meyer and Peterson, 2013). Passage cells are endodermal cells that have not yet become enclosed by suberin lamellae and function to allow the transport of water and ions into the vascular cylinder through the symplast. The number of passage cells decreases with distance from the root tip. The distance that they occur from the root tip is variable as it is strongly determined by environmental conditions, particularly in relation to nutrient and water availability (Meyer and Peterson, 2013). The maturation zone is also identified by the presence of root hairs, which are extensions of the epidermal cell surface.

The oldest zone of the root, which terminates at the root-stem interface, has been termed the cork zone (Peterson *et al.,* 1999). This cork zone is defined by extensive secondary xylem and formation of a thick, outer periderm layer that functions to protect the root following cortical breakdown (Peterson *et al.,* 1999). There is no uniform description for the zone occurring between the maturation zone and the cork zone. In this zone, the root diameter first decreases compared to the zone of maturation as the cortex is sloughed off but periderm has not yet formed (Mckenzie and Peterson, 1995a and 1995b). Pigmentation has been a central factor in describing this zone but the cause of the

brown colouration is not well understood or investigated. It has been loosely correlated with root dormancy, cortical breakdown, periderm formation and CT deposition (McKenzie and Peterson, 1995a).

This chapter is concerned with establishing the localization of CTs and their correlation to pigmentation in *P. tremula* x *alba* roots. Reports of CT localization in roots suggest this varies with plant species with root cap localization in *Populus* and *Rosaceae* (Kao *et al.*, 2002; Hoffmann *et al.*, 2012), brown root localization in *Pinus* and *Eucalyptus* (McKenzie and Peterson, 1995a), or complete absence of root CTs (despite being present in stem and leaf tissues) in *Onobrychis viciifolia* Scop. (sainfoin) (Lees *et al.*, 1993). In *Pinus* and *Eucalyptus*, McKenzie and Peterson (1995a) demonstrated that it was the visibly brown zones, occurring >2 cm from root tip and prior to the cork zone, that stained positively for CTs using the flavonoid stain, vanillin-HCl, and other less commonly used stains, ferrous sulphate and dimethoxybenzaldehyde (DMB). In this zone the staining intensity increased with distance from root tip, whereas the white zone only stained very faintly for CTs. Subsequently, they named this macroscopically brown zone the ‘condensed tannin zone’ (Peterson *et al.*, 1999). This so-called CT zone was characterised by a dying cortex, although water and ion uptake into the vascular cylinder was still possible due to the presence of passage cells in the endodermis in the younger region of this zone. The macroscopic brown pigmentation in this zone was attributed to CTs that were visualised in vacuoles in the younger region of the CT zone, and to the deposition and oxidation of CTs into the cells walls of the dying cortical cells (McKenzie and Peterson, 1995a). Brown pigmentation in the CT zone was not correlated with lignin or suberin, which were also histochemically visualized using phloroglucinol and

berberine hemisulfate, respectively (McKenzie and Peterson, 1995a). In the cork zone, however, the brown colour observed was attributed in part to CTs but also to lignin and suberin deposition within the cork tissue (McKenzie and Peterson, 1995b).

McKenzie and Peterson (1995a and 1995b) used vanillin-HCl histochemical staining for CT localization. It is not an entirely CT specific stain but can also detect all flavan derivatives (Li *et al.*, 1996). Therefore brown pigmented cells in the CT zone that stained positively for CTs by vanillin-HCl may not exclusively have been due to CTs, but perhaps to other flavonoids that were also becoming complexed in cell walls. The lack of vanillin-HCl staining in the white zone strongly indicates that flavonoids (including CTs) are not present in this zone of *Pinus* and *Eucalyptus*. Brown pigmentation in mature *Arabidopsis* seed coats has also been attributed to the oxidation of CTs and other flavonoids (Lepiniec *et al.*, 2006), further supporting this link between CTs and brown pigmentation.

The presence of CTs, however, has not always been found to be correlated with brown pigmentation in roots. In *Populus tremuloides*, *Fragaria* x *ananassa* and *Malus* x *domestica*, CT- specific histochemical staining (4-dimethylaminocinnamaldehyde) detected CTs in the white zone; specifically in the root cap, as well as cortical and epidermal cells within 2 mm of the root tip (Kao *et al.*, 2002; Hoffmann *et al.*, 2012). This difference in CT localization and correlation with pigmentation between these angiosperms and *Pinus* (McKenzie and Peterson 1995a and 1995b) could be explained by differences between genera, but also provides evidence to suggest that CT containing

tissues are not always brown, despite this being a common assumption (McKenzie and Peterson, 1995a; Lepiniec *et al.,* 2006).

The occurrence of CTs in the white zone of the roots is further supported by molecular evidence. Hoffmann *et al.* (2012) showed that CT polymers and flavan-3-ols monomers were present along with seven flavonoid genes responsible for flavan-3-ol synthesis in the root cap of *Fragaria* x *ananassa* and *Malus* x *domestica*. Although *Arabidopsis* does not produce CTs in roots, it has been reported to synthesize other flavonoids e.g. kaempferol and quercetin, in the root cap and not in the older root zones (Saslowsky and Winkel-Shirley, 2001). Flavonoid regulating enzymes were expressed at high levels in the root cap, epidermal and cortical cells of the elongation zone, compared to the rest of the root. This provides molecular evidence for flavonoid synthesis occurring in these regions.

The aim of this chapter is to investigate the relationship between CT distributions and root pigmentation in *Populus*. Using histochemical staining and a quantitative assay, this study will seek to establish CT localization and investigate CT concentrations in specific root zones of *P. tremula* x *alba*.

2.2 Materials and Methods

2.2.1 Plant Material and Growth Conditions

Wild-type *Populus tremula* x *alba* (717) plants were propagated from ~1 cm cuttings of *in-vitro* plantlets and grown in half-strength Murashige-Skoog (Caisson

Laboratories, Inc. Cat # MSP0501) medium supplemented with 0.5 µM indole-3-butyric acid (IBA). Plants were grown in sterilized Magenta boxes for a minimum of eight weeks and until significant shoot and root growth had occurred, i.e. plants were approximately 8 cm in height. Plants were then transplanted into small seedling pots containing vermiculite, covered, and placed in a mist-chamber to acclimate for three weeks. They were then repotted into vermiculite-filled, one gallon round pots and moved into the greenhouse. For histochemical analysis, plants were fertilized with 100 mL of 100 ppm nitrogen, phosphorus and potassium using general purpose 20-20-20 Plant Prod® NPK fertilizer (Plant Products Co. Ltd, Brampton, ON, Canada) three times per week for eight weeks, before harvesting. Plants were supplemented with equal volumes of distilled H_2O (dH_2O) as required to prevent desiccation. Thrips (Order: *Thysonoptera*) were controlled through daily removal by hand.

For CT quantitative analysis, plants were fertilised three times per week with a modified Long Ashton's solution optimised for poplar growth (Luo *et al.*, 2013a) (1 mM NH_4NO_3, 0.9 mM $CaSO_4 + 2H_2O$, 0.6 mM KH_2PO_4, 0.5 mM KCl, 0.04 mM K_2PO_4, 0.3 mM $MgCl_2 + 7\ H_2O$ and 0.03 g L^{-1} standard micronutrient mix (Plant Products Co. Ltd, Brampton, ON, Canada), pH 5.6). Planting procedures, growth substrate and pot size were kept identical to the methods described above.

2.2.2 Histochemical Analysis

Upon harvesting after eight weeks of growth, roots were cut into 1 cm sequential segments sequentially beginning at the root tip. Samples were immediately fixed at room temperature in modified Karnovsky's fixative (25 % glutaraldehyde and 16 %

paraformaldehyde in 0.5 mM sodium phosphate buffer (PBS), pH 7.4). Samples were stored in fixative at 4 ^{o}C for up to four weeks before embedding. Samples were then rinsed three times for 30 minutes each with 0.5 mM PBS, pH 7.4, and dehydrated in sequential ethanol rinses (30 %, 50 %, 70 %, 95 %, and 100 %) over the course of one day. Throughout the following week, plants were infiltrated with increasing concentrations of Technovit® 7100 Glyco Methycrylite (Electron Microscopy Sciences: RT 14653) in 100 % ethanol (Appendix 1), before being cured.

Longitudinal sections (5 µm) were cut using a glass blade microtome (Sorval JB-4). Sections were dried onto slides and stained with the CT specific stain, 0. 1 % 4-dimethylaminocinnamaldehyde (4-DMACA) (w/v) in 0.5 M sulphuric acid in 1-butanol according to the method of Gutmann and Feucht (1991). The slides were covered in 1 mL of stain solution and heated on a Thermolyne Type 1000 hot plate (setting 2.5) for two minutes or until the stain began to evaporate and discolour. The slides were removed from the heat prior to bubbling occurring in the resin. Staining was first attempted using 0.1 % 4-DMACA in 6 N HCl: ethanol (Abeynayake *et al.*, 2011) but this method dissolved and wrinkled the Technovit® resin. Slides were then rinsed three times in 1-butanol for 30 seconds at a time (or until all unbound stain was removed), and cover slips were then secured with Permount^{TM} mounting medium. Sections were imaged within 24 hours on a transmitted light microscope (Zeiss [47-30-12-9902], West Germany) fitted with SPOT RTKE diagnostic 7.2 Colour Mosaic camera. A deep burgundy stain indicated the presence of CTs, consistent with other reports of 4-DMACA stained CTs in

embedded samples hydrolysed by hot sulphuric acid (Abeynayake *et al.*, 2011; Gutmann, 1993).

Freehand cross sections were stained using a custom-made section holder (Brundrett *et al.*, 1988), and submerged in 0.1 % 4-DMACA (w/v) in 0.5 M sulphuric acid:1-butanol for two minutes, washed several times in 1-butanol until all unbound stain was rinsed off, and covered. Whole root specimens were submerged in a reduced concentration of stain (0.01 % 4-DMACA in 2 N HCl:EtOH), rinsed in 70 % ethanol and then kept in dH_2O to prevent desiccation. Roots were imaged within five minutes of staining under a dissecting scope (Wild Macroskop M420, Heerbrugg, Switzerland) fitted with a camera (SPOT Flex 543345, Germany). CTs stained a vibrant blue in fresh sections. The reliability of 4-DMACA in detecting CT was verified through whole root staining using 1 % (w/v) vanillin in 2 N HCl:EtOH, a previously favoured CT stain (McKenzie and Peterson, 1995a; Gardner, 1975). Both stains were consistent in their localization of CTs (Appendix 2).

To test for the presence of an exodermis, freehand cross sections between 0.5 - 1.5 cm from the root tip were stained using the berberine-aniline blue protocol (Brundrett *et al.*, 1988). This was used to determine whether Casparian bands were present in the epidermal layers, indicative of an exodermis. Sections were submerged in 0.1 % berberine hemisulfate in dH_2O for one hour using the custom-made section holder. After two 30 second rinses with dH_2O, sections were placed in aniline blue solution (2.5 % in 2 % acetic acid) for 15 minutes to counterstain by suppressing the background fluorescence of berberine hemisulfate. Sections were then rinsed in dH_2O and placed into

0.1 % (w/v) $FeCl_3$ in 50 % (v/v) glycerol and dH_2O for five minutes before being mounted onto slides in the same solution. Slides were imaged within one hour using a transmitted light microscope (x100) (Zeiss [47-30-12-9902], West Germany) under UV light (365 nm) with Zeiss III RS Filter I [487702]. Unstained controls were also imaged under the same conditions.

To show the distribution of suberin and lignin, which have autofluorescent properties (Ruzin, 1999), freehand sections were first imaged using a transmitted light microscope (x 63) (Zeiss [47-30-12-9902], West Germany) equipped with a UV source and Zeiss III RS Filter I [487702]. Sections were then counterstained for two minutes with the lignin specific stain phloroglucinol (1 % (w/v) in EtOH) that becomes visible following the addition of a drop of concentrated HCl. The slides were then reimaged. The fluorescence of lignin was thus suppressed to allow the distribution of the autofluorescing suberin to be distinguished (Smith *et al.*, 2006).

Cortex viability testing was conducted by submerging whole roots in 5 mL of 10 mM fluorescein diacetate (FDA) in acetone for eight minutes at room temperature and in the dark (Baumann, 2014). Roots were then rinsed three times with dH_2O and imaged immediately under a dissecting scope equipped with epifluorescence and a blue filter (λ_{ex} = 395 nm, λ_{em} =509 nm). Roots were additionally imaged under white light as a control. FDA is retained in living cortical cells and leaks out from non-viable and degrading cells. The extent of cortex viability was therefore proportional to the intensity of fluorescence.

2.2.3 CT Quantification

Roots were harvested after eight weeks of growth, cut into segments according to distance from root tip and root colour, and then pooled into groups from each plant (n>30). Presence or absence of root pigmentation was noted and was a defining factor when dividing root samples into specific zones: root tips were taken as the first 0.5cm from root tip (meristematic and elongation zones), white roots (maturation zone), brown roots without periderm (similar to the description of CT zone (Peterson *et al.*, 1999)) and the cork zone (see Figure 2.6 for precise groupings). The fifth leaf from the shoot apex with the midrib removed was also taken from each plant for comparison. Samples were frozen immediately in liquid nitrogen and then freeze-dried for three days. An aliquot of 8 mg was weighed from each pooled sample. It was not possible to get sufficient material for some samples (mainly root tips) and so the entire sample was weighed and extracted, and the precise weight used in the final calculations.

Soluble CTs from pooled root samples were sequentially extracted in 100 % MeOH by grinding freeze-dried samples in PreCellys 24 homogenizer for two minutes using three 2 mm steel beads per sample, sonicating for ten minutes and centrifuging for five minutes at 1500 rpm. This procedure was followed using 1 x 1.5 mL, and 2 x 1 mL of 100 % MeOH resulting in 3.5 mL of extract. The volume of extract was then made up to 5 mL to ensure it was within the linear range for soluble CT quantification (Appendix 3a). CTs were quantified using the 1-butanol:HCl assay (Porter *et al.*, 1986): 400 µL of extract was added to 2 mL 1-butanol:HCl (95:5 solution) with 67 µL of Fe reagent (2 % (w/v) $NH_4Fe(SO_4)_2$ + 12 H_2O in 2 N HCl) and heated at 95 ^oC for 40 minutes in 15 mL

polypropylene conical tubes with screw cap. The heating process depolymerized CTs into visible anthocyanin monomers (cyanidin and delphinidin) creating a deep red colour which could be quantified by a spectrometer plate reader at 550 nm using 96-well plates (Perkin Elmer Victor^{TM} x5 2030 Multilabel Reader). Spectrophotometric readings for each sample were taken before and after heating. Pre-heated readings were subtracted from heated readings to account for anthocyanins and non-CT compounds which also absorb at 550 nm. Insoluble CTs, which are not extractable using MeOH were quantified by depolymerizing CTs directly from the previously-extracted pellet: 6 mL of 1-butanol:HCl (95:5) and 200 µL Fe reagent were added directly to the dried pellet and heated to 95 ^{o}C for 40 minutes. 400 µL of MeOH was added to each sample before heating to compensate for the volume of soluble extract used in the standard curve (Appendix 3b).

Spectrophotometer readings were converted to CT concentration (µg mL^{-1}) for the total sample using the appropriate standard curve created from purified CT (extracted from *P. tremula* x *tremuloides*). Soluble CTs ranged between 0-300 µg mL^{-1} (Appendix 3a) while the insoluble CTs had a larger range between 0-600 µg mL^{-1} (Appendix 3b). CT concentrations were then converted to mg g dry weight^{-1} using the standardised calculations (Appendix 3c).

2.2.4 Data Analysis

Photographs were edited using Photoshop CC 2014 by removing shadow, blemishes and creating a uniform background colour. Brightness was increased uniformly

across the darker images. No changes were made to contrast, vibrancy or overall appearance of the image.

Data was analysed and graphed using R v.3.0.3. Once model assumptions and normality were checked, data was statistically analysed using two-sample t-test or one-way Analysis of Variance (ANOVA) with Tukey's Honestly Significant Difference (HSD) test.

2.3 Results

2.3.1 *Populus tremula* x *alba* Root Anatomy

Following eight weeks of growth in vermiculite in one gallon pots, *P. tremula* x *alba* roots exceeded 40 cm in length and consisted of an extensive root network absent of mycorrhizae (Figure 2.1). Roots were extremely fine and fragile (<2 mm in diameter) and the majority of the roots were white or cream in colour and had no evidence of secondary growth (Figure 2.1, black arrows). Root tips that had become pot bound had red anthocyanin accumulation and some had begun to degrade. These were excluded from analysis (Figure 2.1, blue arrows). There were no obvious main tap roots, and lateral branching seemed to be random. This made it difficult to accurately section roots according to age and position. Therefore, the distance from root tip and pigmentation were the criteria used to section roots as these were the best proxy for age and developmental stage. Brown pigmentation occurred, on average, over halfway up the length of an individual root, but this was highly variable, as demonstrated when comparing roots A and B (Figure 2.1). The brown zone appears to be similar to the 'CT

zone' described in *Pinus* (Peterson *et al.*, 1999) as this zone had a reduced diameter, presumably due to the loss of cortical cells during maturation (Figure 2.1, brown arrows). Secondary growth was evident above the brown zone and characterized by a thick, waxy, dark red/brown periderm layer making the roots more rigid. This zone of secondary growth is hereafter referred to as the cork zone (Figure 2.1, red arrows). The four described zones of *P. tremula* x *alba* are shown in a simplified root schematic (Figure 2.2).

The absorptive regions of *P. tremula* x *alba* roots were inferred from the absence of an exodermis and the extent of Casparian band and suberin deposition. Their distribution was compared with that of CTs to help delineate functional zones of the root. Berberine-aniline blue staining identified the Casparian band in the endodermis as expected, but not in the epidermal cells (Figure 2.3). This confirms that an exodermis was not present in young *P. tremula* x *alba* roots. The images presented in Figure 2.3 were characteristic of all sections (n=15) taken between 0.5-1.5 cm from the root tip, which corresponds to the zone of maturation. The absence of an exodermis was further verified through the autofluorescence images that clearly showed a strong fluorescence of suberin in the endodermis but only a faint fluorescence in the epidermal layers, even when the brightness of lignin fluorescence from the xylem cells was suppressed through phoroglucinol counterstaining (Figure 2.4). Passage cells within the endodermis, which lacked suberin lamellae (Figure 2.4, yellow arrow), were identified in sections within 3 cm of root tip. However, the distances at which passage cells were present were highly variable between individual roots and cannot be generalized. Due to the reduced diameter

of roots in the brown zone compared to the white and cork zones, no cross sections were successfully cut by hand so suberin deposition in this zone could not be assessed.

Cortex viability staining with fluorescein diacetate (FDA) was conducted to compare the distribution of active, living cortical cells with CT distribution. This experiment showed that only a small region of the root tip (<3 mm) had a viable cortex (Figure 2.5). The brightness observed in the images at the root tip corresponds to the high density of small, living cells in the root meristem. However, under UV light, all white roots showed fluorescence, decreasing in intensity with distance from the root tip. This suggests that most cortical cells were still intact and the cortex was generally living, but this was not accurately captured in the images. Sections from the brown zone and cork zone did not fluoresce under UV light once stained with FDA. This correlates with the loss of living cortical cells in the older portion of the roots (data not shown as images are entirely black).

2.3.2 CT Quantification

CT concentrations of leaves and roots were assayed directly to compare the allocation and distribution of CTs above- and below-ground in young, *P. tremula* x *alba* plants. The white root zone of wild-type greenhouse-grown *P. tremula* x *alba* plants had over fifty times more total CTs than the young leaves (two-sample t-test: DF= 4.41, T= - 9.87, $p<0.001$). CTs accounted for up to 10 % of root dry weight. Insoluble CTs, bound to cell walls and not extractable by methanol, contributed on average <20 % of total CT content in roots. Insoluble CT content in leaves was found to be far more variable, ranging from 10-100 %.

Soluble CT concentrations were found to be significantly higher in the white roots (containing the meristematic, elongation and maturation zones) compared to the brown roots (which lacked secondary growth) and the cork zone (one-way ANOVA: DF=13, $F= 14.59$, $p<0.001$). Tukey's HSD pairwise comparisons showed that almost all the white roots had significantly higher CT levels than brown roots (Figure 2.6). The data suggest that lack of brown pigmentation is a good indicator of CT presence in *P. tremula* x *alba.*

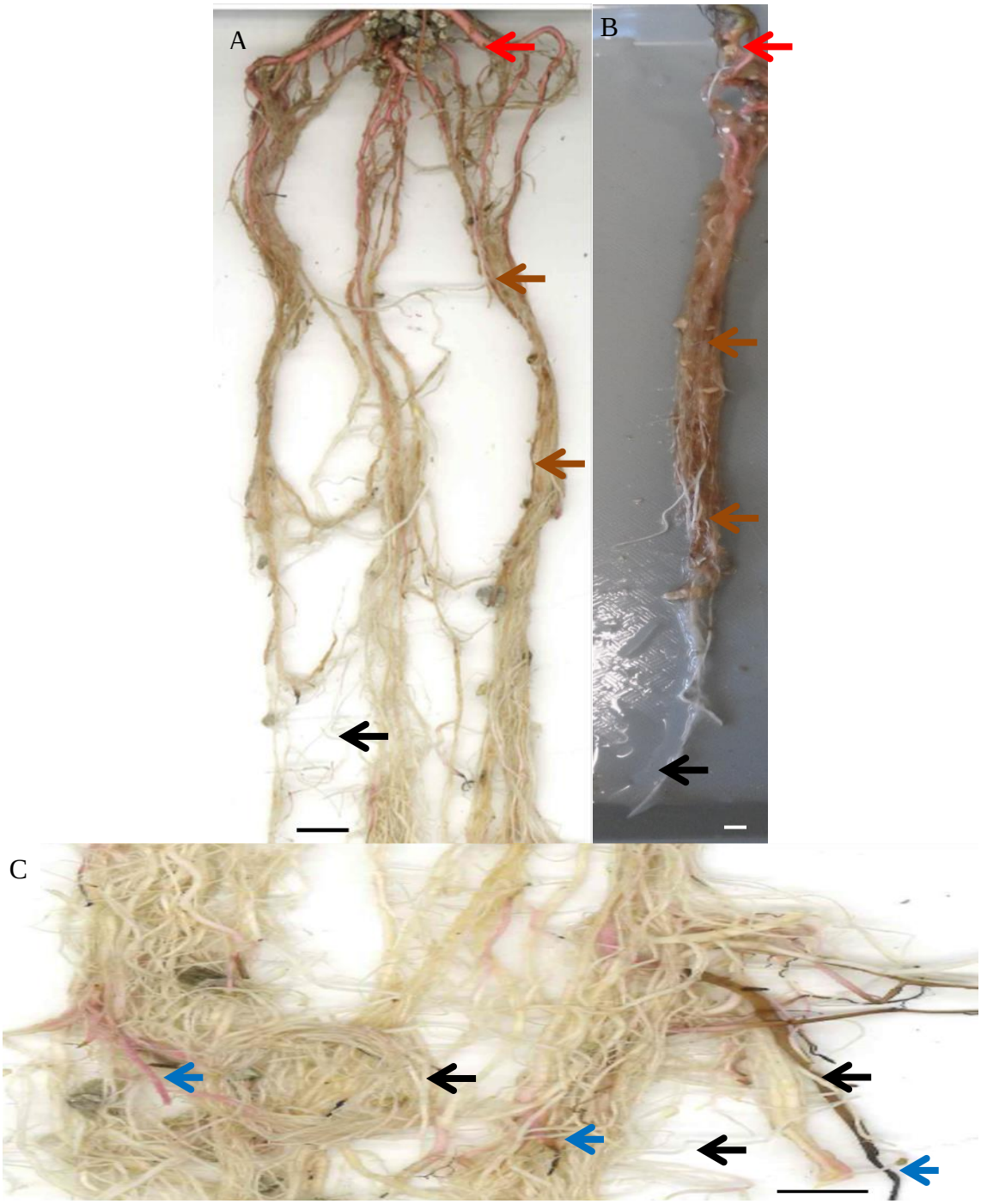

Figure 2.1 Whole root images of typical unstained *Populus tremula* x *alba* root network after eight weeks of growth. A and B. root tips to root collar. C. close up of the area containing the majority of root tips. Blue arrows – typical root tips which were decomposing or had anthocyanin accumulation and were excluded from analysis. Black arrows – typical white zone of roots. Brown arrows – typical brown zone of roots without secondary growth. Red arrows - typical cork zone. Scale bars = 1 cm.

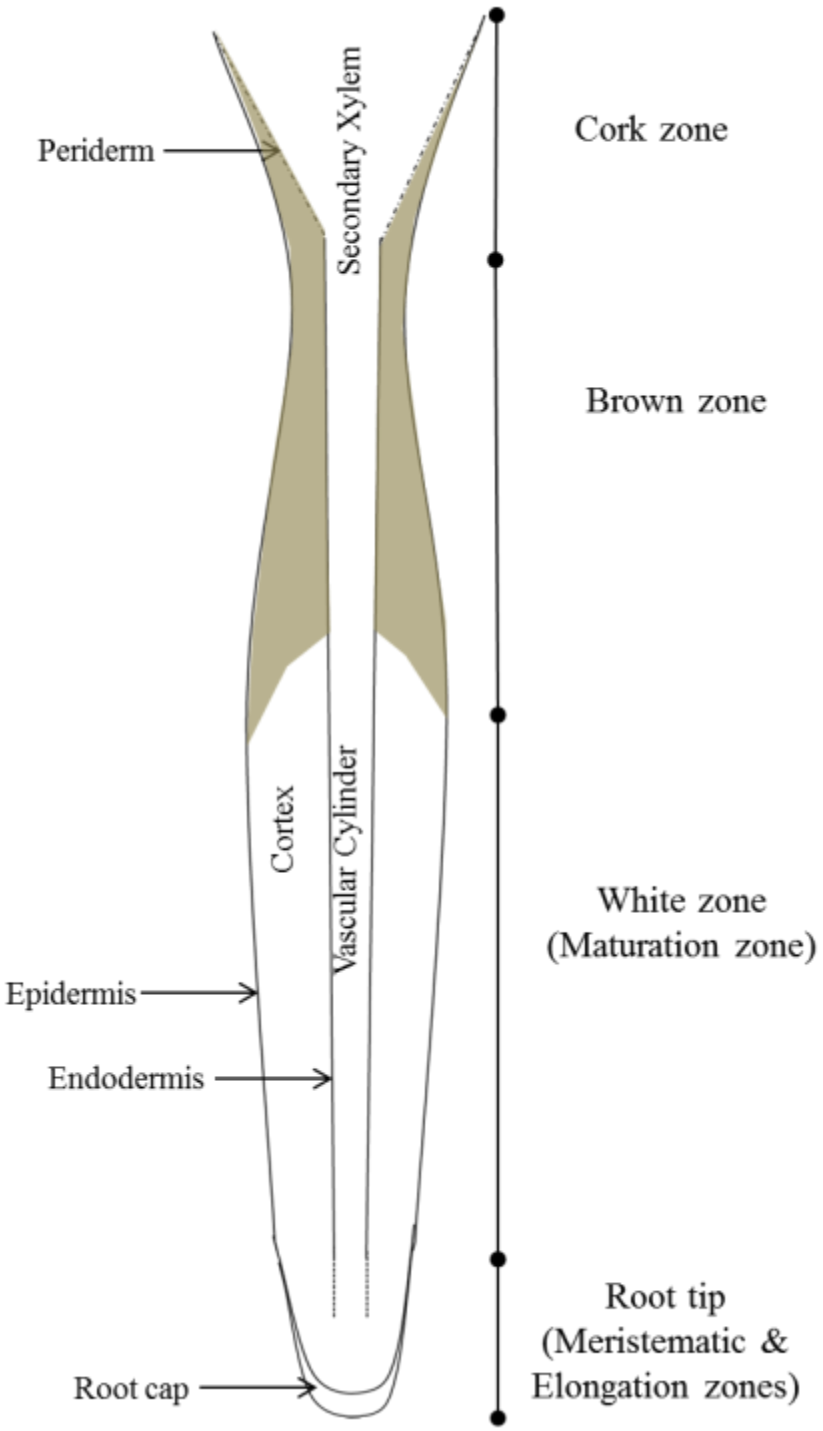

Not to scale

Figure 2.2 Schematic of a typical *P. tremula* x *alba* first order fine root outlining the four main root zones.

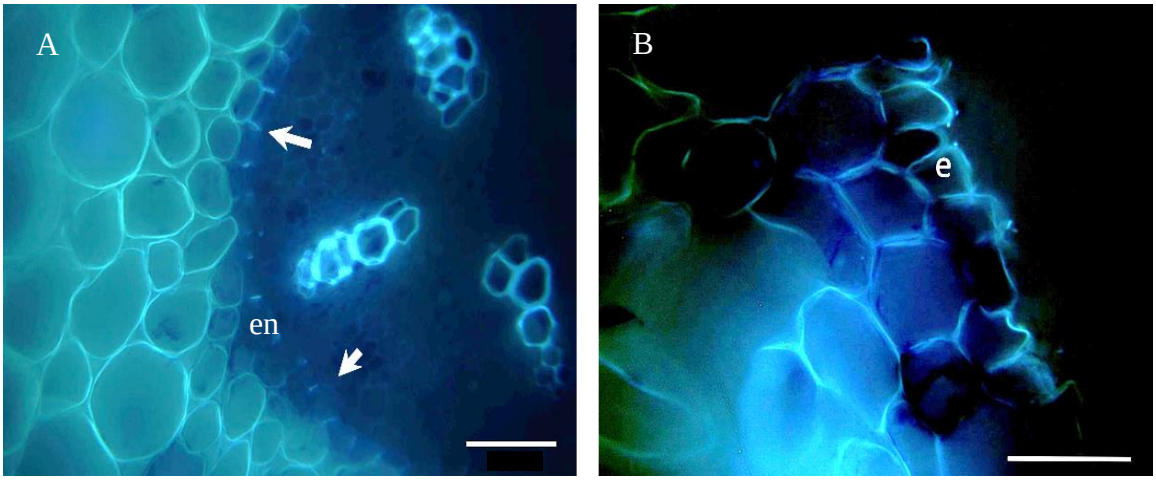

Figure 2.3 Berberine-aniline blue staining to detect the presence of Casparian bands in *P. tremula* x *alba* sections taken 1 cm from root tip (zone of maturation). A. Casparian bands in endodermis (en) (white arrows) B. Absence of Casparian bands in epidermal layers (e). Scale bars = 25 µm.

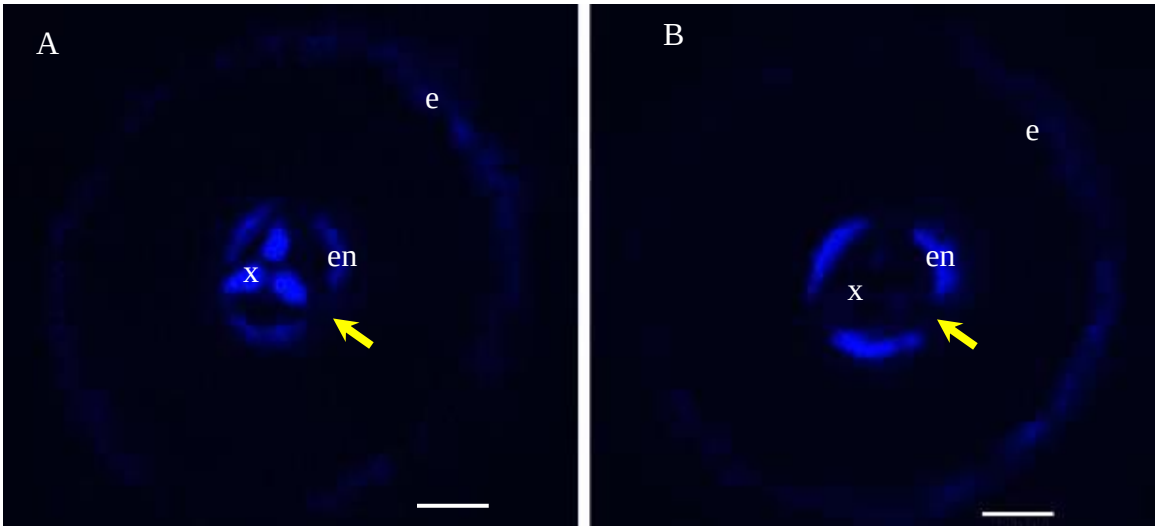

Figure 2.4 A. Autofluorescence of suberin and lignin in cross section 5 mm from root tip (zone of maturation) of *P. tremula* x *alba* . B. Autoflourescence of suberin following lignin counterstaining with 1 % phloroglucinol:EtOH and HCl in cross section taken 5 mm from root tip. Low levels of fluorescence detected in epidermal layers (e) indicate absence of exodermis. Yellow arrow shows passage cells in endodermis, en – endodermis, x- xylem. Scale bar = 100 µm.

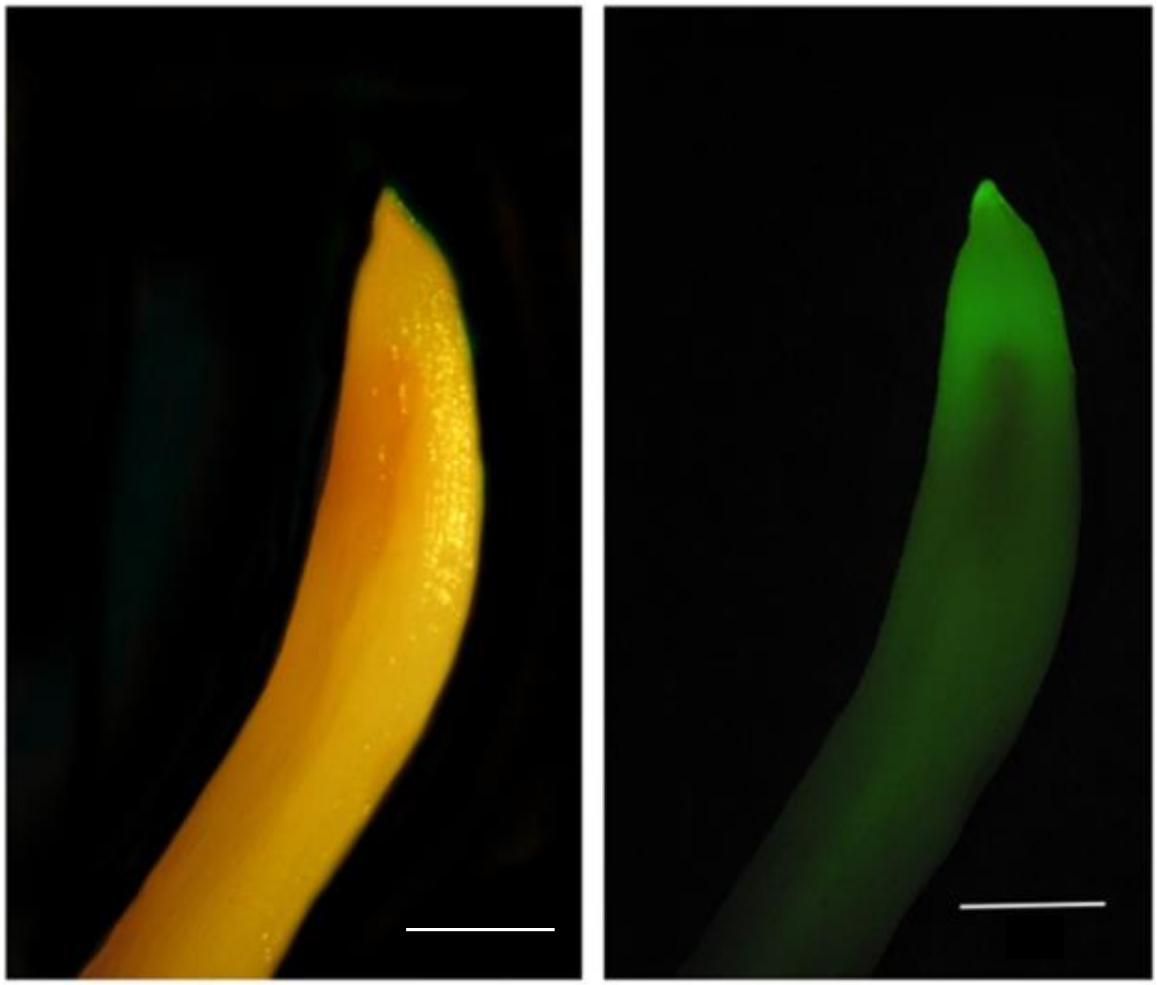

Figure 2.5 Fluorescein diacetate staining to show cortex viability of young white root tips of *P. tremula* x *alba* stained with 10 mM fluorescein diacetate in acetone. Imaged under brightfield (left) and UV (right). Scale bar = 1 mm.

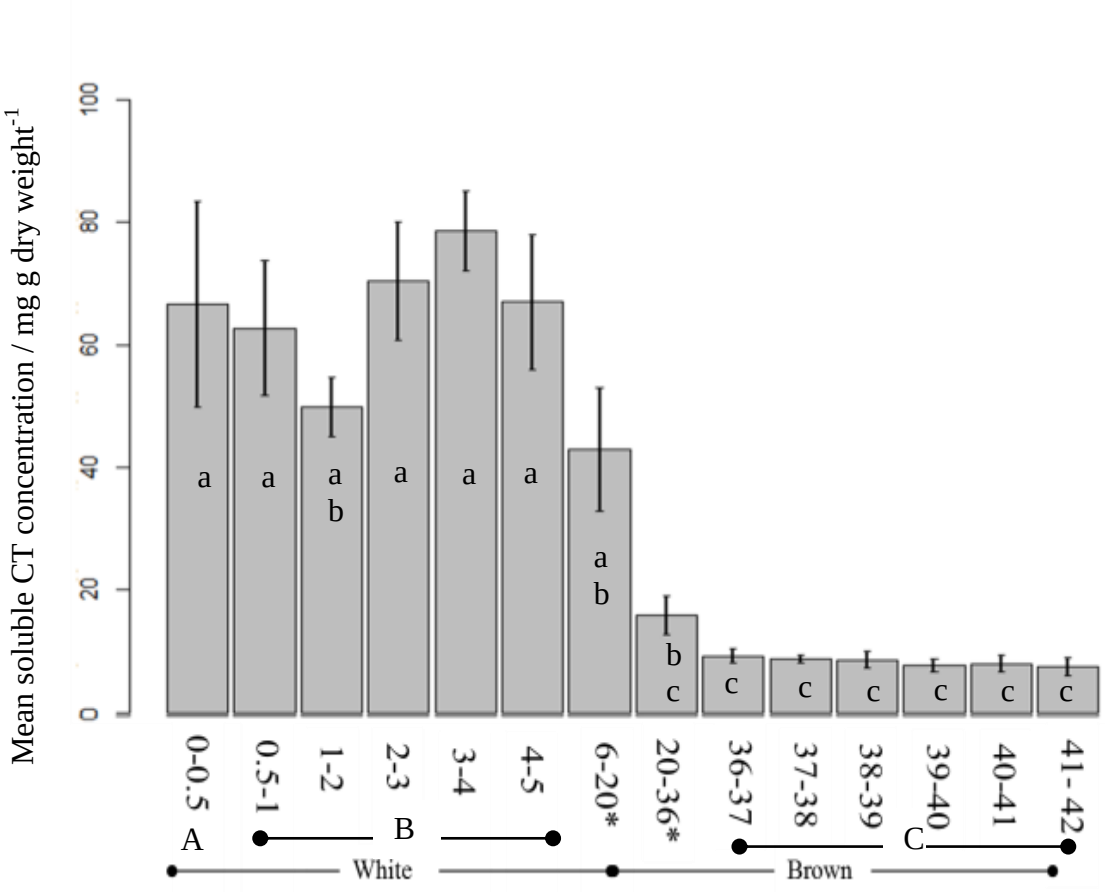

Figure 2.6 Mean soluble condensed tannin (CT) concentrations of root segments sampled at intervals along the root of eight-week-old *P. tremula* x *alba.* Bars indicate +/- standard error (n=6). Note that the x-axis is not linear and that 6-20cm and 20-36cm (*) are a subset of the 1 cm pooled samples which appeared macroscopically identical in appearance. A: Meristematic and elongation zones. B. Maturation zone (without lateral roots). C. Cork zone. Significant pairwise comparisons from Tukey's HSD test are displayed by a, b, c. ($p \leq 0.05$).

2.3.3 Tissue Localization of CTs

In order to visualise CT localization in root tissues and cells, 4-DMACA staining was conducted on whole roots and in both longitudinal and cross sections. Whole root staining showed greater accumulation of CTs in the root tip and white zone (Figure 2.7C and D) compared to the cork zone (Figure 2.7A). The cork zone only had a few sporadic CT-containing cells remaining on the root surface. In contrast, all cells were consistently stained blue near the root tips. Likewise, new lateral roots emerging from the cork zone also showed CT accumulation at the root tips, but less so in the maturation zone (Figure 2.7B). This is different from the longer, white zones which stained dark blue from the tip and throughout the maturation zone of the root (Figure 2.7C and D).

Longitudinal and cross sections were taken at the root tip (containing the meristematic and elongation zones) (Figure 2.8A), in the maturation zone (young white roots, characterised by root hairs but before the emergence of lateral roots) (Figure 2.8B) and in the cork zone (Figure 2.8C). These sections correspond to 0-0.5 cm (A), 1-5 cm (B) and 36-42 cm (C) segments in Figure 2.6, respectively. The 1-butanol:HCl assay (Figure 2.6) showed that CT concentrations were not significantly different between the brown zone (20-36 cm) and the cork zone (36-42 cm), and therefore the brown root zone was not included for histochemical analysis. The longitudinal root sections clearly showed an accumulation of CTs in the root cap (Figure 2.8A) arguably with greater intensity than in the maturation zone (Figure 2.8B). In the quantitative CT assay, the root sections containing the root cap did not have a significantly greater CT concentration than the rest of the sections from the white root zone (Figure 2.6). CTs were absent in the

meristem but were observed in the epidermis of the elongation zone and in some cortical cells. The root tip cross section (Figure 2.8A) also shows a high accumulation of CTs in the root cap cells and an absence in the central cells (presumed to be meristematic cells). The thickness of hand sections makes it difficult to distinguish the cell type, but the overall patterns observed are similar to those in the longitudinal sections.

The zone of maturation was identified by the presence of the discreet tissue types: dermal, ground and vascular, and the occurrence of root hairs. The maturation zone occurred >5 mm back from the root cap within the white root zone (Figure 2.8B). In this zone, there was no secondary vascular development, lateral root initiation or evidence of periderm formation. The longitudinal sections showed that CTs were concentrated predominantly in the epidermal cells, and occurred sporadically throughout the cortex but were absent in the vascular cylinder (Figure 2.8B). The distribution of CTs within cells of the cortex was varied with some stained material enclosed in large concentrated granules while some appeared to be incorporated into cell walls. The distributions of CTs in cross sections corresponded to those in the longitudinal sections, with the epidermal layers stained consistently for CTs and only some cortical cells showing a positive reaction.

CTs were mostly absent from the cork zone (Figure 2.8C) with only occasional red staining present in small granules in some remaining cortical cells. The presence of lignin in the secondary xylem and periderm reduced the clarity of the hand sections. Nevertheless, little blue staining was detected in this zone which is consistent with the results from both the longitudinal sections and the quantitative CT assay (Figure 2.6).

High magnification images (x 400) (Figure 2.9) showed distinct distributions of CTs within different cell types. In the epidermal layer, CTs appeared to be present in large vacuoles filling most of the intracellular space. In the sub-epidermal layer, CTs were observed in slightly smaller, more concentrated vacuolar-like structures. These smaller CT containing vesicles were more prominent in the cortical cells, some being present throughout the cells while others surround a large vacuolar-type space in the centre of the cells. At low magnification this ring-link distribution of CT vesicles around a large central space could be misinterpreted as cell wall distribution (as in Figure 2.8B). CTs were not present in every cortical cell, consistent with the other stained images (Figure 2.8B). The images in Figure 2.9 are taken from sections occurring 5-10 mm from root tip and may not be typical of the whole root, but are considered to be characteristic of the maturation zone and young white roots.

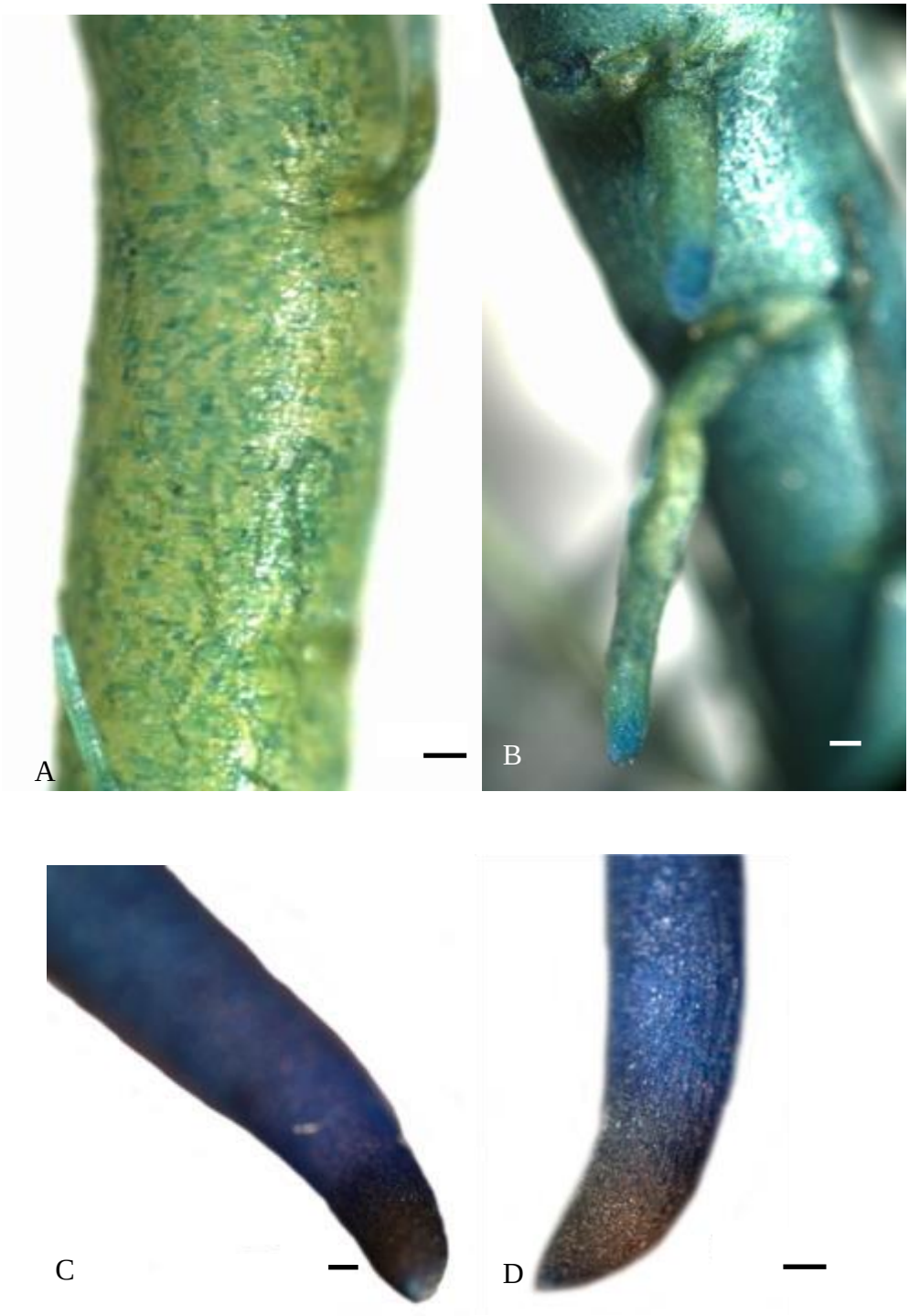

Figure 2.7 Whole root 0.01 % 4-DMACA stained *Populus tremula* x *alba* to detect condensed tannins. A) Cork zone. B) New lateral roots arising from cork zone. C) and D) Main root tips (meristematic, elongation and maturation zone). Scale bars = 500 µm. CTs stained blue.

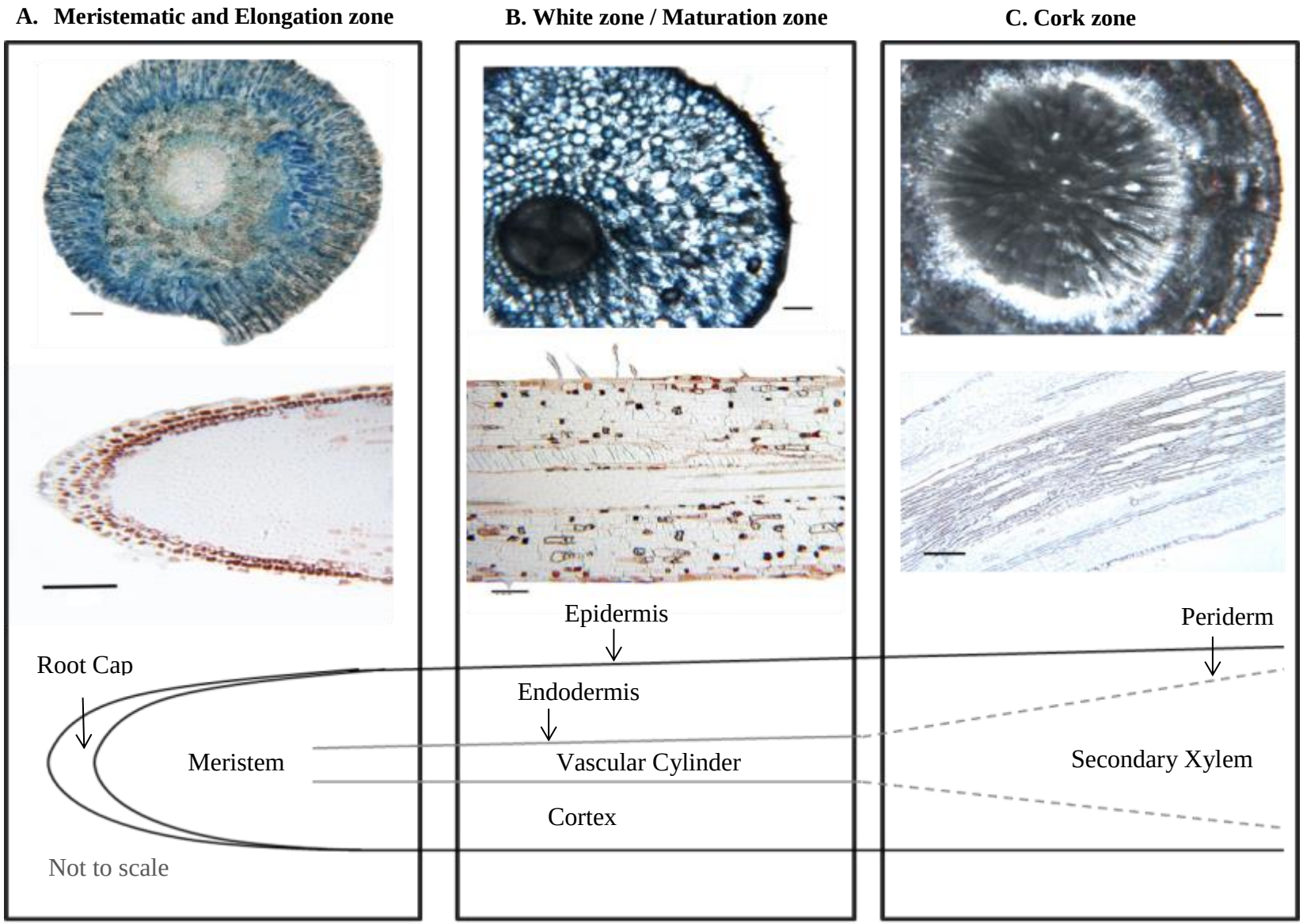

Figure 2.8 Localization of condensed tannins in *P. tremula* x *alba* roots, detected through 0.1 % 4-DMACA staining in embedded longitudinal sections (CT stained red/brown) and fresh cross sections (CTs stained blue). A. Root tip (<2 mm from root). B. White zone / maturation zone (1 cm back from root tip). C. Cork zone (>20 cm back from root tip). Scale bar = 100 µm.

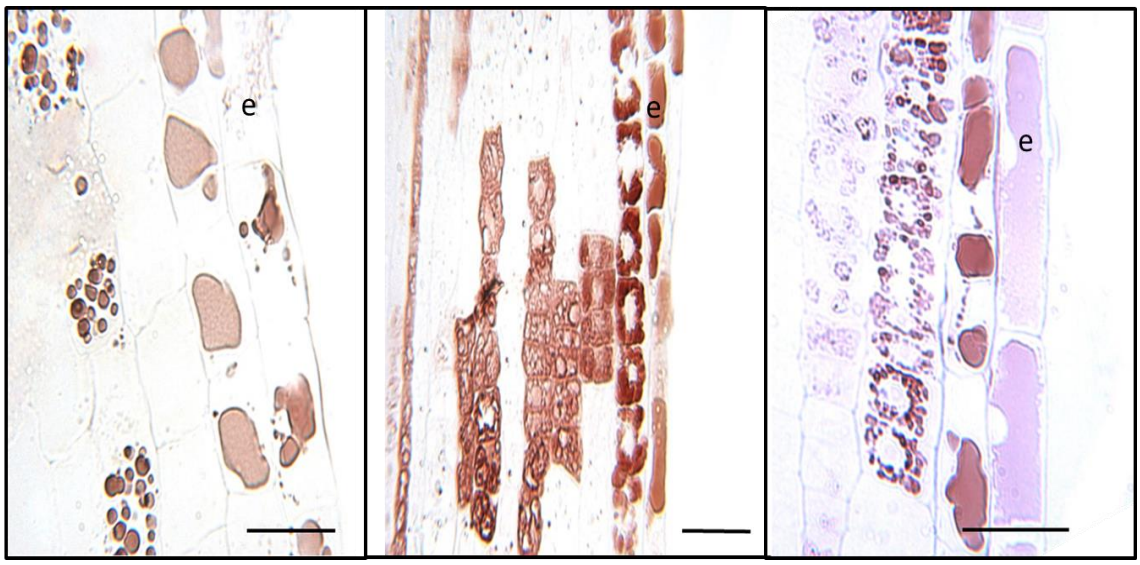

Figure 2.9 Cellular localization of condensed tannins of *P. tremula* x *alba detected* through 0.1 % 4-DMACA staining in embedded longitudinal sections (CTs stained red/brown) between 5-10 mm from root tip in the white zone. e = Epidermis layers. Scale bars=25 µm.

2.4 Discussion

Root CTs accounted for up to 10 % of root dry weight and were found at fifty times higher concentrations than leaf CTs in greenhouse grown *P. tremula* x *alba.* This suggests that CTs are likely to have significant ecological roles within the root system. The *P. tremula* x *alba* genotype has previously been recorded to have lower CT concentrations in the leaves compared to other *Populus* species (Appendix 6a). Low CT concentrations may also result from growth in greenhouse conditions, with minimal environmental stress i.e. UV-B and herbivores. Nevertheless, such a high difference in CT allocation between root and shoot does suggest that root CTs may play important roles during early plant development.

The *P. tremula* x *alba* roots analysed matched the general description of *Populus* roots (Farmer, 1996) with a high number of fine (<2 mm), branching lateral roots. Exodermal cells were not present in this genotype at distances less than 1.5 cm from the root tip, despite previously being recorded at these locations in *Populus deltoides* (Stoláriková-Vaculíková *et al.*, 2015). Several studies have documented that exodermal development can occur closer to the root tip in roots that are exposed to environmental stress (Hose *et al.*, 2001; Redjala *et al.*, 2011). Therefore, the lack of an exodermis cannot be interpreted as a permanent absence in *P. tremula* x *alba*, merely that it was not synthesised in the young maturation zone under the growth conditions of this experiment. Further analysis of older root sections is required to confirm whether an exodermis is absent in *P. tremula* x *alba*.

The cortex viability images taken may not be truly representative of the number of metabolically active cells; only the first 1.5 mm of the root fluoresced brightly, and no fluorescence was visible after 3 mm in a zone where metabolically active cells would be expected. This underestimation in cortex viability is likely an artefact of the camera compensating for the difference in contrast between the very bright root tip and the rest of the root. The high intensity of fluorescence at the root tip is due to the greater cell density in the meristem compared to the rest of the root. Under UV light, white zones of the roots stained with FDA fluoresced brightly. It is, therefore, highly likely that the cortex is viable for a much larger proportion of the white root zone than suggested by the images presented. The brown zone and the cork zone did not fluoresce following FDA staining under UV light. This observation of reduced cortex viability in the cork zone correlates with decreasing root diameter from cortical degradation and the deposition of non-living cork (McKenzie and Peterson, 1995b).

The most significant finding of this study is that CTs accumulated in the white zones of *Populus tremula* x *alba* roots. CT concentrations were not correlated with brown pigmentation as previously reported in other species (McKenzie and Peterson, 1995a). The negative correlation of CT concentration with brown root colouration was demonstrated independently using both histochemical and quantitative CT analysis. The pattern of CT distribution in the root cap is consistent with findings in other angiosperms: *Populus tremuloides* (Kao *et al.,* 2002) and rosaceous species (Hoffmann *et al.,* 2012). In *P. tremuloides,* stained CTs were observed in the root cap and in epidermal cells of zones 0.3 to 2 mm of the root tip. Sporadic staining of cortical cells was also observed in zones greater than 300 µm from the root tips (Kao *et al.,* 2002),

identical to that observed here in *P. tremula* x *alba.* Likewise, CTs also had non-uniform distribution in the cortex in both poplar species. This suggests that the size of the meristematic zone, in which CTs are absent, may be conserved between species and developmental stage, and that CT synthesis occurs in the cortex very soon after differentiation. Kao *et al.* (2002) stated that the intensity of CT staining declined as the root matures, yet no image was provided and specific spatial or anatomical descriptions were not provided. Therefore, no comparisons can be drawn between the CT distributions in regions less than 2 mm from the root tip in *P. tremula* x *alba* (presented here) and in *P. tremuloides* (Kao *et al.*, 2002).

The idea that CTs predominantly give rise to brown colouration, as observed in the roots of *Pinus* and *Eucalyptus* (McKenzie and Peterson, 1995a), is not supported in *Populus*. In *P. tremula* x *alba*, however, the brown zone of the roots occurred at much greater distances (~15 cm) from the root tip compared to ~2 cm recorded in *Pinus*, where passage cells were still present. This suggests that there are differences in root development between rapid-growing *Populus* and slower-growing *Pinus*. Caution must be used when trying to compare these results as there are likely to be other developmental and anatomical differences between the root systems of *Populus* and *Pinus*.

Oxidation and polymerization of CTs were suggested to be the cause of brown pigmentation in *Pinus* roots prior to cork deposition (McKenzie and Peterson, 1995a). In that study, the intensity of CT staining increased with distance from the root tip in the brown zones of *Pinus* roots where cortical cells had begun to degrade. This degradation

of cells was thought to allow CTs to leak from vacuoles and become bound in cell walls (Peterson *et al.,* 1999). By contrast, the evidence gathered here shows a complete contrast in CT distribution in *P. tremula* x *alba* compared to *Pinus* for both root zone and cellular localization. In the current study, CTs were detected by 4-DMACA in the vacuoles of root cells in the white zone of *P. tremula* x *alba* roots, compared to cell walls of dying cortical cells in the brown root zone of *Pinus* roots detected by vanillin-HCl (McKenzie and Peterson, 1995a). The pattern of staining of 4-DMACA compared to vanillin-HCl (used in McKenzie and Peterson, 1995a) was assessed in this study by comparing staining in whole roots. White root zones from the same plant showed consistent staining with both 4-DMACA and vanillin-HCl (Appendix 2). This suggests that the difference in CT localization between *Pinus and P. tremula* x *alba* is more likely to be due to species differences rather than the staining method. The consistency in CT distribution observed in both the histochemical and quantitative assay results, in this study, provides additional confidence in the localization of root CTs in *P. tremula* x *alba*. I conclude that the 'CT zone' varies in localization depending on species, and cannot be used as a general description for the brown zone of the root occurring between the white zone and cork zone.

For methodological reasons, only soluble CTs were quantified along the longitudinal axis of the roots (Figure 2.6). It is possible that insoluble CTs were present in the brown and older roots but were not extracted by methanol. However, quantification of insoluble CTs in other experiments (conducted in Chapter 3) showed that the proportion of insoluble CTs in roots never exceeded 35 % and was not significantly different between root zones (Appendix 4). The highest proportion of root

insoluble CTs were recorded in both the root tips and the cork zone, and did not correlate with brown pigmentation. Due to the relatively low proportion of insoluble CTs in all root samples and significantly lower CT concentration in brown root zones, it is unlikely that the brown colouration observed in *P. tremula* x *alba* roots was due to the presence of insoluble CTs. The brown pigmentation correlated with reduced root diameter due to the degradation of cortical cells and the deposition of periderm in the cork zone. I suggest that the majority of CTs are lost into the soil as cells break down, and do not become oxidised or complexed into the cell walls. In addition, no new CTs appear to be synthesised in brown or cork zones of the roots, supported by the lack of CTs reported in both the histochemical staining and 1-butanol:HCl assay. The cause of browning in plant tissues is generally attributed to the oxidation and polymerization of a variety of phenolics but not necessarily CTs (Dogan *et al.,* 2009). For example, there are multiple studies that demonstrate the cause of browning can be due to the action of the oxidative enzyme, polyphenol oxidase, and subsequent increases of quinones (Tang and Newton, 2004; Constabel and Barbehenn, 2008). The data presented here suggest that the brown colouration in the older zones of *P. tremula* x *alba* was not due to CT oxidation, but rather to other phenolics.

Histochemical analysis with 4-DMACA showed very clear localization of CTs in root cap cells, which has also been observed in longitudinal sections of rosaceous species (Hoffmann *et al.*, 2012). The root cap secretes mucilage to aid its passage through the soil as the root elongates, yet cellular damage on the root-soil interface is inevitable (Barlow, 2003). This may explain why CTs were found to accumulate in the root cap, as the cap functions as a defensive and protective structure for the root

meristem. The intensity of staining in the root cap appeared greater than that observed in the maturation zone (Figure 2.8). However the quantitative CT assay (Figure 2.6) does not show that the root cap had the highest CT levels compared to the other root zones. CTs could be innately synthesised in the root cap for protection or induced in response to mechanical damage during growth. An inducible CT regulatory mechanism, as observed in leaves, could explain the lower than expected root tip CT concentration as some root tips may not have induced CT synthesis. Over thirty root tips per plant were pooled into a single sample to obtain sufficient material for the assay. Root tips may have had very variable CT levels resulting from variations in root damage incurred during development. This was also indicated by the largest standard error bars occurring for the root tips (Figure 2.6). However, all root tip samples taken for histochemical analysis showed discreet root cap localization. The root tip samples taken for histochemical analysis (first 5 mm of root) were also not exclusively root cap but also likely included the meristematic and elongation zones and possibly even some of the early maturation zone. Therefore, the lower than expected CT concentration may also result from dilution by other zones of the roots that were less abundant in CTs. Differences in CT concentration my also arise from the pooling of root tips regardless of branching order or diameter. A recent study has found fundamental differences between fine roots; classified as absorptive and transport roots, which were determined through branching hierarchy (McCormack *et al.*, 2015). Differentiating between these root types in future research may provide interesting insights into CT accumulation in different fine root orders. It would be interesting to investigate the differences in CT concentrations and CT regulating gene expression in root caps that are grown in

aquaponics and receive little disruption or damage to the root cap compared to vermiculite and soil grown roots.

The cellular localization images gathered in this this study show interesting similarities to other studies. CTs have generally been reported to accumulate exclusively in the vacuoles (Gutmann and Feucht, 1991; Hollins and Jaffe, 1997; Visnovitz *et al.*, 2007). A recent study using electron microscopy, however, has claimed to identify a small chloroplast derived organelle which transports the newly polymerized CTs from the thylakoids to the vacuoles in tracheophytes. These small vesicles were named tannosomes (Brillouet *et al.*, 2013). This is the first evidence of CT synthesis in chloroplasts, but it lacks molecular support; as yet, flavonoid enzymes have not been reported within chloroplasts. The cellular localization images here (Figure 2.9) show large, uniformly filled CT vacuoles in the epidermal cells and smaller, distinct, CT-filled vesicles in the cortical cells. The evidence of smaller (~5 µm) CT containing vesicles are similar to images from *Vitis vinifera* (Brillouet and Escoute, 2012), *Vaccinium corymbosum* (Zifkin *et al.*, 2012) and *Onobrychis viciifolia* (Lees *et al.*, 1993), which show comparable granular CT accumulations in the vacuoles and are visibly similar to the tannosome structures observed in Tracheophytes (Brillouet *et al.*, 2013).

The images presented here (Figure 2.9) show good cellular integrity and I am confident that they are a reliable representation of cellular CT localization. This is further supported by the similarity to the other studies. However, it cannot be ruled out that the observed distribution of CTs may be an artefact of the fixation process, during which CTs have been observed to leak from vacuoles (Mueller and Greenwood, 1978).

Additional experiments investigating organelle specific flavonoid enzyme expression will be fundamental in determining the site of CT synthesis within cells.

The data presented here clearly show that CTs accumulate predominantly at the plant-soil interface on the outer cells and tissues of the young, active white zones of the root as well as sporadically in the cortex. This provides useful information when considering physiological roles of poplar root CTs. The accumulation of CTs in the root cap leads to several hypotheses regarding their potential roles. There is strong evidence suggesting active chelation of metal cations by root CTs reducing the toxic effects to plants, as observed in aluminum-rich soils (Osawa *et al.*, 2011; Stoutjesdijk *et al.*, 2001). Anti-pathogen and anti-herbivore defenses are also widely considered roles of CTs due to their protein binding properties. However, to date, there is no strong evidence to suggest anti-herbivory is a function of below-ground CTs. Root defense mechanisms involving CTs have only been investigated using *Melolontha* larvae (Coleoptera, Scarabaeidae). CTs were found to have no negative effect on their growth, development or feeding selection (Sukovata *et al.*, 2015).

Alternative hypotheses for the physiological roles of CTs in roots have been given little consideration. However, the ability of CTs to bind cations does lead to the idea that CTs may have a role in facilitating or modulating nutrient cation uptake. The results of the localization study show CTs occur in the zones of the root anticipated to have maximum nutrient uptake, which is consistent with this hypothesis. Chapter 3 will investigate whether a spatial correlation exists between the distribution of CTs and nutrient ion fluxes in *Populus* roots.

3 Investigating Physiological Roles of Condensed Tannins in *P. tremula* x *alba* Roots – Can They Influence Ion Uptake?

3.1 Introduction

Poplars are fast growing temperate trees. They have wide distributions across differing soil nutrient conditions, but are often grown in nutrient-rich, riparian soils abundant in available nitrogen arising from agricultural runoff (Rennenberg *et al.*, 2010). Some poplars (commonly *P. tremula* x *tremuloides*) are planted commercially on marginal land (Luo *et al.*, 2013a), reflecting an ability to grow on nutrient poor soils. High fine root density and high nitrogen use efficiency of poplars (Luo *et al.*, 2013a), are thought to contribute, in part, to rapid growth. For example, *Populus deltoides* has over twice the rate of nitrogen assimilation of similarly aged *Eucalyptus terticornis* (Bargali and Singh, 1991). Other physiological or biochemical adaptations which facilitate nutrient absorption may also be important, but have been given little consideration (Luo *et al.*, 2013b).

Nitrogen is the primary macronutrient required by plants, and is used in the synthesis of proteins, chlorophyll and other primary metabolites (Luo *et al.*, 2013b). Ammonium (NH_4^+) and nitrate (NO_3^-) are the main forms of inorganic nitrogen accessible for plants and their uptake is mediated by ion specific transporters in the roots (Glass *et al.*, 2001). A preference for nitrogen source is not conserved among *Populus* but appears to be a species specific trait. For example *P. deltoides* has a greater affinity for NO_3^-, whereas *P. tremula* shows preference for NH_4^+ uptake (Rennenberg *et al.*,

2010). There is also evidence to suggest that environmental factors play a role in nitrogen source preference, as transporters can be up-regulated depending on the source of available nitrogen (Glass *et al.,* 2001; Luo *et al.,* 2013b; Rennenberg *et al.,* 2010). The primary purpose of this study is to investigate whether CTs can influence nutrient uptake. This will be achieved through analysis of ion fluxes at discreet spatial positions along the root. In addition to the correlation with CTs, the data will also provide information on patterns of NH_4^+ and NO_3^- uptake in roots of six-week-old *P. tremula* x *alba.*

In leaves of poplar, as in many other plants, synthesis of CTs and phenolics are stimulated by low nitrogen availability (Osier and Lindroth, 2001; Glynn *et al.,* 2007; Stout *et al.,* 1998). By contrast, the effects of low nitrogen on root phenolics are not well investigated in any plant species. It has been proposed that upregulation of phenolics is a mechanism for utilizing excess carbon under limited nitrogen availability, thereby increasing the levels of defensive compounds when growth is limited (Gebauer *et al.,* 1998). Najar *et al.* (2014) showed that *P. tremuloides* with low root nitrogen stores invested more in synthesis of phenolic glycosides and other defense metabolites when stressed by herbivory from forest tent caterpillars, compared to similarly stressed plants with high levels of nitrogen, which invested in rapid growth. In *Solanum lycopersicum*, defensive flavonoids, rutin (Baidez *et al.,* 2007) and kaempferol rutinoside (Mirnezhad *et al.,* 2009), were significantly upregulated under low NO_3^- conditions in all plant organs, while growth was significantly reduced (Larbat *et al.,* 2012). These examples demonstrate the tradeoff between growth (primary metabolites) and defense (secondary metabolites) under low nitrogen conditions. This tradeoff has been termed the growth-

differentiation balance hypothesis (GDBH) (Herms and Mattson, 1992). This effect of nitrogen limitation on increased concentrations of phenolics has also been reported to be far greater in roots than in leaves or stems (Larbat *et al.*, 2014).

As described in Chapter 1, an additional association between CTs and nutrients is their role in regulating soil properties. CTs can reduce nutrient cycling in soil ecosystems by binding to organic nitrogen and complexing proteins to form large insoluble polymers that are less likely to be leached from the soil (Kraus *et al.*, 2004). CTs can also reduce decomposition by inhibiting soil microbes. The observed upregulation of CTs under low nitrogen conditions and the binding of CTs to nutrients within the soil, leads to the speculation that root CTs could have a physiological role in nutrient uptake.

This chapter aims to investigate whether CTs have a physiological role in poplar roots, specifically in modulating or facilitating nutrient acquisition. The results collected in Chapter 2 clearly show that CTs accumulate in cells at the root-soil interface, specifically in vacuoles of root cap and epidermal cells. They were also observed within smaller CT-containing granules in cortical cells of the maturation zone within the white zone. This white zone has a viable cortex and passage cells were present up to 3 cm from root tip, suggesting that this zone is capable of nutrient absorption. CTs have a demonstrated affinity to chelate heavy metal cations (Osawa *et al.*, 2011; Scalbert, 1991; Stoutjesdijk *et al.*, 2001; Kimura and Wada, 1989; see section 1.3). This leads to the speculation that CTs may provide a mechanism for plants to bind and store positively charged inorganic nutrient ions such as NH_4^+, Ca^{2+}, K^+. The storage of nutrient cations

by CTs within the vacuoles could maintain an ion gradient across the cell, and thus enhance cation uptake compared to plants with lower CT concentrations.

Ion-selective microelectrode measurement instruments have been fundamental in providing insights into specific ion fluxes at discreet spatial positions along the roots. Such studies have been conducted in conifers, such as *Pseudotsuga menziesii, Picea sitchensis, Tsuga heterophylla, Pinus monticola, Pinus contorta* and *Thuja plicata* (Hawkins *et al.,* 2008; Hawkins *et al.,* 2014) and also in angiosperms: for example with *Populus popularis* and *P. simonii* (Luo *et al.,* 2013b; Zhang *et al.,* 2014). The oscillating microelectrode ion flux measurement technique (MIFE^{TM}) can simultaneously measure fluxes of three ions to the proximity of a few cells on the root surface. Previous studies have focused on determining differences in ion transport longitudinally up the root and under varied environmental conditions (i.e. salinity, temperature and nutrient availability) and on making both intra- and inter-species comparisons. Maximal nitrogen uptake occurred in the white zone in the elongation and maturation zones, for all of the species analyzed (Hawkins *et al.,* 2008 and 2014; Luo *et al.,* 2013b; Zhang *et al.,* 2014). Precise flux profiles within and between species were variable and were attributed to differences in root growth and maturation rates. To date, no reports have related nutrient fluxes to distributions of phytochemicals or secondary metabolites.

In addition to complexing metal cations, CTs have been shown to bind Ca^{2+} in the vacuoles of pulvini cells of *Mimosa pudica* and *Albizzia julibrissin* (Persian silk tree) (Hollins and Jaffe, 1997). Ca^{2+} is required in high concentrations to initiate action potentials and elicit nastic leaf responses (see Chapter 1, section 1.4.3). To my

knowledge, this is the only study that has demonstrated a direct link between CTs and nutrient cation binding. Due to this link between Ca^{2+} and CTs, as well as the observed link between nitrogen and CT concentration (Osier and Lindroth, 2001; Kosola *et al.*, 2006; Stevens *et al.*, 2014), the experiments in this chapter will measure net fluxes of Ca^{2+}, NH_4^+, and NO_3^- along the root axis of *P. tremula* x *alba* and assess for spatial correlations of ion fluxes with CT distribution.

The potential interaction of CTs with nutrient uptake will be further explored using transgenic poplars with manipulated CT levels. They are unique in allowing for direct comparisons between individuals of the same species that differ only with regards to CT levels. The biosynthesis of CTs is regulated by R2R3-MYB transcription factors that can act either as stimulators or repressors of the CT pathway. High CT lines have been engineered to overexpress MYB 134 (Mellway *et al.*, 2009) and MYB 115 (Franklin, 2013). RNAi knockout lines have also been engineered to eliminate MYB 134 and create low CT lines (Ma, D., Gourlay, G. and Constabel, C.P., unpublished). The MYB 134 and MYB 115 transgenic poplars have been shown to produce high CT levels in leaves; however their effect on CT regulation in roots has not been investigated. To effectively assess whether there is a correlation between nutrient ion fluxes and CTs, transgenic poplars will be selected for comparative study. The concentrations of CTs in roots of three transgenic poplar genotypes (MYB 115, MYB 134 and RNAi MYB 134 knockouts) will first be quantified, in order to select the transgenic genotype with the most significantly altered CT concentrations from wild-type *P. tremula* x *alba*.

The specific objectives of this study are: 1) to test if soil nitrogen availability affects root CT concentration; and 2) to compare the patterns of net fluxes of nitrogen (NO_3^-, NH_4^+) and calcium (Ca^{2+}) with the distribution of CTs in roots, using wild-type and high CT genotypes of *P. tremula* x *alba*. From the evidence showing increased CT synthesis under low nitrogen supply (Osier and Lindroth, 2001; Glynn *et al.*, 2007; Stout *et al.*, 1998) and the evidence linking CTs with cation binding (Hollins and Jaffe, 1997; Osawa *et al.*, 2011; Kimura and Wada, 1989), the hypotheses for this study are: 1) low soil nitrogen availability will increase root CT concentration; 2) zones of the root with high CT concentrations will have highest rates of cation uptake (NH_4^+ and Ca^{2+}) and; 3) the high CT genotypes with elevated root CT concentrations will have higher cation uptake through increased binding by CTs (NH_4^+ and Ca^{2+}) compared to the wild-type trees.

3.2 Materials and Methods

3.2.1 Plant Growth Conditions and Nitrogen Manipulation

To test if nitrogen manipulation influenced root CT concentrations, wild-type *Populus tremula* x *tremuloides* (353) were grown under three nitrogen fertilization treatments in Sunshine Basic Mix #2 (Sungro, Seba Beach, AB, Canada). Prior to harvesting, all aspects of plant care were kindly undertaken by David Ma. Three plants were assigned to each nitrogen condition: 0.1 mM, 1 mM or 10 mM NH_4NO_3 considered to be low, medium (normal) and high nitrogen treatments, respectively. The plants were fertilized on alternate days with 100 mL of the desired NH_4NO_3 concentration within modified Long Ashton's nutrient solution (0.9 mM $CaCl_2$, 0.6 mM KH_2PO_4, 0.5 mM

KCl, 0.04 mM K_2HPO_4, 0.3 mM $MgSO_4$ x $7H_2O$and 0.03 g L^{-1}standard micronutrient mix (Plant Products Co. Ltd, Brampton, ON, Canada) , pH 5.6). All other concentrations of nutrients were standardized in this solution and are the recommended concentrations for poplar growth (Luo *et al.*, 2013a). Plants were grown in greenhouse conditions for 12 weeks and watered with dH_2O as necessary. Upon harvesting, roots were sectioned and divided into groups; root tips (meristematic and elongation zone) (<0.5 cm), white zone (maturation zone) (0.5-10 cm) and cork zone (~20-30 cm). The fifth leaf from the shoot apex was sampled as a control. Root tips that showed necrosis or anthocyanin accumulation from becoming pot bound were excluded. Samples were prepared and soluble and insoluble CTs extracted and quantified using the 1-butanol:HCl assay (Porter *et al.,* 1986) (refer to Methods 2.2.3).

3.2.2 CT Analysis of Transgenic *P. tremula* x *alba* Lines

Preliminary tests were conducted to determine whether concentrations of CTs were elevated in roots of two MYB overexpressing genotypes of *P. tremula* x *alba*: MYB 115 and MYB 134 (Franklin, 2013; Mellway *et al.,* 2009). These genotypic lines were all available as shoot cultures in the Constabel lab. In addition, root CT concentration was also tested in three RNAi MYB 134 knockout transgenic lines (MYB 134-9, MYB 134-11, and MYB 134-12), predicted to have reduced CT levels. As described in Chapter 2, root sections and leaves were analysed for CT concentration with the 1-butanol:HCl assay (Porter *et al.,* 1986) (refer to Methods 2.2.3).

The genotype selected (MYB 115) had the largest difference in root CT levels compared to the wild-type genotype. Two transgenic lines of this genotype were used,

MYB 115-2 and MYB 115-3. An additional 15 plants were grown (five wild-type and five of each of the high-CT transgenic lines MYB115-2 and MYB115-3) (refer to Methods 2.2.1). Fine scale quantification of total CT concentrations (soluble and insoluble) was conducted in sections taken along the root axis using 1-butanol:HCl assay (Porter *et al.*, 1986) (refer to Methods 2.2.3). Plants were grown for eight weeks in vermiculite, fertilised with 100 mL modified Long Ashton's solution containing 1 mM NH_4NO_3 three times per week and watered with controlled volumes of dH_2O, as required.

3.2.3 Micro-electrode Ion Flux Measurement (MIFE^{TM}) Analysis

Fifteen plants, five of the wild-type genotype and five of each of the high-CT transgenic lines (MYB 115-2 and MYB 115-3), were grown for nutrient ion flux analysis. The Long Ashton's solution was altered from previous experiments to match the measuring solution used during MIFE^{TM} analysis, but the overall concentrations of each ion was similar to previous studies (1 mM NH_4NO_3, 0.9 mM $CaSO_4 + 2H_2O$, 0.6 mM KH_2PO_4, 0.5 mM KCl, 0.04 mM K_2PO_4, 0.3 mM $MgCl_2 + 7\ H_2O$ and 0.03 g L^{-1} standard micronutrient mix (Plant Products Co. Ltd, Brampton, ON, Canada), pH 5.6). Plants were grown in pairs in a continuous rotation to ensure that they were all the same age when harvested after six weeks of growth. Originally an eight week growing period was scheduled to match that of the CT quantitative assay study; however early, warm weather significantly accelerated growth and so plants were harvested when they were equal in shoot height to the previous experiment (~30 cm) and before the roots became severely pot-bound. Healthy, individual roots were excised from the plant, and placed in aerated solution containing 500 µM NH_4NO_3 and 500 µM $CaSO_4$ for 30 minutes prior

to measuring to allow the roots to acclimate. Excision was required because the plants were too big and roots too long to fit in the measuring chamber. Excising roots has been shown to have no significant effects on nutrient fluxes for up to 80 minutes (Hawkins *et al.*, 2012).

The MIFE^{TM} technology is a non-invasive method to measure net fluxes of specific nutrient ions at precise root locations (Shabala *et al.*, 1997; Shabala and Newman, 1997). In this study NH_4^+, Ca^{2+} and NO_3^- fluxes were measured and analysed. Borosilicate glass capillaries (1.5 mm diameter) were pulled, dried at 200 ^oC for five hours and silanized with tributylchlorosilane to make sterile, measuring electrodes. Once cooled, electrodes were backfilled with 200 mM NH_4Cl for NH_4^+, 500 mM $CaCl_2$ + $2H_2O$ for Ca^{2+}, and 500 mM KNO_3 + 100 mM KCl for NO_3^-. Electrode tips were then filled with ion-selective resins: NH_4^+ and Ca^{2+} -selective cocktails (Fluka catalog #. 09882 and 21048, respectively), and NO_3^- -selective cocktail containing 0.5 % methyltridodecylammoniumnitrate (MTDDA NO_3^-), 0.084 % methyltriphenylphosphonium (MTPPB) and 99.4 % n-phenyloctylether (NPOE) (Plassard *et al.*, 2002). Electrodes were calibrated using a known set of standards at pH 5.6 (Appendix 5). A reference electrode filled with 100 mM KCl in 1 % agar and electrolysed, chlorided silver wire was placed in the solution for each measurement to complete the electrical current. Calibration was conducted at the beginning and end of each day to ensure readings were representative and reliable.

The electrodes were mounted in a specialised holder (MMT-5, Narishige, Tokoyo, Japan) providing three-dimensional positioning. A maximum distance of 20 µm was

recorded between the electrodes and the root surface, and 4 µm between the electrode tips. Roots were secured and placed in the measuring chamber with fresh measuring solution (500 µM NH_4NO_3 and 500 µM $CaSO_4$). The chamber was moved by a computer-controlled manipulator (PatchMan NP2, Eppendorf AG, Hamburg, Germany). During flux measurements, the MIFE^{TM} computer gently caused the chamber to oscillate over a distance of 40 µm, back and forth from the root surface in a 10 s square-wave cycle. The concentration of each ion was calculated from its electrochemical potential at the two positions (Shabala *et al.*, 1997).

Flux measurements were taken at four discrete positions along the root; at the root tip (<2 mm), and three positions within the maturation zone of the white root zone (0.5 cm, 1.5 cm and 3.5 cm from the root tip) within 80 minutes of excision. These root distances were chosen as they included the zones where uptake is expected to be highest (Hawkins *et al.*, 2008 and 2014; Luo *et al.*,2013; Zhang *et al.*,2014), and also because they corresponded directly to the zones where CT concentrations were assayed with the 1-butanol:HCl assay. The brown zone and cork zone of the root were too far from the root tip to fit in the chamber, and measurements could only have be taken if the meristem was excised. No studies have investigated the effect of meristem excision on ion uptake, and for this reason the brown zone and cork zone were not measured in this study. Ion fluxes were measured for eight minutes at each of the four positions along the root axis to ensure that a reliable average flux measurement was gained for each replicate. Five plants for each genotype were grown and three roots were measured per plant.

To assess for a direct correlation between CT concentrations and the ion fluxes observed, staining of whole roots with 0.01 % 4-DMACA in 2 N HCl:EtOH was conducted to compare CT distribution and ion fluxes in the same root (refer to Methods 2.2.2). Staining was conducted within 24 hours of MIFE analysis, excised roots were stored in aerated solution (500 µM NH_4NO_3 and 500 µM $CaSO_4$) for the interim period.

3.2.4 Data Analysis

CT concentrations from both 1-butanol:HCl assay experiments and ion fluxes from MIFE^{TM} experiments were statistically analysed and graphed using R v3.0.3. CT concentrations were analysed separately for soluble and insoluble CTs and then summed to give total CT concentrations (See Chapter 2 section 2.2.4). Data was tested for normality prior to statistical analysis. Two-way analysis of variance (ANOVA) testing main effects and possible interactions (nitrogen treatment by sample, or genotype by sample for each experiment, respectively) were conducted for each dataset which had two experimental variables. Tukey's Honestly Significant Difference (HSD) test was used to analyse specific pairwise comparisons. Data was plotted as grouped bar charts in ggplot2 with standard error bars.

For the purpose of statistical analysis, the transgenic lines (MYB115-2 and MYB 115-3) were analysed as independent genotypes, as well as the wild-type. For simplicity, the term genotype will be used to describe differences between the wild-type genotype and the two transgenic lines MYB 115-2 and MYB 115-3 (although technically they are not different genotypes).

For MIFE^{TM} experiments, overall fluxes for each ion were averaged over a three minute period, where flux readings showed little variation, to give a single mean flux for each root position and genotype (n=15). Outliers were excluded if they fell more than two standard deviations away from the mean. Fluxes were plotted as grouped line plots in ggplot2 with standard error bars. Negative flux values denote net efflux of an ion from the root. Fluxes were compared between genotype and root position through two-way ANOVA (genotype by root position) and Tukey's HSD test.

3.3 Results

3.3.1 Nitrogen Manipulation Experiment

This experiment was conducted to test whether nitrogen limitation caused an increase in CT concentrations in roots of *P. tremula* x *tremuloides*, since nitrogen limitation has been found to cause upregulation of CTs and other phenolic compounds in leaves (Osier and Lindroth, 2001). Following 12 weeks of growth, phenotypic differences between nitrogen treatments were observed; low nitrogen treated plants showed stunted growth and lighter green leaf colour with sporadic brown necrotic spots compared to medium (normal) and high nitrogen treatments. Under the high nitrogen treatment, *P. tremula* x *tremuloides* had greater shoot height and darker green leaves compared to the medium and low nitrogen treatments. Nitrogen deficiency stimulated enhanced accumulation of CTs, with increasing CT concentrations for all root samples with as nitrogen content of fertilizer decreased (10 mM to 0.1 mM NH_4NO_3). There was a significant interaction between sample and nitrogen treatment (two-way ANOVA: DF= 6, F=4.22, $p<0.01$) (Figure 3.1). Under the low nitrogen treatment CT

concentrations for all root samples were significantly different from each other. Under medium nitrogen treatment, the root tips and white root zone did not have significantly different CT concentrations, whereas under both the high or low nitrogen treatments, CT concentrations in these zones were significantly different from each other.

All root samples had significantly higher CT concentrations when grown in 0.1 mM compared to 10 mM NH_4NO_3. CT concentrations in the white zones were also significantly higher in the medium compared to the high nitrogen treatments. This finding directly supports the first hypothesis that low soil nitrogen availability will increase root CT concentration. By contrast, Tukey's HSD test showed no significant difference in leaf CT concentrations between nitrogen treatments. The negative CT values observed in the leaves are due to the higher spectrophotometer readings from the unheated compared to heated samples and this can be interpreted as no-detectable CTs.

3.3.2 CT Analysis of Transgenic *P. tremula* x *alba* Lines

Root CT concentrations of transgenic *P. tremula* x *alba* were assessed to select the genotype with significantly different CT concentrations compared to the wild-type. Preliminary analysis identified the MYB 115-overexpressing transgenic of *P. tremula* x *alba* as the best genotype as it had significantly higher root CT levels compared to the wild-type. The MYB 134 overexpressing genotype showed significant enhancement of CT concentrations in the leaves, but root CT concentrations did not differ greatly from the wild-type (Appendix 6a). The three putative RNAi MYB 134 knockout lines were found to have no significant difference in root or leaf CT concentrations compared to wild-type *P. tremula* x *alba* (Appendix 6b). It was beyond the scope of this project to

determine whether the RNAi construct had successfully eliminated MYB 134 expression in these transgenics, or if other factors were involved.

Both MYB115 overexpressing transgenic lines (MYB 115-2, MYB 115-3) had almost 30 % higher total CT concentration in the white zone of roots compared to wild-type *P. tremula* x *alba* genotype (one-way ANOVA: DF= 2, F=14.71, $p<0.001$) (Figure 3.2). This result is consistent with the known function of MYB 115 in stimulating CT synthesis in leaves, but this had not previously been documented for roots (Franklin, 2013). Consistent with these data, analysis of all the different root segments also demonstrated this difference in CT concentration between genotypes (two-way ANOVA: DF=2, F=11.842 $P<0.001$) with significantly higher concentrations in the roots of MYB115-2 and MYB115-3 transgenic lines than in the wild-type genotype. Tukey's pairwise comparison, however, showed that CT concentrations were not significantly different between genotypes for any specific root segment, despite being significant overall (Figure 3.3). There were also significantly lower concentrations of CTs in the older portions of the roots from the white-brown transition and through the cork zone (>12 cm from root tip) and in the leaves (#5) compared to the younger white root zones (<12 cm from root tip) regardless of genotype (two-way ANOVA: DF=7, F=32.55, $p<0.001$) (Figure 3.3). This was consistent with other assay results (Figure 2.6 and Appendix 6). Overall analysis through the interaction model (genotype by sample) was also insignificant (two-way ANOVA: DF=14, F=1.182, $p>0.05$). This indicates that the transgenic roots showed the same pattern in CT distribution across the root system as the wild-type roots.

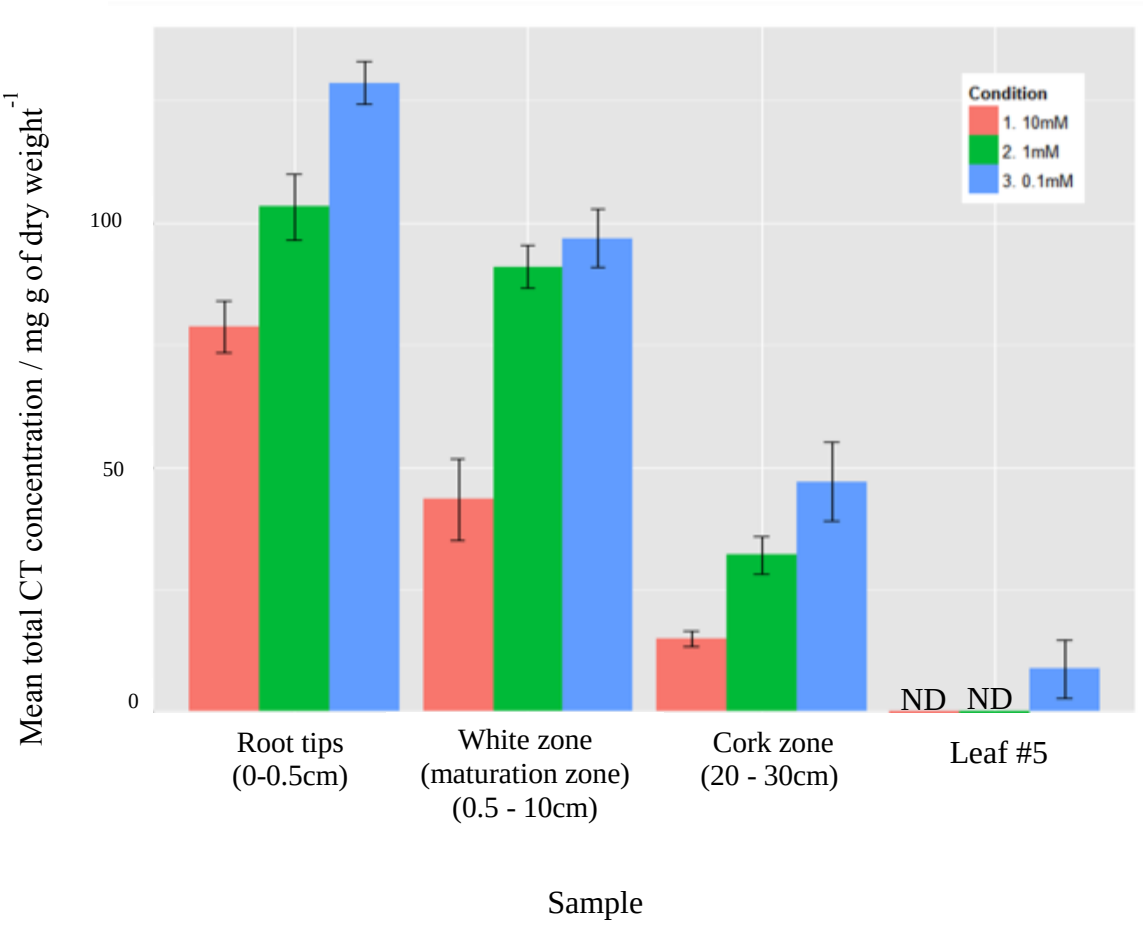

Figure 3.1 Mean total condensed tannin concentrations of three root zones and leaves of wild-type *Populus tremula* x *tremuloides* grown under three NH_4NO_3 concentrations (10 mM, 1 mM, 0.1 mM). ND – no-detectable CTs. Bars indicate +/- standard error (n=3).

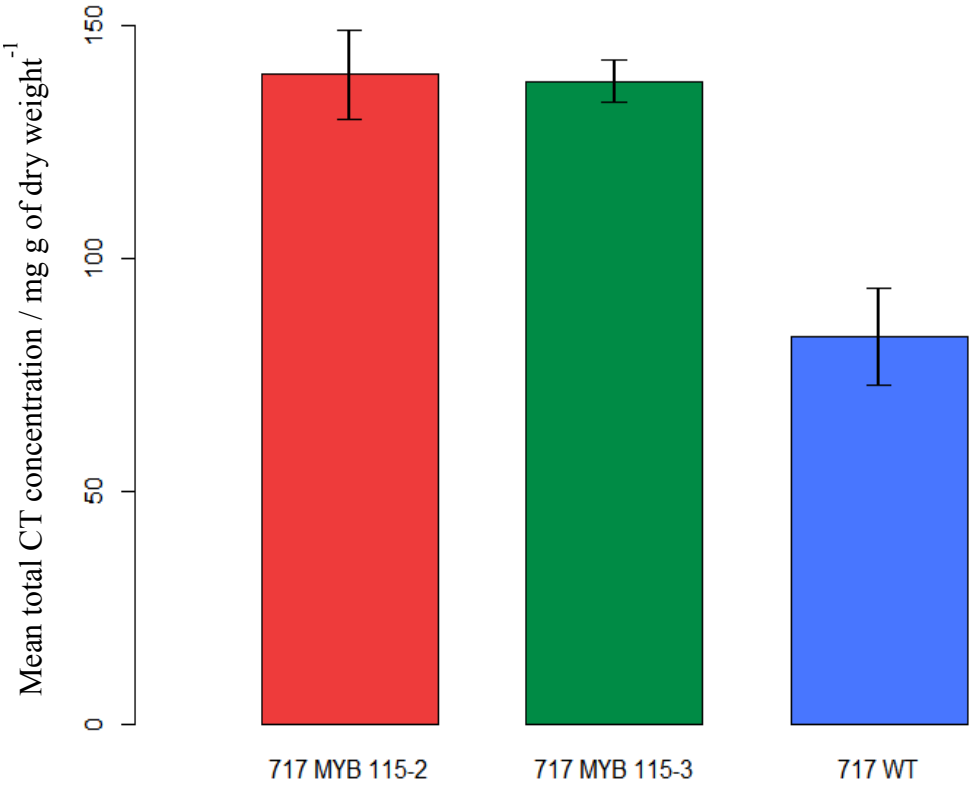

Figure 3.2 Mean total condensed tannin (CT) concentration in the white root zone of three genotypes of *Populus tremula* x *alba* (717): wild-type, and high CT transgenic lines MYB115-2 and MYB115-3. Bars indicate +/- standard error (n=5).

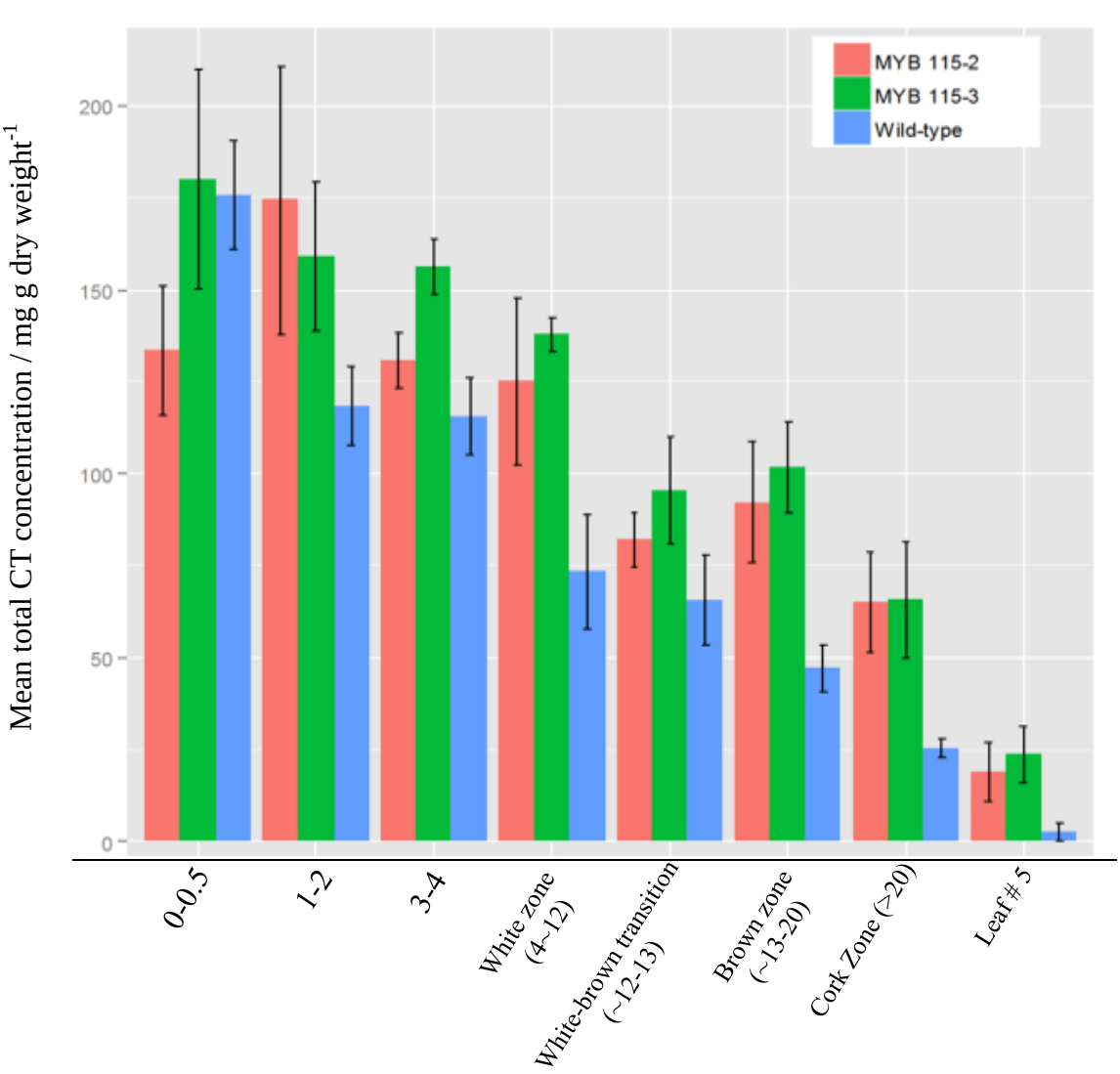

Figure 3.3 Mean total condensed tannin (CT) concentration of root sections and leaves of three genotypes of *Populus tremula* x *alba*: wild-type, and high CT transgenic lines *MYB115*-2 and MYB115-3. Bars indicate +/- standard error (n=5). 0-0.5cm = root tips; 1-12 cm = white root zone / zone of maturation; 12-13 cm = white-brown transition; 13-20 cm = brown root zone, >20 cm = cork zone.

3.3.3 Micro-electrode Ion Flux Measurement (MIFE^{TM}) Analysis

MIFE^{TM} analysis was used to determine if nutrient ion fluxes (NH_4^+, Ca^{2+} and NO_3^-) were spatially associated with distributions of root CTs in both the wild-type and high CT lines (MYB 115-2 and MYB 115-3) of *P. tremula* x *alba*. All genotypes showed consistent patterns in net flux profiles along the root for each ion, with all interaction models (genotype by root position) being insignificant ($p>0.05$). Overall, NH_4^+ and Ca^{2+} showed significant differences in fluxes between genotypes, with MYB 115-2 consistently having the lowest uptake. Root position was also significant when tested as an individual factor for both NH_4^+ and Ca^{2+} net fluxes. NO_3^- fluxes, however, were not significantly different between root position or genotype.

Net fluxes of NH_4^+ were over two fold higher at the root tip than at 0.5 cm and were significantly higher than fluxes recorded at all the other root positions. This was consistent across all genotypes (two-way ANOVA: DF=3, F=25.6, $p<0.001$) (Figure 3.4A). Although, NH_4^+ uptake decreased from the root tip, it remained relatively constant between 0.5 and 3.5 cm. Wild-type and MYB115-2 were significantly different from each other in total NH_4^+ fluxes resulting in the significant genotype result (two-way ANOVA: DF=2, F=3.635, $p<0.001$). MYB 115-3 was not significantly different from either genotype. The wild-type showed the highest influx of NH_4^+ with the exception at 3.5 cm. Net NH_4^+ efflux was recorded in MYB115-2 at distances >1.5 cm from the root tip.

P. tremula x *alba* appeared to preferentially use NH_4^+ as its nitrogen source since uptake was recorded up to ten fold higher than for NO_3^-. Interestingly, NO_3^- influx peaked at 0.5 cm for all genotypes (Figure 3.5A) which was the opposite trend to Ca^{2+} influx (Figure 3.6A). However for NO_3^- fluxes, no significant differences were found between root position or genotype.

Ca^{2+} uptake was lowest at 0.5 cm for all genotypes, but unlike NH_4^+, Ca^{2+} uptake increased further along the root (Figure 3.6A). MYB115-3 showed the highest Ca^{2+} uptake compared to other genotypes and this uptake was maximal at 3.5 cm. Conversely, MYB115-2, showed the lowest influx at this position, but this was still insufficient to yield a significant interaction model (genotype by root position). Genotype and root distance were both significant, however, as individual factors (DF=2, $F=3.717$, $p<0.05$ and DF=3, $F=5.33$, $p<0.001$, respectively). Rates of Ca^{2+} influx were up to 90 nmol m^{-2} s^{-1} lower than NH_4^+ in the root tips of wild-type plants, indicative of the lower requirement for Ca^{2+} compared to NH_4^+.

The observed fluxes of NH_4^+, Ca^{2+} and NO_3^- did not correlate with CT concentrations (Figure 3.4B, 3.5B, 3.6B). The two high CT lines (MYB 115-2 and MYB 115-3), despite their significantly higher overall CT levels compared to the wild-type, showed no significant differences in CT concentrations between genotype, root position or genotype by root position interaction within the first 3.5 cm from the root tip. Positions along the roots at which net ion fluxes were measured in the MIFE™ experiments (<0.2 cm, 0.5 cm, 1.5 cm and 3.5 cm) correlate only to the first three root segments analysed for CT concentration; 0-0.5 cm, 1-2 cm and 3-4 cm (Figure 3.3).

These correlate to <0.5 cm, 1.5 cm and 3.5 cm measured during MIFE^{TM} analysis. It was not possible to collect sufficient root material to run separate quantitative assays for <0.2 cm and 0.5 cm from root tip, so for this reason the single value (<0.5 cm from Figure 3.3) is used to correlate with the first two MIFE^{TM} measurements. In these samples, the CT concentrations were not significantly different between root position or genotype. Nevertheless, significant differences in cation fluxes between some genotypes and root positions were observed for both NH_4^+ and Ca^{2+}. These experiments, therefore, failed to demonstrate any correlation between CT concentration and cation uptake.

As an additional control, whole root 4-DMACA staining for CTs was conducted on the same individual roots used for MIFE^{TM} analysis. The results provide further evidence that suggest that NH_4^+, Ca^{2+} or NO_3^- fluxes were not correlated with CT concentration (Figure 3.7A and B). Surprisingly, some root tips (~30 %) failed to stain with 4-DMACA (Figure 3.7B). This lack of CTs did not correlate with genotype, as a similar proportion of unstained root tips occurred within each genotype. When comparing the ion fluxes at the root tip with the presence or absence of CTs, two-sample t-tests yielded no significant differences in fluxes for any ion (Figure 3.7A). This further suggests that there is no correlation between NH_4^+, Ca^{2+} or NO_3^- fluxes and CT concentrations.

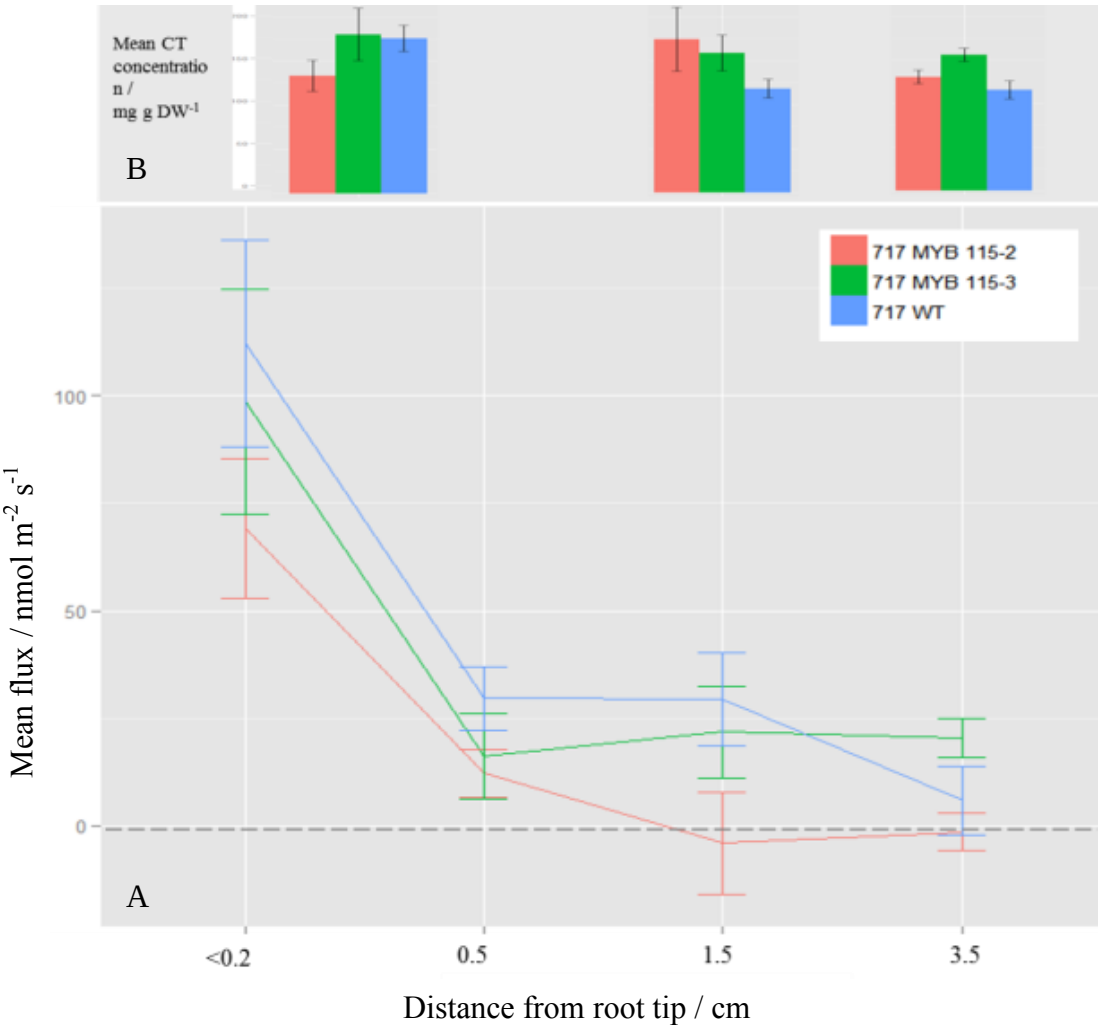

Figure 3.4 A) Mean flux of NH_4^+ at four different root positions (distance from root tip) in three genotypes of *Populus tremula* x *alba* (717): wild-type, and high CT transgenic lines MYB115-2 and MYB115-3. Bars indicate +/- standard error (n=15). Dashed line represents change from net influx (+) to net efflux (-).B) mean total condensed tannin (CT) concentration of roots sections (taken from Figure 3.3) at corresponding distances to flux results. Bars indicate +/- standard error (n=5).

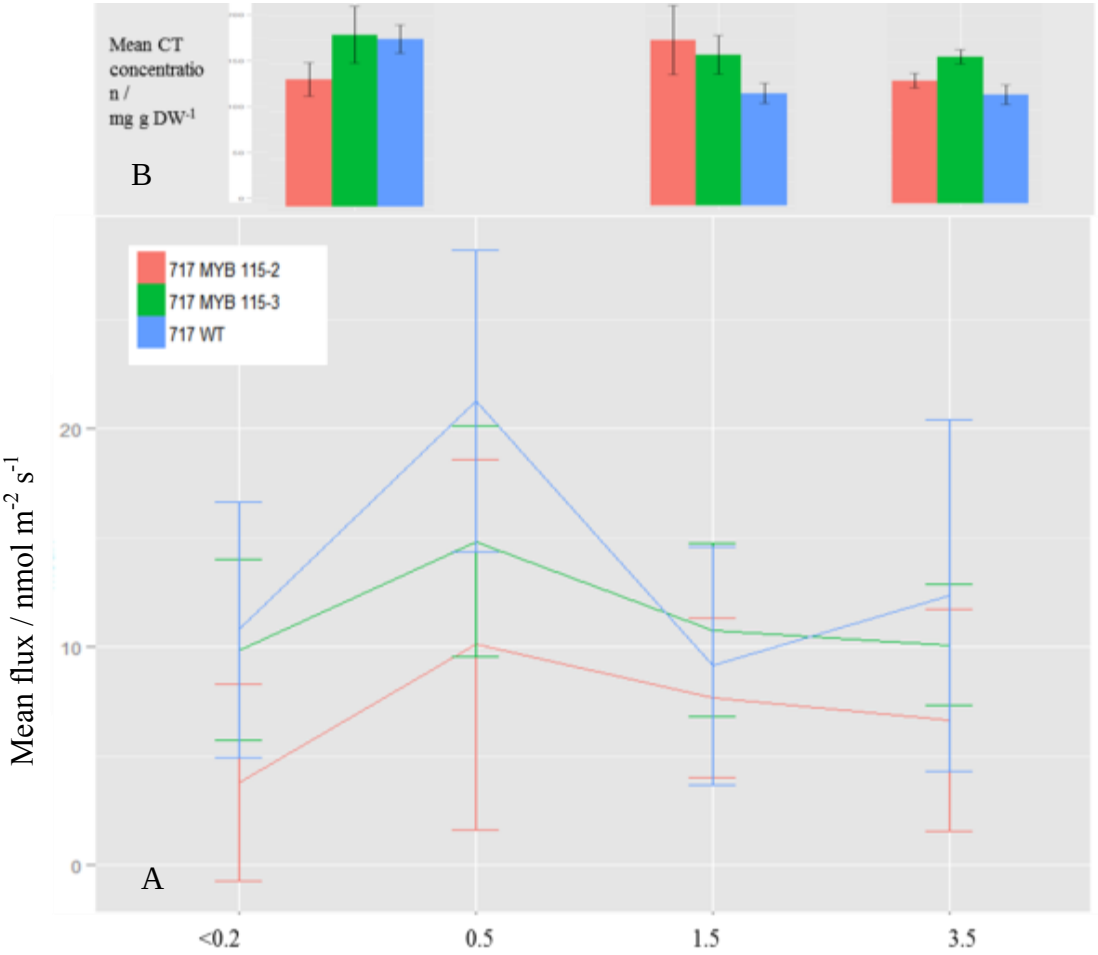

Figure 3.5 A) Mean influx of NO_3^- at four different root positions (distance from root tip) in three genotypes of *Populus tremula* x *alba* (717): wild-type, and high CT transgenic lines MYB115-2 and MYB115-3. Bars indicate +/- standard error (n=15). B) Mean total condensed tannin (CT) concentration of root sections (taken from Figure 3.3) at corresponding distances to flux results. Bars indicate +/- standard error (n=5).

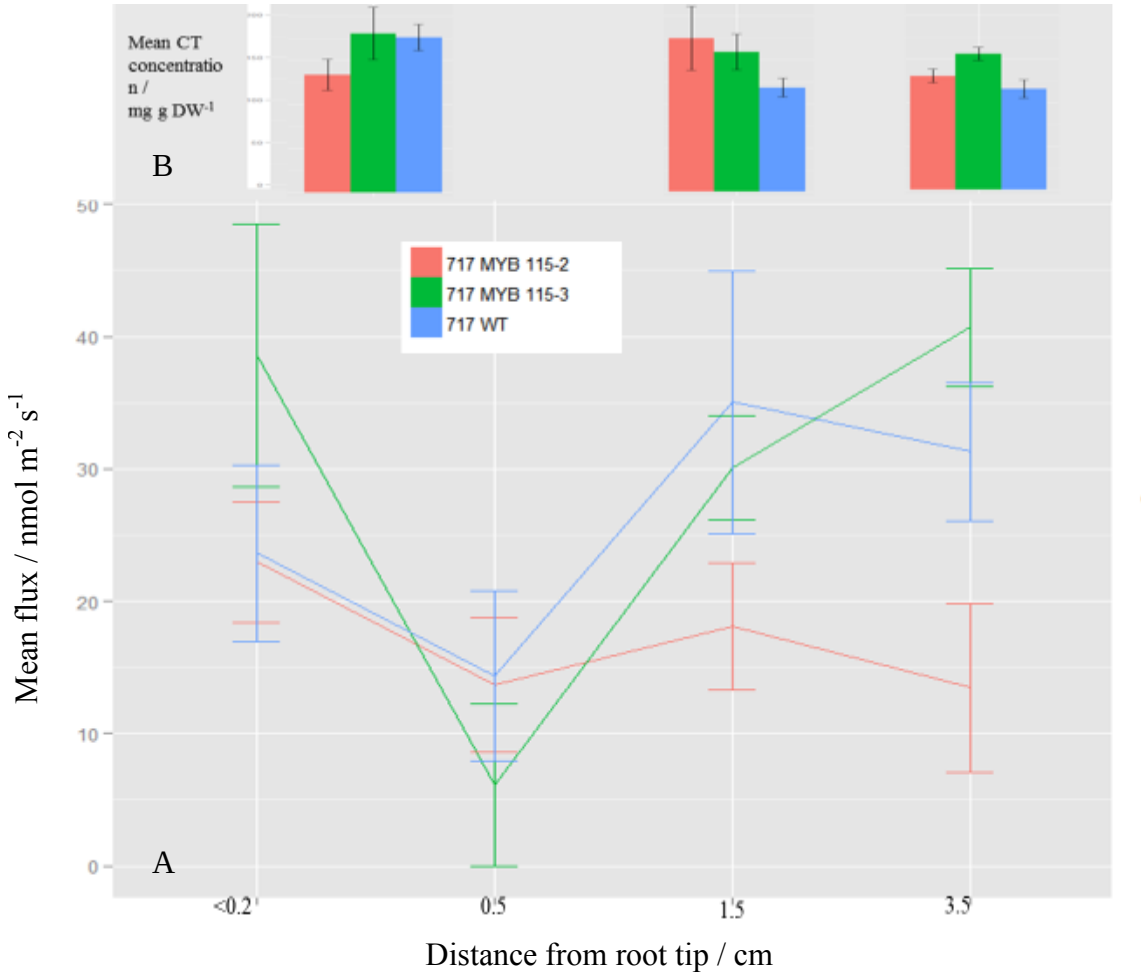

Figure 3.6 A) Mean influx of Ca^{2+} at different four root positions (distance from root tip) in three genotypes of *Populus tremula* x *alba* (717): wild-type, and high CT transgenic lines MYB115-2 and MYB115-3. Bars indicate +/- standard error (n=15). B) Mean total condensed tannin (CT) concentration of root sections (taken from Figure 3.3) at corresponding distances to flux results. Bars indicate +/- standard error (n=5).

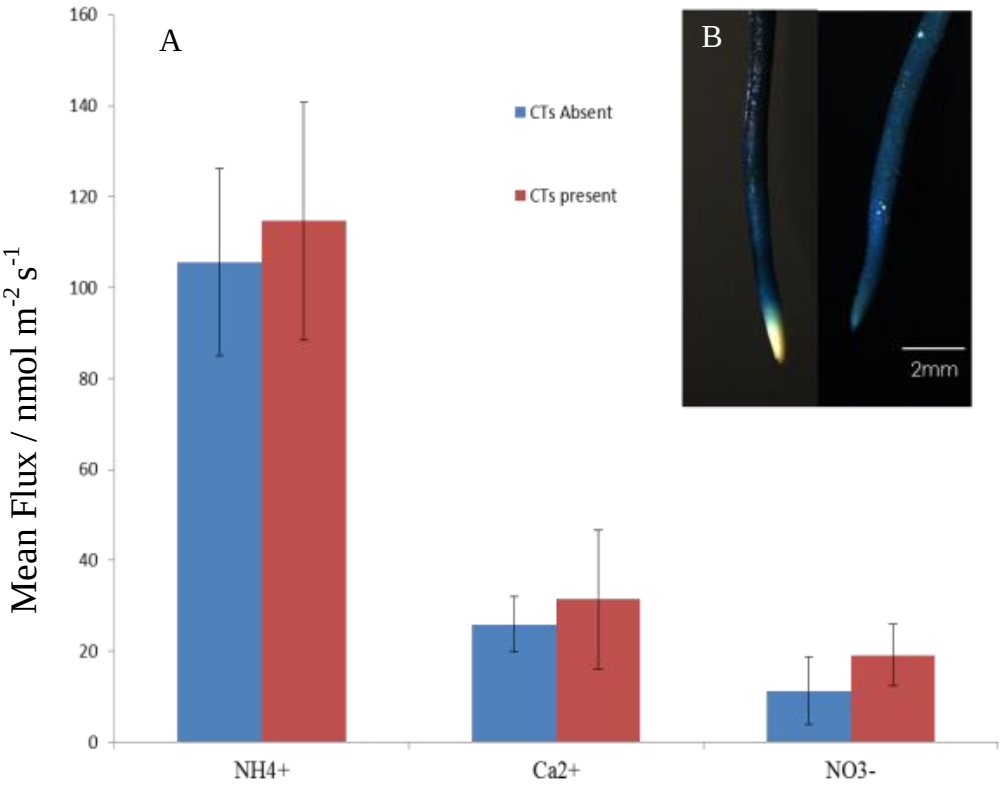

Figure 3.7 A) Mean influx of ions (NH_4^+, Ca^{2+} and NO_3^-) in condensed tannin (CT) containing and non-CT containing *P. tremula* x *alba* root tips used in MIFE™ analysis. Bars indicate +/- standard error (n=15). B) Presence of CTs was detected through 0.01 % 4-DMACA whole root staining (inset) (CTs shown by blue staining).

3.4 Discussion

The nitrogen deficiency experiment demonstrates that root CT concentrations were negatively correlated with soil nitrogen availability. Roots were more sensitive to nitrogen deficiency than leaves, with regards to CT regulation. This provides strong evidence to support the first hypothesis outlined for this study, which states that low soil nitrogen availability will increase root CT concentration. The significant interaction between nitrogen treatment and sample also demonstrates that the response of CTs to nitrogen limitation was not uniform across the whole root. This suggests that CT synthesis can be controlled locally and leads to increases in CT concentrations in specific root zones. For practical reasons, the nitrogen limitation study was conducted using *P. tremula* x *tremuloides* grown in peat soil, rather than *P. tremula* x *alba* grown in vermiculite. Nevertheless, the concentrations of CTs were similar (~10 % of total root dry mass) when grown in 1 mM NH_4NO_3, despite differences in growth substrate and species. This suggests that the response in CT concentration to low nitrogen fertilization is common to the two species tested, and likely to all poplars.

In previous studies, CTs have been observed to bind to Ca^{2+} (Hollins and Jaffe, 1997) and chelate positively charged metals (Osawa *et al.,* 2011; Stoutjesdijk *et al.,* 2001; Scalbert, 1991; Kimura and Wada, 1989). This led to the development of two further hypotheses tested in this chapter: that zones of the root with high CT concentrations will have highest rates of cation uptake (NH_4^+ and Ca^{2+}), and that the high CT genotypes with elevated root CT concentrations will have higher cation uptake through increased binding by CTs (NH_4^+ and Ca^{2+}) compared to the wild-type trees. In

contrast to these hypotheses, NH_4^+ or Ca^{2+} fluxes did not appear to be spatially correlated with CT concentration either along the root or between genotypes. The MIFE^{TM} system measures ion fluxes at discreet positions along the roots and can be used as a proxy for ion transporter activity (Hawkins *et al.*, 2008). In this study, the peak influxes for each ion (NH_4^+, NO_3^- and Ca^{2+}) occurred at different root positions. This provides evidence that ion transporters have different levels of activity in discreet positions along the root. Despite finding no significant correlation between CTs and ion fluxes, this data provides important information on the nature of ion uptake and localization of ion transporters in *Populus*. It also provides new baseline knowledge that can be used to investigate other functional roles of CTs within the root system.

The spatial patterns of fluxes of NH_4^+ and NO_3^- observed are of similar distributions to the fluxes recorded in *P. simonii* (Zhang *et al.*, 2014). In that study, the maximum influx of NH_4^+ occurred near the root tip, similar to the results presented here in *P. tremula* x *alba*. Maximal NO_3^- influx, however, occurred at 1.5 cm from the root tip in *P. simonii*, but at 0.5 cm in *P. tremula* x *alba*. The magnitude of NH_4^+ fluxes in *P. tremula* x *alba* were up to ten fold higher than those recorded in *P. popularis* (Luo *et al.*, 2013b). However NO_3^- fluxes were of similar magnitude. This higher NH_4^+ uptake may be explained by differences in experimental setup and material. The experiment, presented here, used eight-week-old *P. tremula* x *alba* compared to one-year-old cuttings of *P. popularis* used by Luo *et al.*, (2013b). Another microelectrode study, using the same MIFE^{TM} system, compared nutrient fluxes in roots from mature stem cuttings and three-week-old seedlings of *P. trichocarpa* (von Wittgenstein, 2013). Stem cuttings were taken from mature *P. trichocarpa* plants and placed in rooting hormone

(Rootech Original Cloning Gel (Technaflora Plant Products Ltd., Port Coquitlam, B.C., Canada)) to stimulate root growth. Cuttings were then grown in perlite and MIFE^{TM} analysis was conducted on the roots after three weeks of growth. The results showed significant variation in flux profiles between the roots of cuttings and seedlings. MIFE^{TM} analysis of seedlings showed net uptake of NH_4^+ for distances up to 1.5 cm from the root tip. NO_3^- uptake of seedlings was more variable with both influx and efflux being observed. In contrast, MIFE^{TM} analysis of roots from cuttings reported large effluxes of both NH_4^+ and NO_3^-. These large nitrogen effluxes were attributed to the presence of vegetative storage proteins in the mature stem tissue. This reduced the nitrogen demand in older cuttings compared to young, rapidly growing seedlings with no nutrient reserves (von Wittgenstein, 2013). The observed differences in nutrient fluxes between plants of different developmental stages could also explain the lower NH_4^+ uptake observed in one-year-old cuttings of *P. popularis* used by Luo *et al.*, (2013b) compared to the eight-week-old plants used in this study.

Uptake of NH_4^+ was up to 10 fold higher than that of NO_3^-, when both forms of nitrogen were present at equal concentrations, indicating that NH_4^+ is the preferred nitrogen source for *P. tremula* x *alba*. This is contrary to many other poplar species that show greater NO_3^- uptake compared to NH_4^+ (Rennenberg *et al.*, 2010). NO_3^- uptake in other poplars may not be a strict preference but an adaptation to abundant available NO_3^-, with NH_4^+ being scarce in riparian habitats. Net NH_4^+ uptake has been reported to be significantly stimulated in the presence of NO_3^-, yet NO_3^- uptake is inhibited by the presence of NH_4^+ (Luo *et al.*, 2013b). NH_4^+ uptake is passive, whereas NO_3^- uptake is energetically expensive (Taiz and Zeiger, 2010). The results presented here are

consistent with observations that plants preferentially take up NH_4^+ when in solution with NO_3^-.

In conifers, the rate of NH_4^+ uptake has been observed to be five times lower compared to that recorded here for *P. tremula* x *alba* (Hawkins *et al.*, 2014). This likely reflects the adaptations of poplars, characterized by rapid growth and highly efficient nutrient uptake (Eckenwalder, 1996). Behind the root tip (>0.5 cm), NH_4^+ uptake significantly declined to ~25 nmol m^{-2} s^{-1} in two out of the three *P. tremula* x *alba* genotypes (Figure 3.4A). Uptake of NH_4^+ then appears to slowly decline further up the white zone of root within the 3.5 cm measured. This reduction in uptake is consistent with the disappearance of passage cells more than 3 cm from the root tip (Chapter 2). The white zone of *P. tremula* x *alba* roots comprised ~40 % of total root length and only the white zone was analyzed by the MIFE^{TM}. In other woody species, however, the white zone of fine roots accounted for a much smaller proportion of root surface area (<1 %) (Comerford *et al.*, 1994). Although the white zone of roots had the highest influx of nutrient ions per unit area, the brown zone may account for the greater nitrogen uptake overall, due to its larger surface area (Hawkins *et al.*, 2014). The extensive length of *P. tremula* x *alba* roots, particularly the white zone, meant that it was not experimentally possible to measure fluxes in the brown zone as the roots were too long for the measuring chamber. Therefore, whether the brown zone is still capable of nutrient influx, as recorded in conifers, could not be tested. Previous microelectrode studies in *Populus* have also only focused on measuring fluxes within the first 3 cm from the root tip and pigmentation was not described, but measurements would have almost certainly been within the white zone (Luo *et al.*, 2013b; Zhang *et al.*, 2014). The

absence of passage cells in the older portion of the white zone of *P. tremula* x *alba* roots (>3 cm back from root tip) recorded in Chapter 2 may make these roots functionally distinct from those in *Pinus.* In *Pinus,* passage cells were still present within the early brown zones (McKenzie and Peterson, 1995a). Establishing a method to conduct flux analysis on the brown zone of *Populus*, prior to the cork zone, would provide important information regarding nutrient fluxes and cortex viability in this zone.

To date, only a single study has measured Ca^{2+} fluxes using a microelectrode ion flux system (Hawkins and Robbins, 2014), our study is the first to investigate Ca^{2+} fluxes in *Populus* roots. The results in conifers showed large spatial variation in fluxes of Ca^{2+}, with large oscillations between influx and efflux. Overall, however, the differences in Ca^{2+} fluxes at discreet distances along the root were insignificant (Hawkins and Robbins, 2014). The results presented here, however, show significant spatially determined differences in Ca^{2+}, with very low Ca^{2+} influx at 0.5cm. Interestingly, the pattern of Ca^{2+} fluxes appeared to correlate inversely with NO_3^- fluxes. This was not explicitly shown in flux analysis in Hawkins & Robbins (2014). However the authors did find that NO_3^- uptake was inversely correlated to Ca^{2+} fertilization, yet, Ca^{2+} fertilization had no significant effect on NH_4^+ uptake. This supports the idea that there is a link between Ca^{2+} and NO_3^-. The inverse relationship between Ca^{2+} and NO_3^- suggests that the ATPase pumps required for the active uptake of NO_3^- may be using Ca^{2+} as a substrate instead of H^+ (Hawkins and Robbins, 2014) and so might explain the antagonistic relationship between fluxes. The current study did not measure H^+ fluxes and so it is not possible to determine whether Ca^{2+} is a substrate for NO_3^- transporters in place of H^+. Measuring fluxes of NO_3^-, Ca^{2+} and H^+ simultaneously with the MIFE^{TM} is

crucial to understanding this relationship and further investigation into the mechanisms of NO_3^- and Ca^{2+} ion transporters is warranted.

Genotype was a significant factor in both NH_4^+ and Ca^{2+} flux measurements with the high CT transgenic MYB 115-2 having significantly lower ion influxes than the other two genotypes. Observations of growth in the greenhouse during these experiments showed the MYB 115-2 transgenic line has consistently lower growth rates and shoot heights than the other two genotypes, and necrotic spots were observed on the edges of leaves (Figure 3.8). This has not previously been observed in work using this line (Franklin, 2013). The lower rates of ion uptake, observed here, were likely coupled with reduced root and shoot growth in MYB 115-2 transgenic line. However, it was outside of the scope of this project to decipher precisely why this reduced growth rate occurred. A study investigating the expression levels of the genes that encode specific ion transporters would indicate whether the transgene (MYB 115-2) may be affecting transporter regulation and thereby reducing nutrient uptake.

Whole staining of individual roots used in the MIFE™ experiments, showed that CTs were absent in ~30 % of the root tips. This contradicts all the data presented on root tip CT localization in Chapter 2, which consistently showed greater intensity of staining at the root tip compared to the rest of the white zone. In my study, the excised roots were stored in aerated solution (500 µM NH_4NO_3 and 500 µM $CaSO_4$) following flux measurements for up to 24 hours before staining and imaging. One possibility is that under these nutrient rich, hydroponic conditions some roots were still capable of growth, despite being excised, and synthesized a new root cap while in solution. Alternatively,

the CT-containing cells may have been washed off into the solution. Due to the fact that the staining was conducted on excised roots, the results may be artificial. However, the results may demonstrate that CTs are not immediately accumulated in the root cap, and may be only synthesized upon damage at the soil-plant interface. This would explain the high root tip accumulation observed in the vermiculite grown trees.

Figure 3.8 Necrotic spots frequently observed in the MYB 115-2 transgenic *P. tremula* x *alba* line.

The growth-differentiation balance hypothesis (GDBH) (Herms and Mattson, 1992) states that under low nitrogen conditions there should be a tradeoff between growth (primary metabolites) and defense compounds (secondary metabolites). This hypothesis was supported in roots by the results of the nitrogen manipulation experiment: CTs were induced to higher concentrations in roots under low nitrogen

compared to high nitrogen fertilization. This is also consistent with previous results in *P. tremuloides;* Stevens *et al.* (2014) found 47 % higher CT concentrations in roots in the unfertilized condition compared to the fertilized treatment (using Osmocote slow release fertilizer). In this experiment CT concentrations in leaves of *P. tremula* x *alba*, were not significantly different between high and low nitrogen treatments, and so are inconsistent with the GDBH. This is likely due to the very low leaf CT concentrations observed in all conditions. This low level of CT synthesis is expected to be due to greenhouse conditions that minimize external stressors. Furthermore, the selection for young leaves may have caused these low levels as they may not have induced CT synthesis at this early age. Correlating CT concentrations with other physical factors such as height, C/N ratios and root/shoot biomass would provide useful information on regulation and trade-off between growth and defenses (GDBH) specific to CT regulation.

In summary, NH_4^+ and Ca^{2+} fluxes were not spatially correlated with root CT concentration. Nevertheless a significant inverse relationship between nitrogen limitation and CT concentration was observed. Pest and pathogen defense, as well as detoxification of heavy metal soils need to be tested as potential physiological roles of root CTs in *Populus* in future experiments.

4 Conclusions and Future Directions

The aims of this MSc project were to determine localization of CTs in the roots of *P. tremula* x *alba* and investigate the hypothesis that root CTs can modulate or facilitate nutrient uptake. Root CT localization was analysed using both quantitative assays and histochemical techniques. This is the first study to quantitatively measure the distribution of CTs along the root axis.

CT concentration was significantly higher in the white zone compared to the brown zone of *P. tremula* x *alba* roots. This finding was unexpected as the brown zone of woody roots of *Pinus*, between the white zone and cork zone has been found to be highest in CTs (and is often called the 'CT zone'). The longitudinal and cross sections show that CTs accumulate in the root cap cells and the epidermal layers of the young white zone of poplar roots. In *P. tremula* x *alba*, this white zone of young sapling roots accounts for ~40 % of the total root length. In contrast, the white zone has been recorded to comprise only 0.3 % of root length in *Pinus taeda* (Comerford *et al.,* 1994). The high proportion of white zone in the roots of *P. tremula* x *alba*, as grown in our experimental conditions, may explain the differences in CT distribution with previous reports. This high volume of white root zones in poplar means there is extensive surface for nutrient uptake to occur, almost certainly contributing to the rapid growth observed in many poplar species. However, the white zones of fine roots are very soft and delicate and more vulnerable to environmental stressors, which creates a demand for phytochemical defenses (Gebauer *et al.*, 1998; Rasmann *et al.,* 2011) compared to the cork zone where the periderm forms an outer protective layer.

The data on CT localization (Chapter 2) provided important information when considering potential ecological roles of root CTs. In Chapter 1, I outlined three potential roles of root CTs: 1) CTs function as anti-microbial and anti-herbivore defenses in the roots; 2) CTs can chelate heavy metal cations and provide a mechanisms for plants to adapt to heavy metal soils; 3) CTs can function by binding nutrient cations and modulate or facilitate nutrient cation uptake. CT localization at the soil-plant interface in the root cap and epidermal cells of active, young roots suggests that CTs may play a role in plant defenses in these zones and could therefore be consistent with any of the above-proposed roles. The spatial relationship between CTs and nutrient ion fluxes were considered in this thesis, thus I focused on the third proposed role of roots CTs and addressed the question: are root nutrient ion fluxes spatially correlated with root CT concentration?

CTs were significantly upregulated under low nitrogen conditions, consistent with a connection to nutrient uptake. Significant differences were observed in NH_4^+ and Ca^{2+} influx at different positions along the root, while CT concentration was constant. This strongly suggests that there is no correlation between CT concentration and fluxes of NH_4^+, NO_3^- or Ca^{2+}, and does not lend support to the hypothesis that CTs could modulate or facilitate cation uptake.

The upregulation of CTs under low nitrogen suggests that *P. tremula* x *alba* may be investing carbon in CT synthesis. This maybe a mechanism to increase defenses while growth is limited by nitrogen availability as previously proposed through the growth-differentiation balance hypothesis (Herms and Mattson, 1992). The evidence for

anti-herbivore properties of CTs in leaves has been inconsistent. Consistent negative effects of CTs are observed frequently in mammalian herbivores but not lepidopterans (Barbehenn and Constabel, 2011). A major knowledge gap, however, still exists regarding below-ground herbivory and defenses (Rasmann *et al.*, 2011). Only a single study has investigated the role of CTs as below-ground anti-herbivore defense compounds. Sukovata *et al.* (2015) found no correlation between root CT concentration and root-feeding *Melolontha* (Coleoptera, Scarabaeidae) grub performance which supports the idea that CTs are not an effective anti-herbivore defense in this system. Herbivory from mammals and some invertebrates, specifically nematodes, is responsible for high levels of damage below-ground and affects the overall fitness of the plant (Wallis *et al.*, 2012; Rasmann and Agrawal, 2008). Therefore, further study is needed to investigate whether high root CT levels can act as effective anti-herbivore mechanisms to other invertebrate and vertebrate root-feeders.

Currently, a physiological role of root CTs, with the most supporting evidence, is their ability to chelate heavy metals as observed in *Cinnamomum camphora* and *Lotus pedunculatus.* Evidence suggests that CTs can sequester Al^{3+} in vacuoles of root surface cells of the elongation zone (Osawa *et al.*, 2011; Stoutjesdijk *et al.*, 2001). These CT-Al^{3+} cells are then rapidly detached from the root and replaced with new CT containing cells (Osawa *et al.*, 2011). This turnover of CT cells allows *C. camphora* to grow on toxic Al^{3+} soils, whereas *G. max,* a non-CT producing species, was significantly stunted (Osawa *et al.*, 2011). Evidence for CTs binding Al^{3+} *in situ* has also been discovered in *L. pendunculatus* (Stoutjesdijk *et al.*, 2001). CTs have also been shown to chelate Fe^{3+}

and reduce toxic effects to mangroves (Kimura and Wada, 1989). However, a metal-chelating function for CTs in roots has only been investigated in very few species.

The availability of *Populus* transgenic plants with manipulated CT levels provides an excellent study system to address the physiological functions of CTs in roots. With the evidence to support metal chelation as a key physiological role of root CTs, a logical next step would be to extend the growth and survival study of Osawa *et al.* (2011) to poplar, and grow high-CT and wild-type *P. tremula* x *alba* in soils with a range of Al concentrations. In addition, testing the defense capabilities and resistance of high and low- CT *Populus* genotypes to different herbivores and fungal pathogens will provide further information on the impact of CT concentrations on anti-herbivore and anti-microbial defenses.

In summary, the significantly higher CT concentrations observed in roots compared to leaves clearly suggest that CTs play a key role in the roots of young *P. tremula* x *alba* saplings. This MSc project rigorously tested the hypothesis that root CTs may modulate or facilitate uptake of positively charged nutrient ions, but there proved to be no correlation between the two factors. Below-ground anti-herbivore/anti-pathogen defences and heavy metal chelation are other proposed roles and are logical areas for further investigation to address the functional roles of CTs in roots of *Populus.*

Literature Cited

Abeynayake, S. W., Panter, S., Mouradov, A. and Spangenberg, G. (2011) A high-resolution method for the localization of proanthocyanidins in plant tissues. *Plant Methods* **7:** 13.

Ayres, M.P., Clausen, T.P., Mclean, S.F., Redman, A.M. and Reichart, P.B. (1997) Diversity of structure and antiherbivore activity in condensed tannins. *Ecology* **78:** 1696-1712.

Baidez, A.G., Gomez, P., Del Rio, J.A. and Ortuno, A. (2007) Antifungal capacity of major phenolic compounds of *Olea europaea* L. against *Phytophthostructans* (Zinssm.) Scholten. *Physiological and Molecular Plant Pathology* **69:** 224-229.

Bailey, J.K., Deckert, R., Schweitzer, J.A., Rehill, B.J., Lindroth, R.L., Gehring, C. and Whitham, T.G. (2011) Host plant genetics affect hidden ecological players: links among *Populus*, condensed tannins, and fungal endophyte infection. *Canadian Journal of Botany* **83:** 356-361.

Bailey, J.K., Schweitzer, J., Rehill, B. and Lindroth, R.L. (2004) Beavers as molecular geneticists: a genetic basis to the foraging of an ecosystem engineer. *Ecology* **85:** 603–608.

Banso, A. and Adeyemo, S. (2007) Evaluation of antibacterial properties of tannins isolated from *Dichrostachys cinerea*. *African Journal of Biotechnology* **6:** 1785-1787.

Barbehenn, R.V. and Constabel, C.P. (2011) Tannins in plant–herbivore interactions. *Phytochemistry* **72:** 1551-1565.

Barbehenn, R.V., Jaros, A., Lee, G., Mozola, C.,Wier, W. and Salminen, J.P. (2009) Tree resistance to *Lymantria dispar* caterpillars: importance and limitations of foliar tannin composition. *Oecologia* **159:** 777-788.

Barceló, J. and Poschenrieder, C. (2002) Fast root growth responses, root exudates, and internal detoxification as clues to the mechanisms of aluminum toxicity and resistance: a review. *Environmental and Experimental Botany* **48:** 75–92.

Barlow, P.W. (2003) The root cap: Cell dynamics, cell differentiation and cap function. *Journal of Plant Growth Regulation* **21:** 261–286.

Bargali, S.S. and Singh, S.P. (1991) Aspects of productivity and nutrient cycling in an 8-year-old *Eucalyptus* plantation in a moist plain area adjacent to central Himalaya, India. *Canadian Journal of Forest Research* **21:** 1365-1372.

Baumann, N. (2014) Live/dead staining with FDA and PI. *Ibidi Cells in Focus. Application* **Note 33.**

Bernays, E.A. (1978) Tannins: an alternative viewpoint. *Entomologia Experimentalis et Applicata* **24:** 244-253.

Bernays, E.A., Chamberlain., D.J. and McCarthy, P. (1980) The differential effects of ingested tannic acid on different species of Andridoida**.** *Entomologia Experimentalis et Applicata* **24**: 244-253.

Boeckler, G., Towns, M., Unsicker, S., Mellway, R.D., Yip, L., Hilke, I., Gershenzon, J. and Constabel, C.P. (2014) Transgenic upregulation of the condensed tannin pathway in poplar leads to a dramatic shift in leaf palatability for two tree-feeding Lepidoptera. *Journal of Chemical Ecology* **40:** 150-158.

Bogs, J., Jeffe, F.W., Takos, A.M., Walherand, A.R. and Robinson, S.P.R. (2007) The grapevine transcription factor VvMYBPA1 regulates proanthocyanidin synthesis during fruit development 1. *Plant Physiology* **143:** 1081-1082.

Brillouet, J-M., Romieu, C., Schoefs, B., Solymosi, K., Cheynier, V., Fulcrand, H., Verdeil, J-L. and Conéjéro, G. (2013) The tannosome is an organelle forming condensed tannins in the chlorophyllous organs of Tracheophyta. *Annals of Botany* **112:** 1003-1014.

Brillouet, J-M. and Escourte, J. (2012) A new technique for visualizing proanthocyanidins by light microscopy. *Biotechnic and Histochemistry* **87:** 195-200.

Brundrett, M.C., Endstone, D.E. and Peterson, C. A. (1988) A berberine-aniline blue fluorescent staining procedure for suberin, lignin, and callose in plant tissue. *Protoplasma* **146:** 133-142.

Castells, E., Peñuelas, J. and Valentine, D.W. (2005) Effects of plant leachates from four boreal understorey species on soil N mineralization, and white spruce (*Picea glauca*) Germination and seedling growth. *Annals of Botany* **95:** 1247-1252.

Comerford, N.B., Smethurst, P.J. and Escamilla, J.A. (1994) Nutrient uptake by woody root systems. *New Zealand Journal of Forestry Science* **24:** 195-212.

Constabel, C.P. and Barbehenn, R. (2008) Defensive roles of polyphenol oxidase in plants. In *Induced Plant Resistance to Herbivory.* Edited by A. Schaller, Springer Science pp. 253-270.

Constabel, C.P., Yoshida, K. and Walker, V. (2014) Diverse ecological roles of plant tannins: plant defense and beyond. In *Recent Advances in Polyphenol Research, Vol 4* Edited by Romani, A., Lattanzio and, V and Quideau S. Wiley-Blackwell, Oxford, pp.115-142.

DeGabriel, J.L., Ben Moore, D., Foley, W.J. and Johnson, C.N. (2009) The effects of plant defensive chemistry on nutrient availability predict reproductive success in a mammal. *Ecology* **90:** 711-719.

Dogan, S., Dogan, M. and Arslan, O. (2009) Enzymatic browning in foods and its prevention. *Food Processing: Methods, Techniques and Trends* 385-421.

Eckenwalder, J.E. (1996) Systematics and evolution of *Populus*. In *Biology of Populus and its implications for management and conservation.* Part 1, Chapter 1. Edited by R.F Stettler, H.D, Bradshaw, Jr., P.E. Heilman, and T.M Hinckley. NRC Research Press, National Research Council of Canada, Ottawa, ON, Canada. pp. 7-32.

Farmer, R.E., Jr. (1996) The genecology of *Populus*. In *Biology of Populus and its implications for management and conservation*. Part 1, Chapter 2. Edited by R.F Stettler, H.D, Bradshaw, Jr., P.E. Heilman, and T.M Hinckley. NRC Research Press, National Research Council of Canada, Ottawa, ON, Canada. pp. 33-55.

Feeny, P.P. (1968) Effect of oak leaf tannins on larval growth of the winter moth *Operophtera brumata*. *Journal of Insect Physiology* **14:** 805-817.

Franklin, A.M. (2013) Functional characterization of PtMYB115, a regulator of condensed tannin synthesis in poplar. MSc thesis, University of Victoria, pp. 68-78.

Gallagher, K.L. (2013) Cellular Patterning of the Root Meristem. In *Plant Roots the Hidden Half. Fouth Edition.* Part II Chapter 3. Edited byA. Eschel and T. Beeckman.CRC Press, Taylor and Francis Group, Florida, USA. pp.3-1 – 3-24.

Gardner R.O. (1975) Vanillin-hydrochloric acid as a histochemical test for tannin *Biotechnic and Histochemistry* **50:** 315-317.

Gebauer, R., Strain, B., and Reynolds, J. (1998) The effect of elevated CO2 and N availability on tissue concentrations and whole plant pools of carbon-based secondary compounds in loblolly pine (Pinus taeda). *Oecologia* **113:** 29-36.

Glass A. D. M., Brito D. T., Kaiser B. N., Kronzucker H. J., Kumar A., Okamoto M., Rawat S. R., Siddiqi M. Y., Silim S. M., Vidmar J. J., Zhou D. (2001) Nitrogen transport in plants, with an emphasis on the regulation of fluxes to match plant demand. *Journal of Plant Nutrition and Soil Science* **164:** 199-207.

Glynn, C. Herms D.A., Orians, C.M., Hansen, R.C. and Larsson, S. (2007) Testing the growth-differentiation balance hypothesis: dynamic responses of willows to nutrient availability. *New Phytologist* **176:** 623-634.

Gucker, C.L. (2010) *Populus alba* and hybrids. In: *Fire Effects Information System*, [Online]. U.S. Department of Agriculture, Forest Service, Rocky Mountain

Research Station, Fire Sciences Laboratory (Producer). Available: c [2015, August 4].

Gutmann, M. and Feucht, W. (1991) A new method for selective localization of flavan-3-ols in plant tissues involving glycolmethacrylate embedding and microwave irradiation. *Histochemistry* **96:** 83-86.

Gutmann, M. (1993) Localization of proanthocyanidins using in situ-hydrolysis with sulfuric acid. *Biotechnic and Histochemistry* **68:** 161-165.

Hawkins, B.J., Boukcim, H. and Plassard, C. (2008) A comparison of ammonium, nitrate and proton net fluxes along seedling roots of Douglas-fir and lodgepole pine grown and measured with different inorganic nitrogen sources. *Plant, Cell and Environment* **31:** 278-287.

Hawkins, B.J., Robbins, S. and Beinhauer, E. (2012) Shoot excision has no effect on net flux of protons, ammonium or nitrate in seedling roots of a conifer and three crop species. *Journal of Plant Physiology* **169:** 924-928.

Hawkins, B.J., Robbins, S. and Porter, R.B. (2014) Nitrogen uptake over entire root systems of tree seedlings. *Tree Physiology* **34**: 334-342.

Hawkins, B.J. and Robbins, S (2014) Contrasts in growth and nitrogen nutrition of species in the Cupressaceae and Pinaceae in response to calcium. *Plant Soil* **380:** 315-325.

Heilman, P.E., Ekuan, G. and Fogle, D. (1994) Above- and below-ground biomass and fine roots of 4-year-old hybrids of *Populus trichocarpa* x *Populus deltoides* and parental species in short rotation culture. *Canadian Journal of Forest Research* **24:** 1186-1192.

Herms, D.A. and Mattson, W.J. (1992) The dilemma of plants: to grow or defend. *Quarterly Review of Biology* **67:** 283-335.

Hishi, T. (2007) Heterogeneity of individual roots within the fine root architecture: causal links between physiological and ecosystem functions. *Journal of Forest Research* **12:** 126-133.

Hoffmann, T., Friedlhuber, R., Steinhauser, C., Tittel, I., Skowranek, K., Schwab, W. and Fischer, T.C. (2012) Histochemical screening, metabolite profiling and expression analysis reveal *Rosaceae* roots as the site of flavan-3-ol biosynthesis. *Plant Biology* **14:** 33-40.

Hollins, D.L. and Jaffe, M.J. (1997) On the role of tannin vacuoles in several nastic leaf responses. *Protoplasma* **199:** 215-222.

Hose, E., Clarkson, D.T., Steudle, E., Schreiber, L. and Hatung, W. (2001) The exodermis: a variable apoplastic barrier. *Journal of Experimental Botany* **52:** 2245-2264.

Hunter, M.D. (2001) Out of sight, out of mind: the impacts of root-feeding insects in natural and managed systems. *Agricultural and Forest Entomology* **3:** 3-9

Hwang, S.Y. and Lindroth, R.L. (1997) Clonal variation in foliar chemistry of aspen: Effects on gypsy moths and forest tent caterpillars. *Oecologia* **111:** 99-108.

Jones, D.L., Prabowo, A.M. and Kochian, L.V. (1996) Kinetics of malate transport and decomposition in acid soils and isolated bacterial populations: the effect of microorganisms on root exudation of malate under Al stress. *Plant Soil* **182:**239-247.

Kao, Y., Harding, S.A. and Tsai, C. (2002) Differential expression of two distinct phenylalanine ammonia-lyase genes in condensed tannin-accumulating and lignifying cells of quaking aspen. *Plant Physiology* **130:** 796-807.

Kaplan, I., Halitschke, R., Kessler, A., S, Sardanelli, S., Sardanelli, R. and Denno, R. F. (2008) Constitutive and induced defences to herbivory in above- and below-ground plant tissues. *Ecology* **89:** 392-406.

Karowe, D.N. (1989) Differential effect of tannic acid on tree feeding Lepidoptera: Implications for theories of plant-herbivore chemistry. *Oecologia* **80:** 507-512.

Kimura, M. and Wada, H. (1989) Tannins in mangrove tree roots and their role in the root environment. *Soil Science and Plant Nutrition* **35:** 101-108.

Kosola, K. R., Dickmann, D. I., Hall, R. B. and Workmaster, B. A. (2004) Cottonwood growth rate and fine root condensed tannin concentration. *Tree Physiology* **24:** 1063-1068.

Kosola, K., Parry, D. and Workmaster, B. (2006) Responses of condensed tannins in poplar roots to fertilization and gypsy moth defoliation. *Tree Physiology* **26:** 1607-1611.

Kraus, T., Dahlgren, R. and Zasoski, R. (2003) Tannins in nutrient dynamics of forest ecosystems-a review. *Plant and Soil* **256:** 41-66.

Kraus, T. E. C., Zasoski, R. J., R, Dahlgren, R. A., Dahlgren, Y. A., Horwath, W. R. and Preston, C. M. (2004) Carbon and nitrogen dynamics in a forest soil amended with purified tannins from different plant species. *Soil Biology and Biochemistry* **36**: 309-321.

Larbat, R., Paris, C., Le Bot, J. and Adamowicz, S. (2014) Phenolic characterization and variability in leaves, stems and roots of Micro-Tom and patio tomatoes, in response to nitrogen limitation. *Plant Science* **224:** 62-73.

Larbat, R., Le Bot, J., Bourgaud, F., Robin, R. and Adamowicz, S. (2012) Organ-specific responses of tomato growth and phenolic metabolism to nitrate limitation. *Plant Biology* **14:** 760-769.

Lees, G.L., Suttill, N.H. and Gruber, M.Y. (1993) Condensed tannins in sainfoin. 1. A histological and cytological survey of plant tissues. *Canadian Journal of Botany* **71:** 1147-1152.

Lepiniec, L., Debeaujon, I., Routaboul, J., Baudry, A., Pourcel, L., Nesi, N., and Caboche, M. (2006) Genetics and the biochemistry of seed flavonoids. *Annual Review of Plant Biology* **57:** 405-430.

Leser, C., and Treutter, D. (2005) Effects of nitrogen supply on growth, contents of phenolic compounds and pathogen (scab) resistance of apple trees. *Physiologia Plantarum* **123:** 49-56.

Li, Y., Tanner, G. and Larkin, P. (1996) The DMACA–HCl protocol and the threshold proanthocyanidin content for bloat safety in forage legumes. *Journal of the Science of Food Agriculture* **70:** 86-101.

Luo, J., Li, H., Liu, T., Polle, A., Peng, C. and Luo, Z-B. (2013a) Nitrogen metabolism of two contrasting poplar species during acclimation to limiting nitrogen availability. *Journal of Experimental Botany* **64:** 4207-4224.

Luo, J., Qin, J., He, F., Li, H., Liu, T., Polle, A., Peng, C. and Luo, Z-B. (2013b) Net fluxes of ammonium and nitrate in association with H^+ fluxes in fine roots of *Populus popularis*. *Planta* **237:** 919-931.

Lynch, J. P. and St Clair, S. (2004) Mineral stress: the missing link in understanding how global climate change will affect plants in real world soils. *Field Crops Research* **90:** 101-115.

Marsh, K.J., Foley, W.J., Cowling, A. and Wallis, I.R. (2003) Differential susceptibility to Eucalyptus secondary compounds explains feeding by the common ringtail (*Pseudocheirus peregrinus)* and common brushtail possum (*Thicosurus Vulpecula). Journal of Comparative Physiology B* **173:** 69-78.

McArt, S. H., Spalinger, D. E., Collins, W. B., Schoen, E. R., Stevenson, T. and Bucho, M. (2009) Summer dietary nitrogen availability as a potential bottom-up constraint on moose in south-central Alaska. *Ecology* **90:** 1400-1411.

McCormack, M.L., Dickie, I.A., Eissenstat, D.M., Fahey, T.J., Fernandez, C.W. *et al.* (2015) Redefining fine roots improves understanding of below-ground contributions to terrestrial biosphere processes. *New Phytologist* **207:** 505-518.

McKenzie, B.A., and Peterson C.A. (1995a) Root browning in *Pinus banksiana* Lamb. and *Eucalyptus pilularis* Sm. 1. Anatomy and permeability of the white and tannin zones. *Botanica Acta* **108:** 127-137.

McKenzie, B.A., and Peterson C.A. (1995b) Root browning in *Pinus banksiana* Lamb. and *Eucalyptus pilularis* Sm. 1. Anatomy and permeability of the cork zone. *Botanica Acta* **108:** 138-143.

Mellway, R., Tran, L., Prouse, M.B., Campbell, M.M. and Constabel, C.P. (2009) The wound-, pathogen-, and ultraviolet B-responsive MYB134 gene encodes an R2R3 MYB transcription factor that regulates proanthocyanidin synthesis in poplar. *Plant Physiology* **150:** 924-941.

Meyer, C.J. and Peterson, C.A. (2013) Structure and Function of Three Suberized Cell Layers. In *Plant Roots the Hidden Half. Fouth Edition.* Part II Chapter 5. Edited byA. Eschel and T. Beeckman.CRC Press, Taylor and Francis Group, Florida, USA. pp.5-1 – 3-20.

Mirnezhad, M., Romeo-Gonzalez, R.R., Leiss, K.A., Choi, Y.H., Verpoorte, R. and Klinkhamer, P.G.L. (2009) Metabolomic analysis of host plant resistance to thrips in wild and cultivated tomatoes. *Phytochemical Analysis* **21:** 110-117.

Mueller, W.C. and Greenwood, A.D. (1978) The ultrastructure of phenolic-storing cells fixed with caffeine. *Journal of Experimental Botany* **29:** 757-764.

Mueller-Harvey, I. (2006) Unravelling the conundrum of tannins in animal nutrition and health. *Journal of Science and Food Agriculture* **86:** 2010-2037.

Nagata, T., Hayatsu, M. and Kosuge, N. (1992) Identification of aluminum forms in tea leaves by 27Al NMR. *Phytochemistry* **31:** 1215-1218.

Nichols-Orions, C. (1991) Differential effects of condensed and hydrolyzable tannin on polyphenol oxidase activity of attine symbiotic fungus. *Journal of Chemical Ecology* **17:** 1811-1819.

Osawa, H., Endo, I., Hara, Y. and Matsushima, Y. (2011) Transient proliferation of proanthocyanidin-accumulating cells on the epidermal apex contributes to highly aluminum-resistant root elongation in camphor tree. *Plant Physiology* **155:** 433-446.

Osier, T., and Lindroth, R.L. (2001) Effects of genotype, nutrient availability, and defoliation on aspen phytochemistry and insect performance. *Journal of Chemical Ecology* **27:** 1289-1313.

Osier, T. and Lindroth, R.L. (2006) Genotype and environment determine allocation to and costs of resistance in quaking aspen. *Oecologia* **148:** 293-303.

Pei, Y., Xiang, Y-F., Chen, J-N., Lu, C-H., Hao, J. *et al.* (2011) Pentagalloylglucose downregulates cofilin1 and inhibits HSV-1 infection. *Antiviral Research* **89:** 98–108.

Peters, D. and Constabel, C.P. (2002) Molecular analysis of herbivore-induced condensed tannin synthesis: cloning and expression of dihydroflavonol reductase from trembling aspen (*Populus tremuloides*). *The Plant Journal* **32:** 701-712.

Peterson, C.A., Enstone, D. E., and Taylor, J.H. (1999) Pine root structure and its potential significance for root function. *Plant and Soil* **217:** 205-213.

Peterson, C.A and Enstone, D.E. (1996) Functions of passage cells in the endodermis and exodermis of roots. *Physiologia Plantarum* **97:** 592-598.

Plassard, C., Guérin-Laguette A, Véry A-A., Casarin, V. and Thibaud J-B. (2002) Local measurements of nitrate and potassium fluxes along roots of maritime pine. Effects of ectomycorrhizal symbiosis. *Plant Cell Environment* **25:** 75-84.

Porter, L.J, Hrstich, L.N. and Chan, B.G. (1986) The conversion of procyanidins and prodelphinidins to cyaniding and delphinidin. *Phytochemistry* **25:** 223-230.

Pregitzer, K.S., Zak, D.R., Curtis, P.S., Kubiske, M.E., Teeri, J.A. and Vogel, C.S. (1995) Atmospheric CO_2, soil nitrogen and turnover of fine roots. *New Phytologist* **129:** 579-585.

Pregitzer, K.S. and Friend, A.L. (1996) The structure and function of *Populus* root systems. In *Biology of Populus and its implications for management and conservation. Part II, Chapter 14*. Edited by R.F Stettler, H.D, Bradshaw, Jr., P.E. Heilman, and T.M Hinckley. NRC Research Press, National Research Council of Canada, Ottawa, ON, Canada. pp. 331-354.

Quideau, S., Deffieux, D., Douat-Casassus, C. and Pouységu, L. (2011) Plant polyphenols: chemical properties, biological activities, and synthesis. *Angewandte Chemie International Edition* **50:** 586-621.

Rasmann, S. and Agrawal, A.A. (2008) In defense of roots: a research agenda for studying plant resistance to below-ground herbivory. *Plant Physiology* **146:** 875-880.

Rasmann, S., Bauerle, T.L., Poveda, K. and Vannette, R. (2011) Predicting root defense against herbivores during succession. *Functional Ecology* **25:** 386-379.

Redjala, T., Zelko, I., Sterckeman, T., Legue, V. and Lux, A. (2011) Relationship between root structure and root cadmium uptake in maize. *Environmental and Experimental Botany* **71:** 241-248.

Rennenberg, H. Wildhagen,, H. and Ehlting B. (2010) Nitrogen nutrition of poplar trees. *Plant Biology* **12:** 275–291.

Ruzin, S.E. (1999) Plant microtechnique and microscopy. Oxford University Press, New York. p. 174.

Saslowsky, D. and Winkel-Shirley, B. (2001) Localizaton of flavonoid enzymes in *Arabidopsis* roots. *The Plant Journal* **27:** 37-48.

Scalbert, A. (1991) Antimicrobial properties of tannins. *Phytochemistry* **30:** 3875-3883.

Schimel, J.P., Cates, R.G. and Ruess, R. (1998) The role of balsam popular secondary chemicals in controlling soil nutrient dynamics through succession in Alaskan taiga. *Biogeochemistry* **42:** 221-234.

Schweitzer, J., Madritch, M., Bailey, J., LeRoy, C., Fischer, D.G., Reholl, B.J., Lindroth, R.L., Hagerman, A.E., Wooley, S.C., Hart, S.C. and Whitham ,T.G. (2008) From genes to ecosystems: the genetic basis of condensed tannins and their role in nutrient regulation in a Populus model system. *Ecosystems* **11:** 1005-1020.

Shabala, S.N., Newman, I.A. and Morris, J. (1997) Oscillations in H^+ and Ca^{2+} ion fluxes around the elongation zone of corn roots and effects of external pH. *Plant Physiology* **113:** 111-118.

Shabala, S.N. and Newman, I.A. (1997) H^+ flux kinetics around plant roots after short-term exposure to low-term exposure to low temperature: identifying critical temperatures for plant chilling tolerance. *Plant Cell Environment* **20:** 1401-1410.

Shaw, T., Moore, J. and Marshall, J.D. (1998) Root chemistry of Douglas-fir seedlings grown under different nitrogen and potassium regimes. *Canadian Journal of Forest Research* **28:** 1566-1573.

Smith, A., Zoetendal, E., and Mackie, R. (2005) Bacterial mechanisms to overcome inhibitory effects of dietary tannins. *Microbial Ecology* **50:** 197-205.

Smith, A.H, Pinkard, E.A., Hunter, G.C., Wingfield, M.J. and Mohammed, C.L. (2006) Anatomical variation and defence responses of juvenile *Eucalyptus nitens* leaves to *Mycosphaerella* leaf disease. *Australasian Plant Pathology* **35:** 725-731.

Smolander, A., Kanerva, S., Adamczyk, B. and Kitunen, V. (2012) Nitrogen transformations in boreal forest soils—does composition of plant secondary compounds give any explanations? *Plant and Soil* **350:** 1-26.

Steinly, B.A. and Berenbaum, M. (1985) Histopathological effects of the tannins on the midgut epithelium of *Papilio polyxenes* and *Papilio glaucus*. *Entomologia Experimentalis et Applicata* **184:** 111-118.

Stevens, M.T, Gusse, A.C. and Lindroth, R.L. (2014) Root chemistry in *Populus tremuloides:* Effects of soil nutrients, defoliation, and genotype. *Journal of Chemical Ecology* **40:** 31-38.

Stevens, C.E. and Hume, I.D. (2004) Comparative physiology of the vertebrate digestive system. Cambridge University Press pp.11-23.

Stolá riková-Vaculíková, M., Romeo, S., Minnocci, A., Luxová, M., Vaculík, M., Lux, A. and Sebastiani, L. (2015) Anatomical, biochemical and morphological responses of poplar *Populus deltoides* clone Lux to Zn excess. *Environmental and Experimental Botany* **109**: 235–243.

Stout, M.J., Brovont, R.A. and Duffey, S.S. (1998) Effect of nitrogen availability on expression of constitutive and inducible chemical defenses in tomato, *Lycopersicon esculentum. Journal of Chemical Ecology* **24:** 945-963.

Stoutjesdijk, P.A., Sale, P.W. and Larkin, P.J. (2001) Possible involvement of condensed tannins in aluminum tolerance of *Lotus pedunculatus*. *Australian Journal of Plant Physiology* **28:** 1063-1074.

Sukovata, L., Jaworski, T., Karolewski, P. and Kolk, A. (2015) The performance of *Melolontha* grubs on the roots of various plant species. *Turkish Journal of Agriculture and Forestry* **39:** 107-116.

Tahara, K., Hashida, K., Otsuka, Y., Ohara, S., Kojima K. and Shinohara, K. (2014) Identification of a hydrolyzable tannin, oenthein B, as an aluminum-detoxifying ligand in a highly aluminum-resistant tree, *Eucalyptus camaldulensis. Plant Physiology* **164:** 683-693.

Tang, W. and Newton, R.J. (2004) Increase of polyphenol oxidase and decrease of polyamines correlate with tissue browning in Virginia pine (*Pinus virginiana* Mill.). *Plant Science* **167:** 621–628.

Taiz, L. and Zeiger, E. (2010) Plant Physiology, Fifth Edition. Sinauer Associates Inc, Massachusetts, USA. pp.132-157.

Tegelberg, R. and Julkunen-Titto, R. (2001) The effects of long-term elevated UV-B on the growth and phenolics of field-grown silver birch (*Betula pendula*). *Global Change Biology* **7:** 839-848.

Treutter, D. (2006). Significance of flavonoids in plant resistance: a review. *Environmental Chemistry Letters* **4:** 147-157.

Tsai, C., Harding, S. and Tschaplinski, T. (2006) Genome-wide analysis of the structural genes regulating defense phenylpropanoid metabolism in Populus. *New Phytologist* **172:** 47-62.

Turnquist, H., Allen, N. and Jaffe, M.J. (1993) A pharmacological study of calcium flux mechanisms in the tannin vacuoles of *Mimosa pudica* L. motor cells. *Protoplasma* **176:** 91-99.

Tuskan, G.A., DiFazio, S.P., Jansson, S., *et al.* (2006) The genome of black cottonwood, *Populus trichocarpa* (Torr. and Gray). *Science* **313:** 1596–1604.

USDA, NRCS. 2015. The PLANTS Database (http://plants.usda.gov, 18 August 2015). National Plant Data Team, Greensboro, NC 27401-4901 USA.

Visnovitz, T., Világi, I., Varró, P. and Kristóf , Z. (2007) Mechanoreceptor cells on the tertiary pulvini of *Mimosa pudica* L. *Plant Signaling and Behaviour* **2:** 462-466.

von Wittgenstein, N.J.B. (2013) Nitrogen transporters: comparative genomics, transport activity, and gene expression of NRTs and AMTs in Black Cottonwood (*Populus trichocarpa*). MSc thesis, University of Victoria pp. 48-63.

Wallis, I., Edwards, M., Windley, H. and Krockenberger, A. (2012) Food for folivores: nutritional explanations linking diets to population density. *Oecologia* **169:** 281-291.

Waterman P.G. and Mole S. (1994) Analysis of phenolic plant metabolites. *Blackwell Scientific Publishing* pp.13-15.

Whitham, T., Bailey, J., Schweitzer, J., et *al.* (2006) A framework for community and ecosystem genetics: from genes to ecosystems. *Nature Reviews Genetics* **7:** 510-523.

Yoneda, S. and Nakatsubo, F. (1998) Effects of the hydroxylation patterns and degrees of polymerization of condensed tannins on their metal-chelating capacity. *Journal of Wood Chemistry and Technology* **18:** 193-205.

Yoshida, K., Ma D. and Constabel, C.P. (2015) The MYB182 protein down-regulates proanthocyanidin and anthocyanin biosynthesis in poplar by repressing both structural and regulatory flavonoid genes. *Plant Physiology* **167:** 693-710.

Zhang, C., Meng S., Yiming L. and Zhao, Z. (2014) Net NH_4^+ and NO_3^- fluxes, and expression of NH_4^+ and NO_3^- transporter genes in roots of *Populus simonii* after acclimation to moderate salinity. *Trees* **28:** 1813-1821.

Zifkin, M., Jin, A., Ozga, J.A., Zaharia, I., Schernthaner, J.P., Gesell, A., Abrams, S.R., Kennedy, J.A. and Constabel, C.P. (2012) Gene expression and metabolite profiling of highbush blueberry fruit indicates transcriptional regulation of flavonoid metabolism and activation of abscisic acid metabolism. *Plant Physiology* **158:** 200-224.

Appendix

Appendix 1

Protocol for Embedding Using Technovit® 7100 Glyco Methycrylite Resin

Ratio	Solution	Infiltration time
1:1	100 % Ethanol : Technovit® 7100 base	12 hours
1:2	100 % Ethanol : Technovit® 7100 base	24 hours
	Technovit® 7100 base	48 hours
	Technovit® 7100 base + Hardener I	72 hours
	Technovit® 7100 base + Hardener I	72 hours
	Technovit® 7100 base + Hardener I + Hardener II	Cured in blocks

Appendix 2

Whole root condensed tannin staining of *Populus tremula* x *alba* roots with 0.01 % 4-DMACA in 2 N HCl:EtOH (blue/green) and 1 % vanillin-HCl (red).

Appendix 3a

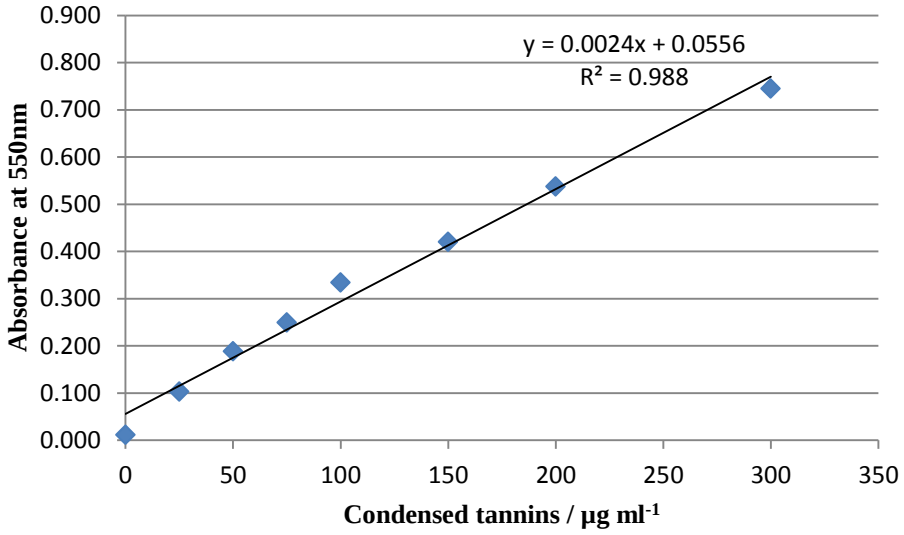

Standard curve used to calculate soluble CT concentration from spectrophotometer reading at 550 nm. CTs extracted in 5 mL of MeOH and 400 µL added to 2 mL 1-butanol:HCl (95:5).

Appendix 3b

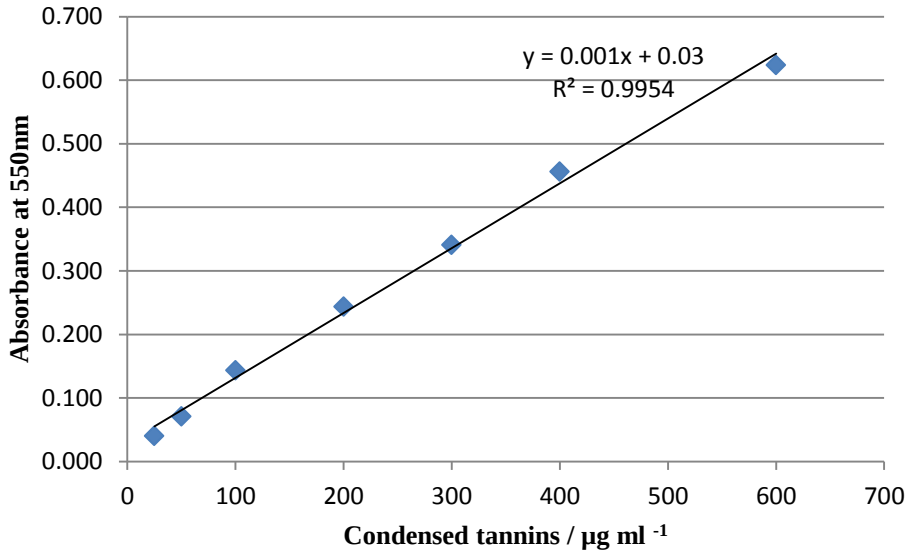

Standard curve used to calculate insoluble CT concentration from spectrophotometer reading at 550 nm. Boiled in 6 mL 1-butanol:HCl (95:5) with 400 µL CT extract in MeOH

Appendix 3c

Standardized calculations used to gain concentrations of CTs (µg mL^{-1}) for both soluble and insoluble CTs

Soluble CTs

µg mL^{-1} = ((heated-unheated absorbance)-0.0556) / 0.0024.

mg g of dry $weight^{-1}$ = (µg mL^{-1} * vol MeOH (5 mL))/dry weight sample (mg)

Insoluble CTs

µg mL^{-1} = ((heated-unheated absorbance)-0.03) / 0.001

mg g of dry $weight^{-1}$ = (µg mL^{-1} * 0.4) /dry weight sample (mg)

Appendix 4

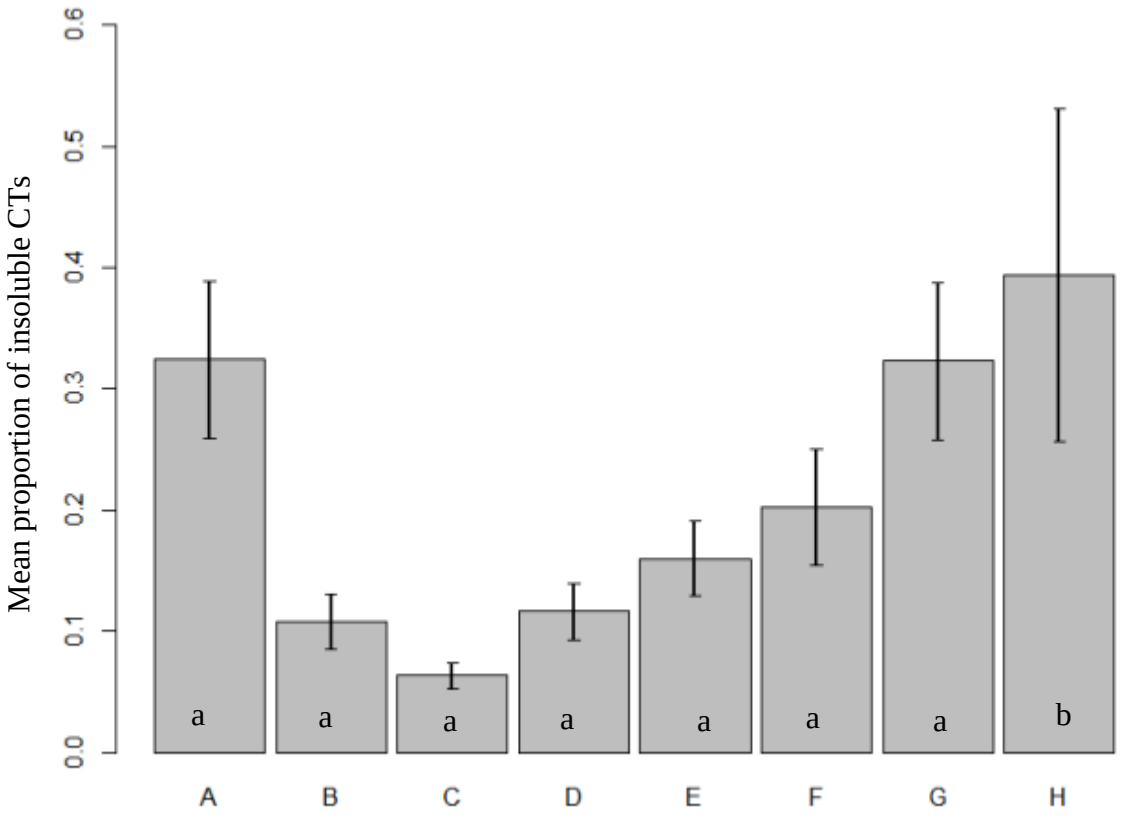

Mean proportion of insoluble condensed tannins from three genotypes of *Populus tremula* x *alba;* wild-type, and high CT transgenic lines *MYB115*-2 and MYB115-3. Bars indicate +/- standard error (n=5). Samples are recorded as distance from root tip. A. 0-0.5cm, B. 1-2cm, C. 3-4cm, D. White zone (4~12cm), E. white-brown transition (~12-13cm), F. Brown zone (~13cm-20cm), G. Cork zone (>20cm), H. Leaf # 5. Significant pairwise comparisons through Tukey's HSD is indicated by a and b ($p \leq 0.05$).

Appendix 5

Calibration Solutions used for MIFE experiment. All corrected to pH5.6 using KOH and H_2SO_4.

Calibration solution for NH_4^+ and NO_3^-

Concentration of NH_4NO_3 (µM)	**Concentration of $CaSO_4$ (µM)**
250	500
500	500
1000	500

Calibration solution for Ca^{2+}

Concentration of NH_4NO_3 (µM)	**Concentration of $CaSO_4$ (µM)**
500	250
500	500
500	1000

Measuring Solution - 500µM NH_4NO_3, 500 µM $CaSO_4$.

Appendix 6a

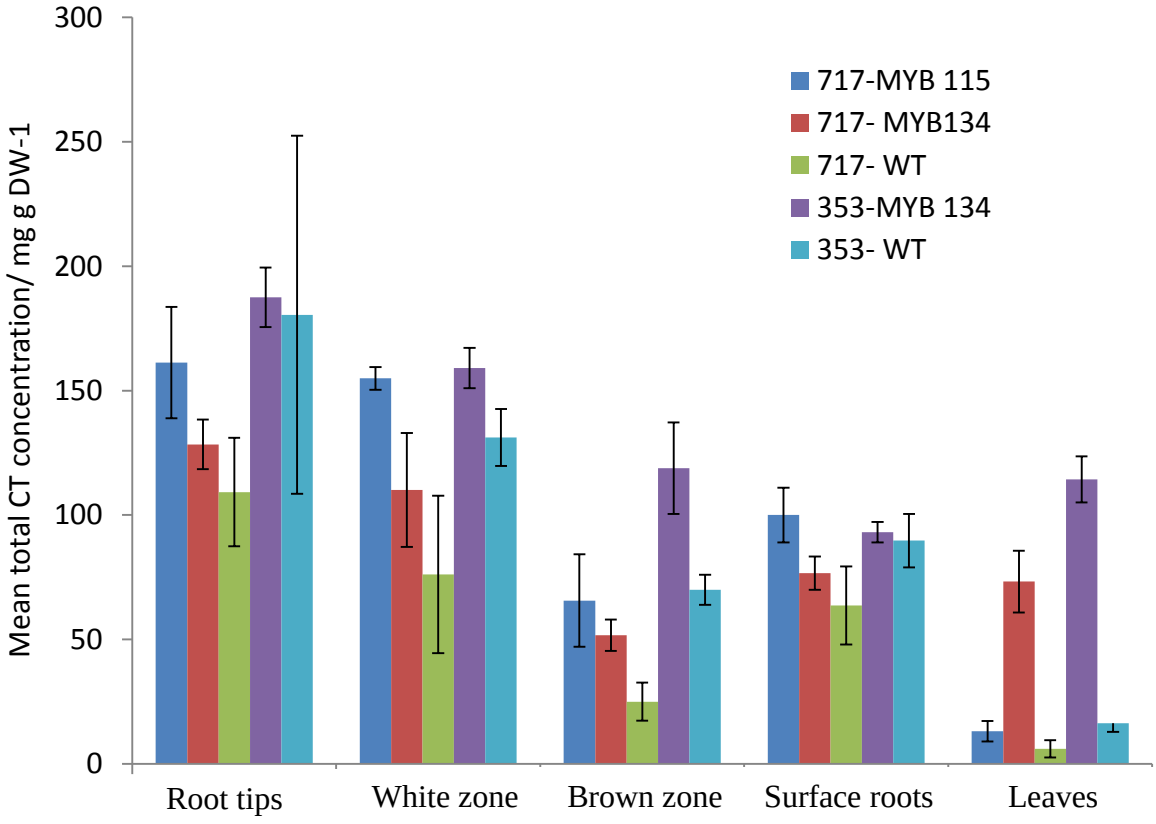

Mean total CT concentration in wild-type and MYB-overexpressing transgenics in the *Populus tremula* x *alba* (717) and *Populus tremula* x *tremuloides (353)* genetic backgrounds. Bars indicate +/- standard error (n=3). Note: surface roots were a mix of white and brown root zones.

Appendix 6b

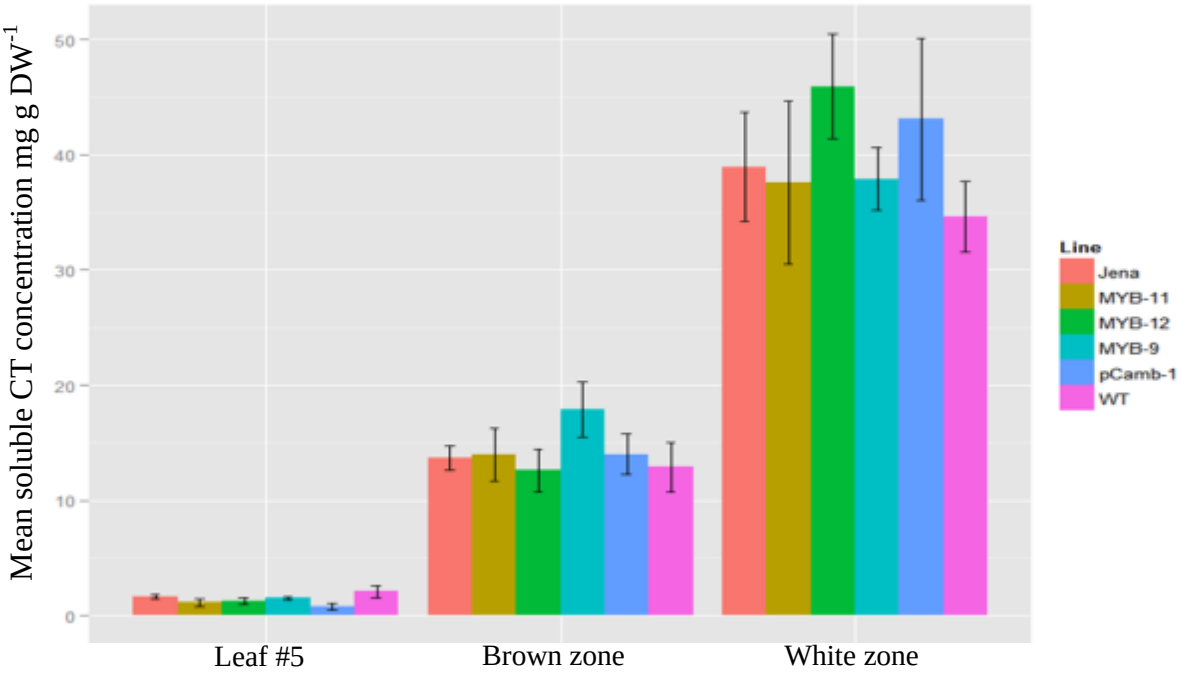

Mean soluble CT concentration of putative RNAi MYB 134 knockdown transgenics and control *Populus tremula* x *alba:* two wild-types (Jena and WT), empty vector control (pCamb-1), RNAi-MYB 134 knockout lines (MYB-9, MYB-11, and MYB-12). Bars indicate +/- standard error (n=4).